Master thesis project at Delft University of Technology

Mechanical properties of timber foundation piles derived from small-scale compression tests

Evaluating the impact of defects and decay on the mechanical properties of spruce foundation piles

by
Ing. M.P. Struik

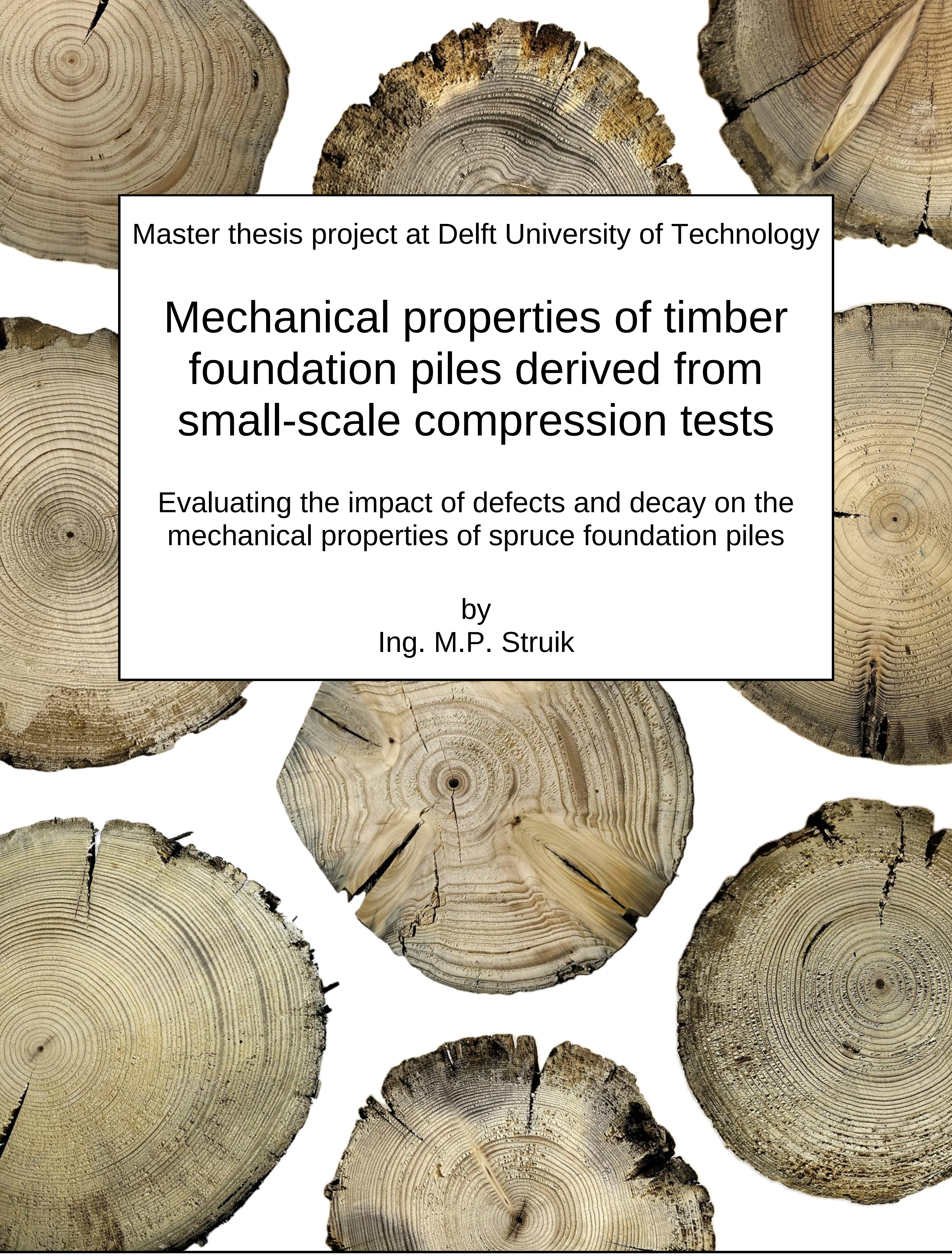

Cover photos: Cross-sections of spruce piles with defects and decay that were included in the project

Mechanical properties of timber foundation piles derived from small-scale compression tests

Evaluating the impact of defects and decay on the mechanical properties of spruce foundation piles

by
Ing. M.P. Struik

A master thesis project carried out for
Department of Bio-based Structures and Materials
Faculty of Civil Engineering and Geosciences
Delft University of Technology

In partial fulfilment of the requirements for the degree
Master of Science in Civil Engineering

Thesis committee

Prof. Dr. Ir. J.W.G. van de Kuilen
Dr. Ir. G. Pagella
Dr. Ir. G.J.P. Ravenshorst
Dr. Ir. M. Mirra
Ir. P.A. de Vries

Delft
28 March 2025

Preface

This thesis marks the end of my studies at the Delft University of Technology. It is the final component to conclude my master track in Structural Engineering and my specialization in Steel and Timber Structures. This study was carried out for the Department of Bio-based Structures and Materials.

As a part of my graduation research in 2019 for my bachelor's degree at the Rotterdam University of Applied Sciences, I went through the entire design process for the reconstruction of a timber pile foundation for a row of residential houses. Here I have seen firsthand the consequences of degraded timber pile foundations and the amount of effort required to restore these deteriorated foundations. It was during this research that my interest in timber foundations became apparent.

Afterwards I went to the Delft University of Technology to finish the bridging programme and to complete the courses of the Civil Engineering master curriculum. When I came across a master thesis topic on aged timber foundation piles at my faculty, it immediately got my attention because it matched my interests and prior knowledge nicely. After some initial preparations I started the testing of the specimens, analysing of the results and writing down the findings. Now I have reached the point where my thesis is finished and I feel very grateful and proud to successfully complete this research. This entire project has been a great experience and I hope that this sentiment will also be reflected in the texts of this thesis.

My sincere thanks go to Dr. Ir. Giorgio Pagella for making this research topic available to me, supervising my project, being patient, sharing his expertise and guiding me throughout the process. I would like to extent my gratitude to the other members of my thesis committee Prof. Dr. Ir. Jan-Willem van de Kuilen, Dr. Ir. Geert Ravenshorst, Dr. Ir. Michele Mirra and Ir. Peter de Vries for their feedback and knowledge. I am also thankful to Ruben Kunz from the Department of Electronic and Mechanical Development (DEMO) for his skilfulness, humour, assistance and all the free coffee I received while working together in the laboratory.

Lastly, I would like to thank my family, parents and friends for their unwavering confidence and encouragement throughout my studies. In particular, I want to express my heartfelt gratitude to my partner Shinara for her emotional support and believing in me more than I believed in myself: this dissertation would not have been possible without you.

Thank you for your interest in this thesis and I hope you enjoy reading it.

Mark Struik

Delft, March 2025

Abstract

Timber pile foundation piles are important structural components of historic buildings and constructions throughout the Netherlands. Many of these piles have been in service for a long time and start showing serious signs of biological degradation that affects their load-bearing capacity. It is essential to preserve these aged timber piles and, in order to make an estimate of the remaining functionality, it is essential to compute their wet mechanical properties. The conventional method for determining the wet compressive strength is by performing large-scale compression tests on segments from the pile. In this project it is researched whether it is also possible to determine the wet compressive strength by performing small-scale compression tests on discs taken from the pile, which could possibly save both time and resources during future investigations.

For this experimental study a total of 6 spruce foundation piles were selected that originated from 1727, 1886, 1922 and 2019. These piles brought forth 45 round wooden discs with each a height of 15 centimeters extracted from the pile head, middle and tip. The discs contained different amounts of bacterial degradation and high concentrations of knots in order to investigate their effects on the strength. The degradation was quantified using micro-drill measurements and the presence of the knots was specified as a knot ratio. From the results of the small-scale compression tests on the discs it can be concluded that the strength of the discs is well correlated with the strength from the large-scale tests. It was observed that the degraded wood hardly contributes to the strength of the pile and that the section with the highest knot ratio governs the strength of the pile. All in all, it was found possible to obtain accurate values for the wet compressive strength of aged timber piles by performing small-scale tests on discs from the piles, as long as the effects of the biological degradation and the knots are taken into account.

Keywords: Spruce timber foundation piles, round wooden discs, wet compressive strength, small-scale compression testing, bacterial degradation, micro-drill integrity testing, knot ratio

Contents

* *The appendices are supplementary to the thesis and provide detailed information on all individual tests and measurements that have been performed. They are in a separate document and will only be distributed upon request.*

List of Figures

List of Tables

1. Introduction

Several historic European cities, including some old city centers in the Netherlands, were founded on timber piles. Many iconic architectural buildings and civil engineering works were constructed on wooden foundations. Timber pile foundations are a major part of the cultural heritage and the aim is to maintain and preserve these foundations including their historical importance.

1.1 Problem description

Nowadays there are approximately still 25 million timber piles in service throughout the Netherlands. About fifty percent of these piles are located under buildings and the other fifty percent are located underneath marine constructions like bridge piers and quay walls. Many of these timber foundation piles have been in use for a long time. Some famous Dutch examples of 17th century buildings with a timber pile foundation that are still standing are the Amsterdam Royal Palace, which rests on 14,000 spruce piles, and the Rotterdam Saint Laurens church, which was built on 500 pine piles. [1]

There are several degradation processes that can occur, which in combination with the old age and high loads drastically reduce the load-bearing capacity of timber foundation piles. One of the most common reasons for degraded timber foundations is biological attack by wood-destroying fungi and bacteria that break down the cells in the wood structure [2]. The fungi can cause a very fast degradation of the timber foundations but they need oxygen to survive [3]. Most timber foundation piles are submerged because they are installed below the groundwater level which means that there is no oxygen unless the water level drops. In these cases the bacterial degradation is decisive because the bacteria can thrive in anaerobic environments. The bacteria have a slower rate of degradation but they can cause significant damage over a longer period of time [4].

The presence of degradation can have a serious negative effect on the functionality of timber foundation piles, which in turn may impact the stability of the superstructure. This can well be illustrated by some pine foundation piles with a diameter of approximately 14 centimeters that were used in the Dutch city of Haarlem which, after only 70 years in the ground with bacterial decay, had an effective cross-section with a diameter of less than 3 centimeters, meaning that the building is supported by foundation piles that resemble broomsticks [1]. Generally it is important to examine the foundations properly, identify any problems in time, make a good estimate of the residual lifespan and administer structural adjustments when necessary to prevent cracks and other damages.

In practice it remains challenging to investigate timber pile foundations, especially when there is limited accessibility to inspect the foundations. Each pile foundation is different which asks for a case-by-case analysis to identify its condition. In addition, it is not always visible whether and to what extent the degradation has occurred. Degraded timber piles often have an unchanged colour and shape, which means that in-situ testing is required to determine their soundness [5]. And, in order to acquire a good estimate of the residual load-bearing capacity, it is necessary to determine the mechanical properties of the timber piles.

The mechanical properties, such as strength and stiffness, depend on the moisture content of the wood structure. Timber piles are often submerged and therefore saturated with water, which means that all the pores are filled with water and the moisture content is way above the fibre saturation point with a value that can be higher than 100%. [3]

The European standards for wood design are covered in Eurocode 5 which provides guidelines and design values for the use of structural timber [6]. This also includes characteristic values for the mechanical properties of structural timber. However, these values are derived from tests that have been conducted in a standardized dry environment for wood with a moisture content of 12% [6]. Since timber foundations have a much higher moisture content, the mechanical properties should be determined specifically for wet wood to make them applicable for a research on timber foundation piles. The standard is not really useful for this thesis and therefore it is needed to look at what is available in literature.

In the past there have been two prominent studies on the wet compressive strength of round timber. The first study dates back to 1994, it was performed by J.W.G. van de Kuilen and it covered a total of 93 samples from spruce, douglas fir and larch trees with a mean moisture content of 100% [7]. The second study originates from 2016, it was carried out by S. Aiker and G. Stapf on a total of 17 spruce specimens with a mean moisture content of 89% [8]. Both studies provide useful values for the wet mechanical properties of roundwood just like timber foundation piles. Having said that, the results are not specifically suitable for the evaluation of aged timber piles because they do not include the effects of biological degradation.

A study into the wet mechanical properties of aged timber piles has been initiated by the Delft University of Technology in 2020 and is still ongoing at the time this thesis was written [9]. The study is executed by researchers of the department Biobased Structures and Materials to gain more insight into degradation mechanisms, defects such as knots and their effect on the wet properties. Timber piles that have been in service since 1922, 1886 and 1727 were extracted from bridges in the city of Amsterdam and numerous experiments were performed including computer tomography (CT) scans, micro-drilling and compression tests.

The researchers from TU Delft have already achieved promising results that are in particular of interest for this thesis project. Especially the findings from the large-scale compression tests on segments from the aged timber foundation piles are meaningful. These tests have been performed by G. Pagella on more than 200 wet spruce and fir segments with a length of approximately six times the smallest diameter [10]. The tested segments contained different levels of degradation which makes it possible to map out the wet mechanical properties of aged timber foundation piles. From these tests it occurred that that in more than 70% of the cases the pile segments failed in compression at the section with the highest amount and/or bigger sizes of knots [11]. The sections with knots are considered critical weak spots which, in combination with the decay, appear to be decisive for the wet compressive strength and the load-bearing capacity of aged timber piles.

In addition, a total of 6 small-scale compression tests have been conducted on discs with a height of about 100 millimeters [12]. The discs were taken from some of the same segments as the large-scale compression tests which makes it possible to directly compare the results. It turned out that the resistance of a disc with knots is similar to the resistance of a segment with the same knots. While this similarity is an encouraging development, it is important to note that it has been demonstrated so far through the results of only a few tests. Also, these tests only involved new piles without degradation and it is still unknown if this trend also holds for aged timber piles.

1.2 Research questions and scope

This thesis project is created to investigate whether performing small-scale compression tests on discs from aged timber piles can give representative values for their wet mechanical properties. The small-scale testing could provide an alternative to the conventional large-scale testing, saving both time and resources. This study can also contribute to a better understanding of the different defects and degradation mechanisms that affect the wet mechanical properties. The broad objective is to help improve and facilitate future research into aged timber foundations.

The main research question can be formulated as follows:
How can the wet mechanical properties of a degraded spruce timber pile be determined through small-scale mechanical tests on discs sawn from the pile?

In order to break down the main research question, several sub-questions are formulated:

- *How does the wood structure change over the length of the tapered pile and how does this impact the mechanical properties of the pile?*
- *In which ways do the knots influence the compressive strength of the large-scale segments and the small-scale discs taken from the pile?*
- *How is it possible to quantify the amount of degradation by performing non-destructive micro-drill tests on the pile?*
- *To what extent is there a relation between the resistance from the micro-drill tests and the mechanical properties of the pile?*
- *How do the physical and mechanical properties of the small-scale discs relate to the properties of the whole pile?*
- *What is the correlation between the results of the compression tests of the large-scale segments and the small-scale discs?*

A total of 45 discs with varying amounts of degradation are selected for this study. They are taken from 6 different spruce (picea abies) timber foundation piles that originate from the building years 2019, 1922, 1886 and 1727. The piles were retrieved from 2 historical bridges in the Dutch city of Amsterdam. They were installed below the water level so the cause of the degradation is believed to be from bacterial decay only.

For about half of the discs it is decided to capture only clear wood sections without any knots. Whereas for the other discs it was chosen to confine the sections with the bigger knots to isolate the weak spots of the pile. As a consequence, it is possible to examine the effect of a high knot content and compare it directly to the sections without knots.

The discs are sawn with a height of 150 millimeters and they are tested in compression with an axial load parallel to the fibre direction in a displacement controlled set-up. The mechanical properties that are considered are in particular the short-term wet compressive strength and the wet static modulus of elasticity.

The discs are taken from different locations on the pile in order to examine the distribution of the properties over the length of the pile. Also, the discs are sawn from segments that have previously been subjected to large-scale compression testing. This makes it possible to use the results from the large-scale tests of the segments to validate the results from the small-scale tests of the discs.

1.3 Outline

In Chapter 2 there is an elaborate literature review which covers all the aspects of timber foundation piles. It starts with the basics and gives a brief explanation of some practicalities of timber foundations and the way their trees are cultivated. Then it goes into more depth about the wood structure, defects, physical properties, mechanical properties, degradation mechanisms and methods to examine the decay. The last part is dedicated to the recent and relevant research that has been performed by the Delft University of Technology on timber foundation piles.

Chapter 3 contains information about the materials, specifically the spruce discs, that are selected to be tested during this study. It presents important background details about the discs and the piles from which they were sawn. This chapter goes through the origin of the piles, the way the piles are subdivided into segments and discs, the sample size of the discs for the upcoming tests and all relevant data of the selected segments from the previous large-scale compression tests.

The methodology is covered in chapter 4 and all steps are worked out in chronological order. It describes how the discs are sawn, the storing and handling of the discs, the integrity tests with the micro-drill and the piercer tool, the compression tests with the sensor locations and the oven-drying process to get rid of all bound water. The different tests do provide essential values such as the density, moisture content, level of decay, compressive strength and modulus of elasticity. The details of how these values are computed with corresponding formulas are outlined at each step.

Chapter 5 gives all the results from the tests that are performed on the discs. This chapter begins with an explanation about the assumptions that are made during the testing and the processing of the results. Next, the results are presented in tables and some overall relations are highlighted in graphs. Several values are checked to see if they are in line with the expectations and to review if they were computed correctly.

In chapter 6 there is the analysis, in particular about the examined wet compressive strength and the wet modulus of elasticity of the discs. First the relationship between the strength and the degradation is considered. After that, the presence of the knots and its effect on the strength is discussed. Lastly the differing values and irregularities regarding the computed values for the elasticity of the discs are explained.

Finally, chapter 7 contains the conclusions by summarizing the key findings of the research. This provides an answer to the main research question. A close discussions of the results regarding the defects and degradation is conducted to point out any limitations.

The appendices form a comprehensive collection of all the data of the individual tests that are performed. This is a separate document because it consists of too many pages, making it insufficient to add directly to this thesis. The appendices can be provided to interested parties upon request.

2. Preliminary research

Thorough research to gain more knowledge about timber foundation piles.

2.1 Timber piles

Background information about timber piles.

2.1.1 What are timber piles

Timber refers to wood that has been specifically processed and manufactured to be used as structural element. Hereby the shape and dimensions of the wood are engineered in such a way to fulfil a structural purpose for buildings and constructions. Timber foundation piles are generally made from the tree trunks of grown conifer trees. The tree species spruce, pine and fir are most commonly used for the production of timber piles in the Netherlands [1]. The main steps that need to be taken to convert a tree trunk into a timber pile are essentially felling of the tree, sawing off the branches and stripping the bark. So, once a tree trunk has been processed and shaped to be used as a foundation pile, it is referred to as a timber foundation pile.

The growth process of the tree is eventually decisive for the structure of the timber pile, that is why it is important to understand the anatomy and composition of the tree. A tree can generally be divided in two fragments, the overhead part which consists of the trunk that supports the crown and the subterranean part which consists of the root system. The crown is the top part of the tree where the branches and the foliage emerge from the trunk. The tree is covered with scaly bark and the branches are arranged in a whorl around the trunk. The trunk has the shape of a tapered cylinder, the sectional area at the top of the trunk is smaller than the sectional area at the base of the tree as shown in Figure 2.1.

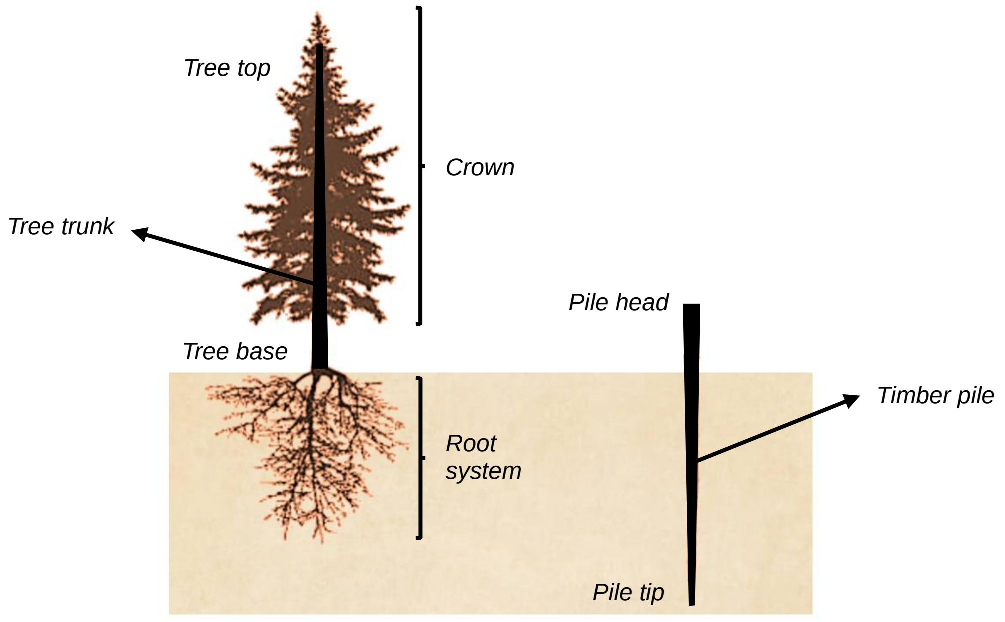

Figure 2.1: Schematic representation of a conifer tree and a timber pile

After the timber pile is installed, its orientation is upside-down in comparison with the natural orientation of the tree trunk. The top of the trunk will become the pile tip and the base of the trunk will be the pile head.

2.1.2 Brief history of timber piles

After the Middle Ages, stone was increasingly used as a construction material for houses to prevent the expansion of a possible city fire. Foundation piles were needed in the Western parts of the Netherlands because the weak peat soil is unable to support the heavy stone structures [13]. Long timber piles were used to transfer the loads from the ground level to the deeper load-bearing sand layer. The depth of the load-bearing sand layer is different for each location, in Amsterdam timber piles with a length of 10 to 12 meters were used [1]. Nowadays it is customary to use longer piles of approximately 22 meters to reach the second sand layer [13]. A schematic representation of old and new pile foundations is in Figure 2.2.

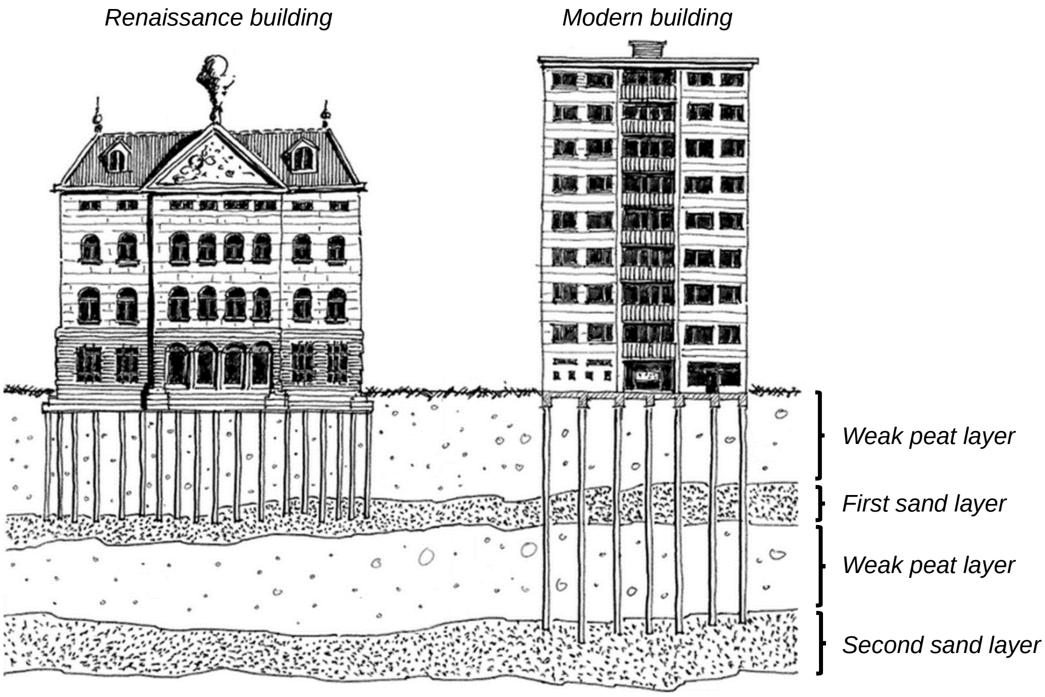

Figure 2.2: Examples of pile foundations throughout the years [13]

During the beginning of the 16th century there was a need for coniferous wood in the Dutch ship building industry because the coniferous tree species are lighter in comparison with deciduous tree species. In addition, certain conifer species are known for their long stems, relative straightness and fast growing speed. The conifer trunks were also used for the production of timber piles because of their availability, shape and cheap price [14]. The wood was imported from Scandinavia, Poland, Germany and Belgium. Often pine was used for short piles and spruce or fir was used for longer piles. For example, the Royal Palace on the Amsterdam Dam square was built in 1640 with 14,000 spruce piles of 11 meters imported from the southern part of Sweden. [1]

Most of the old pile foundations were designed based on trial-and-error, experience and accustomed building methods [15]. There was no implementation of design codes and standards which makes it hard to retrace the building steps. The piles were driven manually, often using manpower or horses to repeatedly lift a heavy block and let it fall on the pile head. It was assumed that the load-bearing layer was reached when the pile encountered significant resistance [13]. The pile driving was stopped and the excrescent part was sawn off. In general, there is no certainty that the pile is in the right position and that the pile tip has sufficient load-bearing capacity.

There can be a great variety of mechanical and physical properties for the different timber elements. Visual grading is a method that has been used since ancient times to differentiate the optic macroscopic characteristics of timber. Currently all rules regarding the visual grading and quality of timber piles are laid down in standard EN 1995-1-1 [6]. Here attention is paid to the presence of irregularities, damage and deterioration which can affect the strength and stiffness of the wood. For instance, wood with macroscopic defects such as forked growth, crooked stems and spiral grain are rejected for the use as timber piles because of their inferior quality.

The use of concrete foundation piles has become customary for the building industry since the 1950s. Concrete piles are favoured over timber piles because of their long life span and dimensional flexibility. Timber piles are still used in niche markets like sewerage systems, small buildings, greenhouses and renovation projects. Still up to 200.000 timber piles are installed every year in the Netherlands [1]. New timber foundation piles that are installed must comply with current regulations. The guidelines for the design and the quality of timber piles from European coniferous wood is described in standard NEN 5491. This standard describes the use of the tree species spruce, larch and douglas fir.

2.1.3 Felling and forestry

The way the trees grow mainly depends on the space and distance between the trees. If a tree has more space, it will grow wider and not as tall as a tree that has less space around it. The trees that are used to make timber foundation piles are often deliberately planted and actively managed after which they are harvested. [16]

Nowadays the trees are felled using mechanical harvesters and, to a lesser extent, using ground crews with chain saws. The harvesters are equipped with an extensible boom that has a felling head consisting of a chain saw, feed rollers, delimbing knives and sensors. Each tree is selected by the operator, it is grabbed with the felling head near the tree base and cut down using the chain saw. The thicker part at the bottom part of the tree, at the transition between the trunk and the roots, is cut off. Also, the top of the tree is removed and all the scrap wood can be used to make particleboards. Then the trunk moves through the feed rollers and all branches are automatically removed by the delimbing knives. The sensors in the felling head measures the diameter and the length of the tree trunk. At this point the operator decides whether the tree trunk is good enough to be made into a timber pile or whether it will be cut into smaller pieces for other applications.

Tree farm *Tree harvester* *Timber piles*

Figure 2.3: Process of harvesting trees at a pine tree farm in the Netherlands

Each tree has a maximum life of about 100 years old, after this point the tree grows very slowly and it is no longer profitable to leave the tree for the production of wood. However, most trees are felled earlier after approximately 50 years when they have the right size to be made into a timber pile. It is desirable to have timber piles with a uniform shape and size. The preferred length is roughly 15 meters with a pile head diameter of about 20 centimeters and a pile tip diameter of approximately 13 or 14 centimeters. [16]

There are some differences in the way the forests are managed depending on the location and country where the trees are grown. For example, Germany has quite a lot of forests for the production of timber and they manage the forests with the creed “früh, oft und mäßig” which literally translates to “early, often and moderately”. It means that they go and harvest the trees when they are relatively young, they do it often and take only a little at a time. This way only the big trees are felled, the smaller trees have more space to grow and at the same time saplings are planted at the open spaces to ensure the next harvest.

On the other hand, the forestry in the Netherlands is done on a much smaller scale. Most of the forest are reserved for the conservation of nature only and may not be used for the production of wood. If a plot of land is used for the production of timber, it is done quite exhaustive and unconstrained in comparison to Germany. Most of the Dutch trees are left standing for too long and most are felled all at once. [16]

The result between the different management styles is a difference in quality and size. Generally, the German piles are considered to be of superior quality in comparison to the Dutch piles. The Dutch timber piles are generally less straight and have a smaller pile tip. Also, the Dutch timber piles have a tapering of about 1.0 centimeters per meter and the German timber piles have a tapering of approximately 0.7 or 0.8 centimeters per meter. [16]

2.1.4 Complexity of foundation problems

This section covers some of the possible issues regarding aged timber foundations to give an impression of how complicated these issues can be. Most of these statements come from personal experiences by working on the designs for the strengthening of degraded timber foundations for residential buildings.

Degradation mechanisms can occur that have a negative effect on the condition of the timber elements which can lead to foundation issues. Each pile foundation is different which asks for a case-by-case investigation analysis to identify its condition. The investigation can be challenging, especially when there is limited accessibility to inspect the foundation. Also, there is generally insufficient documentation present in the archives and the lack of information is a typical problem.

There are many different causes for foundation issues and several degradation mechanisms can occur at the same time. Alterations in the surroundings can trigger the degradation to start or accelerate. For example, a common and ongoing problem is that the soil can dry out during the summer whichever can lead to three possible issues. First, the dehydrated ground can cause the subsoil to subside which results in settlements. Second, it may happen that the subsoil shrinks and causes a negative skin friction along the foundation pile which causes an extra load on the pile. And lastly, a lower groundwater level can result in the fungal decay of timber elements when they get exposed to oxygen.

An other known problem is that the vehicles we use have become increasingly heavier in the past century which means that the foundation piles of historic bridges and old quay walls have to carry bigger loads. Or another example, when new foundation piles cause stressed zones in the subsoil which result in extra loads for the existing piles. The way that existing structures are loaded has changed over the years which makes it hard to deduce the time dependent behaviour of the timber elements, like creep and load-duration effect.

A deteriorating foundation can result in misalignments and a skewed position of the structure above. It is important to recognize foundation issues in time and react accordingly to conserve the structural integrity of the building. A construction is often monitored for a long time in order to map out the development of damage patterns and settlement behaviour.

It may be necessary to take action if the state of the timber foundation elements are found to be in bad shape. Additionally, the condition of the superstructure can be decisive in determining whether measures are needed. For instance, according to a study done by Deltares in 2009 [17], measures are needed if the skewness of a masonry building in vertical direction becomes greater than 1:67. In that case tensile forces can occur in the masonry due to the self-weight and eccentricity of the heavy brickwork. Stabilisation of the foundation is deemed necessary to prevent cracks and a permanent loss of cohesion. The strengthening of the foundation consists of installing complicated and expensive tailor-made adjustments to the construction.

Note that it is not always necessary to take action when irregularities are observed. For example, if a timber pile is tested in the lab and it is considered to have insufficient strength, then this does not necessarily mean that the foundation is failing because there may be some structural redundancy. Also, the occurrence of settlements does not indicate that measures are required, especially when it is sinking uniformly and the superstructure is not affected.

In practice it would be desirable to know the exact residual life of a timber foundation so it is possible to arrange the logistical and financial resources when necessary. However, it remains challenging to make a good estimate of the condition of timber foundations because of the many different aspects and elements, with each their own limitations and interactions, and more research is needed to make the investigations easier in the future.

2.2 Wood structure

Structure and characteristics of wood.

2.2.1 Macrostructure

Wood is a natural product from a multicellular photosynthesizing organism and it is a inhomogeneous material. The tree trunk can grow in height but also in radial direction. A distinction is made between different kinds of wood structures inside the trunk which are formed in different stages of the tree's life. The different wood structures are visible in the cross-sectional surface of a tree trunk as shown in Figure 2.4.

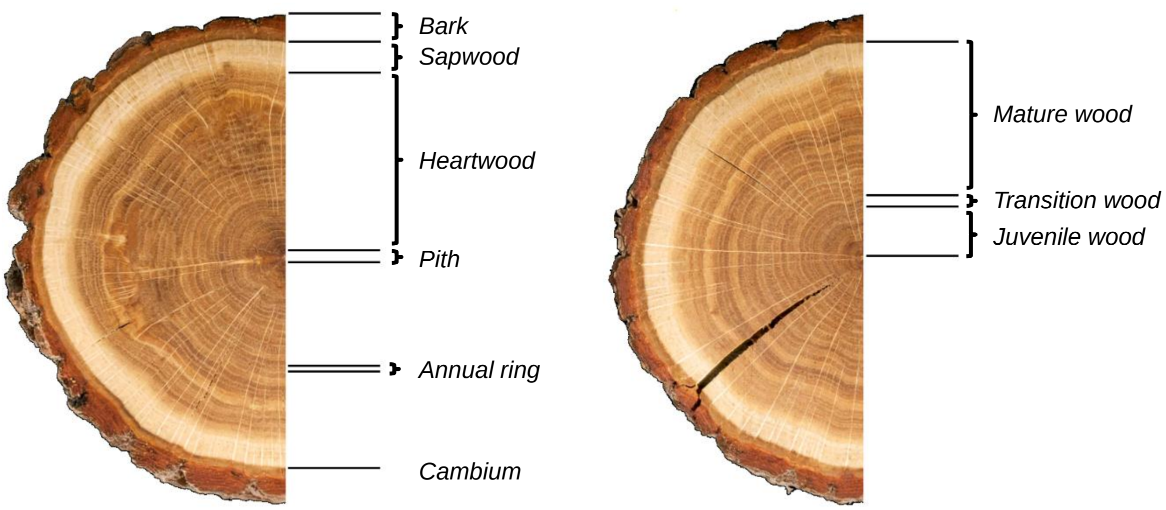

Figure 2.4: Cross-sectional surface of a tree trunk

The bark is the scaly brown exterior of the trunk. A distinction is made between the outer bark and the inner bark. The outer bark consists of deceased cells and it protects the tree against insects, extreme temperatures and damage. The inner bark is comprised of living cells and it functions as a transport of nutrients from the crown to the cambium layer. The cambium layer is not visible to the naked eye and it is positioned between the bark and the sapwood. This is the layer where the cell divisions occur which causes the tree to grow in radial direction. The cells that are formed inward are a part of the sapwood and the cells that are formed outward are a part of the bark. [3]

Sapwood has living cells which store nutrients and conduct water from the root system to the crown. The sapwood cells are connected with adjacent cells by pits so that nutrients can be exchanged. Only the younger external part of the trunk consists of sapwood. The older and inner part of the tree consists of dead heartwood cells which provide strength and stability. The transition of living sapwood cells into heartwood cells is known as the heartwood formation. Heartwood formation is a biochemical process whereby the cells perish, starch is consumed and constituents are stored. The pits in the sapwood close off during heartwood formation. [3]

The sapwood and heartwood have capillary pores which can hold and transport water. The porosity is somewhere between 50% to 70% depending on the density of the wood and the tree species. The center of the trunk is called the pith, which should not be confused with the aforementioned pits. The pith is only a couple of millimeters wide and it consists of deceased cells which are a remnant of when the tree was still a young scion. [3]

Rays are small openings which run in radial direction from the center of the cross-section towards the outside. The rays enable the transport of nutrients and water in radial direction. All trees have rays but the size and amount of rays can vary depending on the tree species. The rays can be visible in a cross-section as thin lines with a thickness smaller than 1 millimeter.

The sectional surface of the tree increases each year over the width of a growth ring, also known as an annual ring. The width of the growth ring depends on the weather conditions, the ring will be narrower in a dry year than in a year with a lot of rain. A growth ring consists of earlywood and latewood. A tree’s age and history can be deduced from the amount and width of its growth rings.

Trees subjected to seasonal changes will have different needs throughout the year, depending on the temperature and weather conditions. At the beginning of the year, during springtime, there is a need for fresh water and nutrients in the crown. The cambium layer will form earlywood. Earlywood has a large pore volume and thin cell walls so they can transport water better. At the end of the year, during the fall, the need for water is lower. The cambium layer will form latewood. Latewood has small cell cavities and thick cell walls to strengthen the tree. The earlywood is often lighter in colour than the more dense latewood and therefore growth rings can be distinguished at the cross-section of a tree. [3]

Besides seasonal changes, there are also differences in wood structure noticeable depending on the age of the tree. Juvenile wood is formed during the first years and mature wood is produced during later years. The wood between juvenile and mature is called transition wood. Juvenile trees tend to grow more rapidly in the spring and they experience less competition from surrounding trees. That is why juvenile wood has much wider earlywood and thus also a wider growth ring. The mature wood has longer cells and the mature latewood has generally thicker cell walls. That is why mature wood has a higher density in comparison with the juvenile wood. The difference between juvenile wood and mature wood can particularly be observed in conifer species as presented in Figure 2.5. [18]

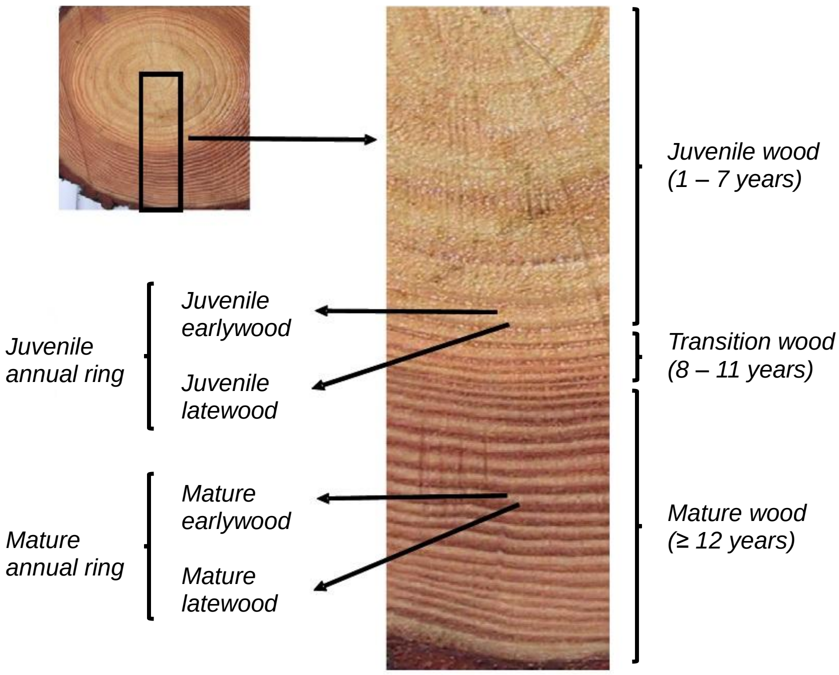

Figure 2.5: Cross-section of a 30 year old radiata pine tree [18]

2.2.2 Microstructure

Different tree species can be divided in two groups, namely softwood species and hardwood species, which are distinguished based on their microscopic structures.

A conifer tree has a softwood microstructure, see Figure 2.6.

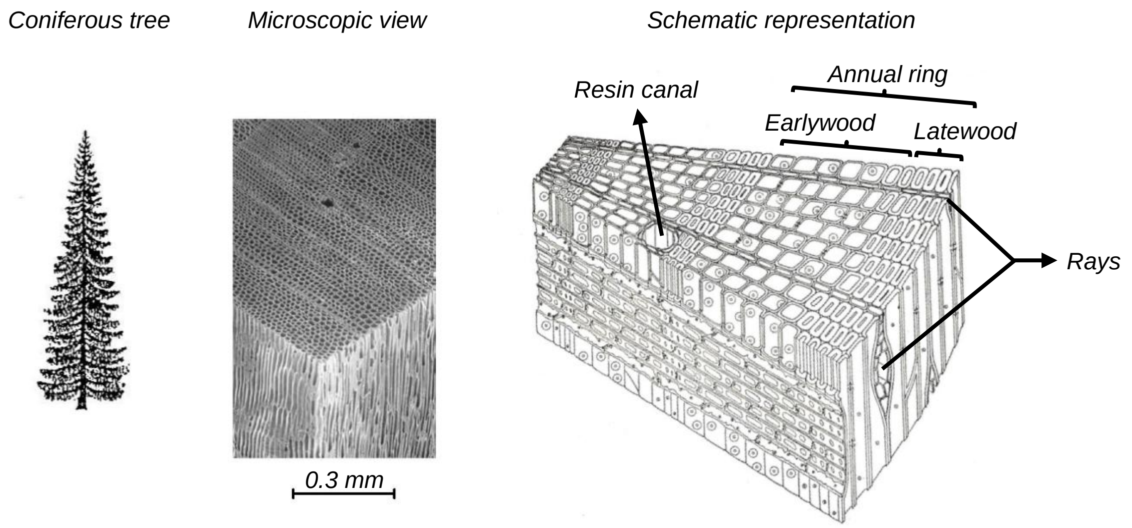

Figure 2.6: A typical coniferous tree and the microscopical structure of softwood [3]

Softwood is comprised of tracheid cells and parenchyma cells. The tracheids are long cells and are mostly orientated in longitudinal direction along the trunk. The cells are often compared with fibres because of their stringlike shape and longitudinal orientation. Tracheid cells provide strength and water transport. The parenchyma cells are located at the rays and resin canals. Rays and resin canals are small and have a single row of parenchyma cells [3]. The resin can seal any wounds and prevent the draining of internal fluids. Examples of softwood species are fir, spruce, cedar, pine and larch.

A deciduous tree has a hardwood microstructure, see Figure 2.7.

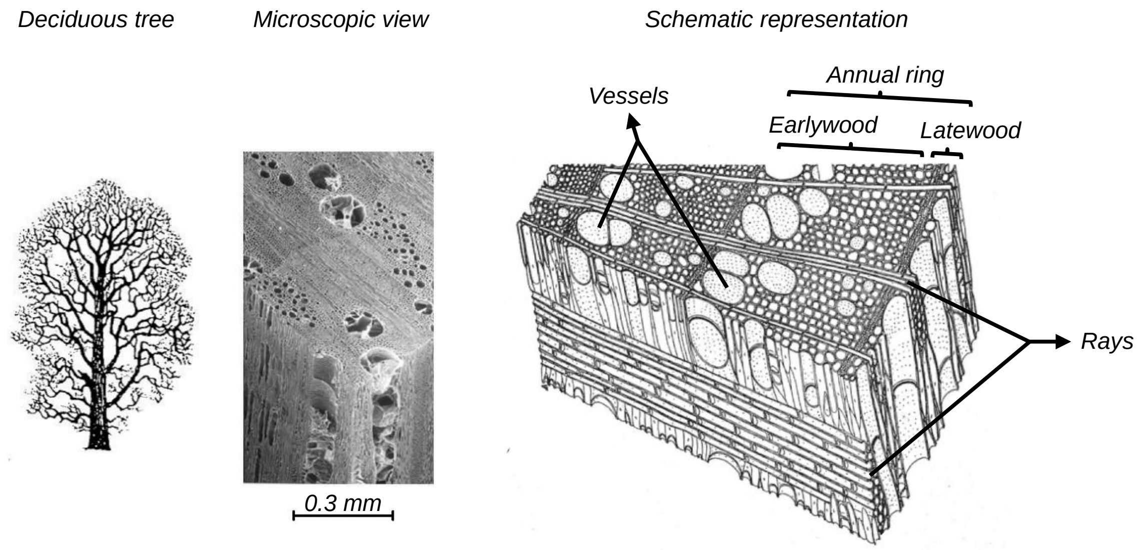

Figure 2.7: A typical deciduous tree and the microscopical structure of hardwood [3]

Hardwood is more evolved than softwood and consists of considerably more specialised cells. There are libriform fibres which only provide strength and tracheid cells which contribute to the strength and water transport. The hardwood has no resin canals, instead there are vessels comprised of dead cells and their function is to hold water. The rays in hardwood are bigger and more clearly visible because they have multiple rows of parenchyma cells [3]. Examples of hardwood species are beech, oak, teak, birch and elm.

The chemical composition of wood can be seen as natural polymer composites made of mainly carbon. Wood contains 40%-47% cellulose which are organic polymers from glucose and provide tensile strength. Also 25%-35% hemicellulose, which are organic polymers from mannose or xylose, and 16%-31% lignin are in the wood and contribute to the stiffness and the compressive strength of the timber. The amounts are different depending on the tree species and the type of wood structure. [19]

2.2.3 Local defects

Local disruptions of the wood structure can have a negative impact on the resistance of the timber pile. The defects are caused by the growth process of the tree and events during the life of the tree. Common local defects are knots, reaction wood and cracks. Note that the defects are elaborated in the standards NEN 5461 and NEN-EN 1310.

A knot is a remnant of a branch that is contained in the wood structure of the trunk. Knots are visible as dark brown areas and the wood is substantially more hard, dense and brittle than the regular wood. The branches grow radially out of the trunk and the branch fibres run in the same direction as the branch. The longitudinal fibres in the trunk are locally disrupted at the location of the knot because the fibres have to run around the knot. A lengthwise cut gives the knot a spiked shape and a crosswise cut result in a circular shape.

There are two types of knots: intergrown knots and encased knots, see Figure 2.8. A knot is encased when the wood of the trunk and the wood of the branch are not continuous. It occurs when the trunk produces growth rings while the branch is deceased. The growth rings of the trunk are formed without continuing along the branch. A knot is intergrown when the wood of the trunk and the wood of the branch are continuous. The continuity is created when the branch is alive and the growth ring of the trunk is uninterrupted with the growth ring of the branch. Note that every knot starts as an intergrown knot and can only become encased after the branch has died. The wood structure is more disturbed with knots that are intergrown because the angle of the grain around the knot locally deviates more. [2]

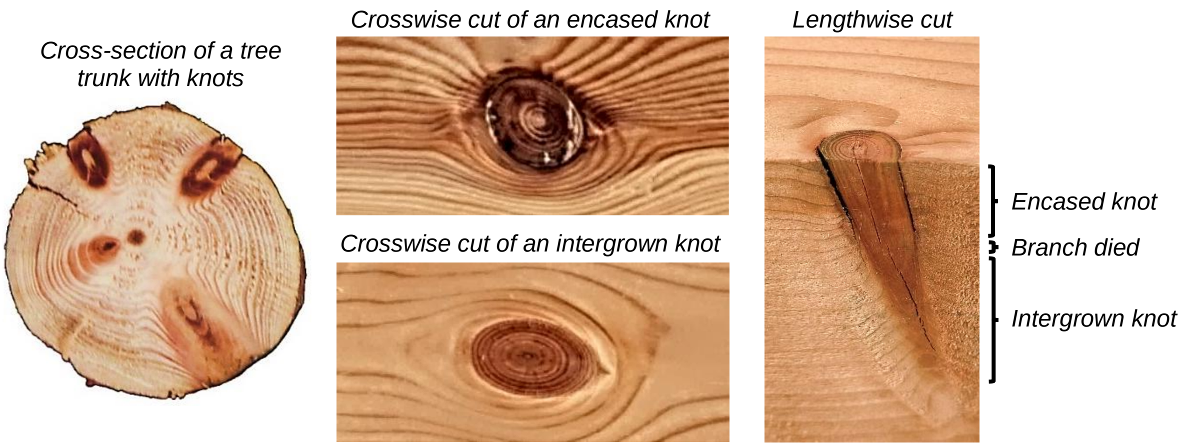

Figure 2.8: Different types of knots

Reaction wood can be formed in the trunk or branches of the tree to bring these segments in a certain position. Any limb with a deflection of more than one or two degrees from vertical orientation produces reaction wood. When, for example, a tree grows on a slope or it is slanted due to wind pressure, the trunk will form reaction wood to keep its vertical orientation. Reaction wood is the reason why all non-vertical branches can maintain their position. [2] The formation of reaction wood can cause differences in densities throughout tree. In some cases it results in uneven thicknesses of the growth rings, an eccentric pith and an oval cross-section.

Softwood trees and hardwood trees have a different type of reaction wood, see Figure 2.9. A softwood tree produces compression wood on the underside of the sloping limb and a hardwood tree produces tension wood on the topside of the sloping limb. The compression wood has an increased amount of lignin which gives it its higher density, hardness and brittleness. The tension wood has a reduction in lignin and more cellulose in the cell walls which provide a higher tensile resistance. [3]

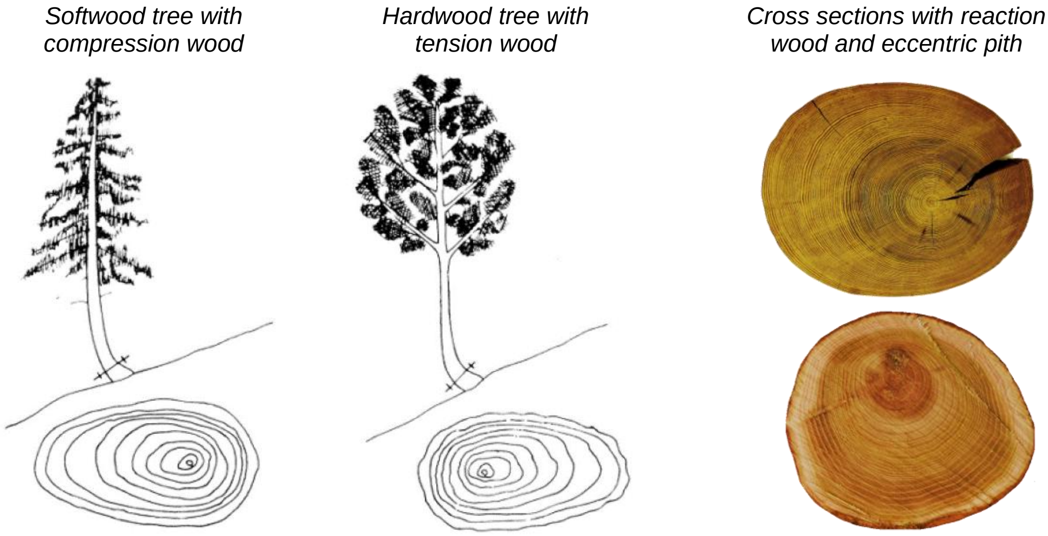

Figure 2.9: Cross-sections with reaction wood [3]

Reaction wood is only formed on one side of the stem and it is often considered to be disadvantageous due to its uneven distribution in the tree. A piece of timber can warp because the reaction wood is more prone to axial shrinkage and swellage than normal wood. Also, reaction wood is weaker than a normal wood type with a similar specific gravity. [2]

A tree can get wounds by experiencing physical damage or broken branches. The wound cannot seal itself if a part of the cambium layer dies. A callus is formed when the surrounding living cambium layer starts to grow over the wound [20]. The surrounding wood can cover the wound entirely and the scar can become invisible after a couple of years. The wood structure at the location of the overgrowth will be irregular.

Growth stresses can occur inside the stem due to the ageing process in combination with bending stresses caused by the wind and the self-weight of the tree. In general, the newly formed sapwood develops tensile stresses in longitudinal direction and the heartwood near the pith experiences compressive stresses in longitudinal direction. The growth stresses increase as the tree gets older and the diameter of the stem expands. [3]

Cracks can develop throughout the life of the tree due to internal stresses and external loads. Large cracks are generally caused by excessive loads and are often easy to spot, especially if the fibres are broken. There may also be smaller cracks between the fibres of the wood without tearing them. This type of crack is known as a shake, which is characterized by a separation of fibres along the grain of the timber structure. Shakes often occur after a section is cut because then the fibres are locally discontinued and the wood structure experiences some relieve from the internal stresses.

A shake can develop in different locations depending on the circumstances, see Figure 2.10. Cup shakes form between the growth rings due to extreme bending caused by storms and lateral loads. Ring shakes are comparable with cup shakes but in this case the growth ring is completely separated. Heart shakes develop at the pith and spread along the rays due to the maturing of the wood and the shrinkage of the pith. Star shakes are wide open cracks at the outside of the wood due to severe heat or frost. [20]

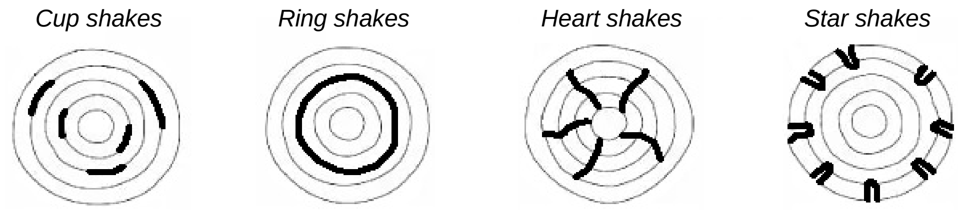

Figure 2.10: Different kinds of shakes in a tree cross-section [20]

Radial shakes can form radially from the bark to the pith due to seasoning of the wood and exposure to sunlight. They look similar to star shakes but expand further into the wood structure. The radial shakes can be small and develop in an irregular pattern along the rays and growth rings. A bigger radial shake can form a significant separation of the fibres and leave a void in the wood structure.

2.2.4 Irregularities along the height

The tapering and curvature of the trunk are influenced by the height of the tree. There are also irregularities in the wood, like the distribution of knots and the change in wood structure, which seem to have a relation with the tree height. Other deformations, such as spiral grain and forked growth, are not relevant for the investigation of timber piles because the affected trees can easily be recognized and cast out during visual grading.

A tree trunk generally has a tapered shape and a non-prismatic cross-section due to its growing process. The sectional area at the top of the tree is often smaller than the sectional area at the base of the tree. In standards it is usually assumed that a pile has the shape of a frustum of a cone, with a circular cross-section and a linear taper along the height. In reality, most assessments show that the taper is not linear and the degree of taper changes with the position along the height [2].

The degree of taper can be described by evaluating the decline in diameter over the height. A tree is considered to be tapered when the reduction in diameter is larger than 1 centimeter per meter tree height, otherwise the shape of the trunk is prismatic [3]. Another way to describe the degree of taper is by evaluating the decrease in circumference along the height. For example, a douglas-fir has an average decrease in circumference of 1.7 cm per meter, whereas a red pine has an average reduction in circumference of 2.5 cm per meter [2].

The straightness of a tree is often related to the orientation of the centroidal axis of the trunk. A non-straight tree trunk can be characterized by the dimensional properties sweep and crook. The sweep of a tree is associated with the gradual change of the centroidal axis, so the amount of curvature or bow in the trunk. A crook is a sudden change of the centroidal axis, often resulting in a bended trunk. Trees with large curvatures and big crooks are unwanted for the production of timber piles. A general trick that is used in practice consist of imagining a straight line from the center of the bottom section towards the center of the top section. A non-straight pile is considered suitable for the use as a foundation pile if the straight line remains completely within the body of the pile. [21]

Certain coniferous trees such as pine, fir and spruce have a branch formation where the branches are positioned in a whorl around the trunk. The vertical branch distribution is characterized by the presence of several clusters of branches on certain heights and longitudinal branch-free segments in between, see Figure 2.11. A segment with branches is called a whorl or a growth unit and a branch-free segment is known as an interwhorl. In general, the tree will develop one growth unit each year depending on the weather conditions. The lower branches die off as the tree gets higher and these knots are eventually grown over and covered by the wood of the trunk. [22]

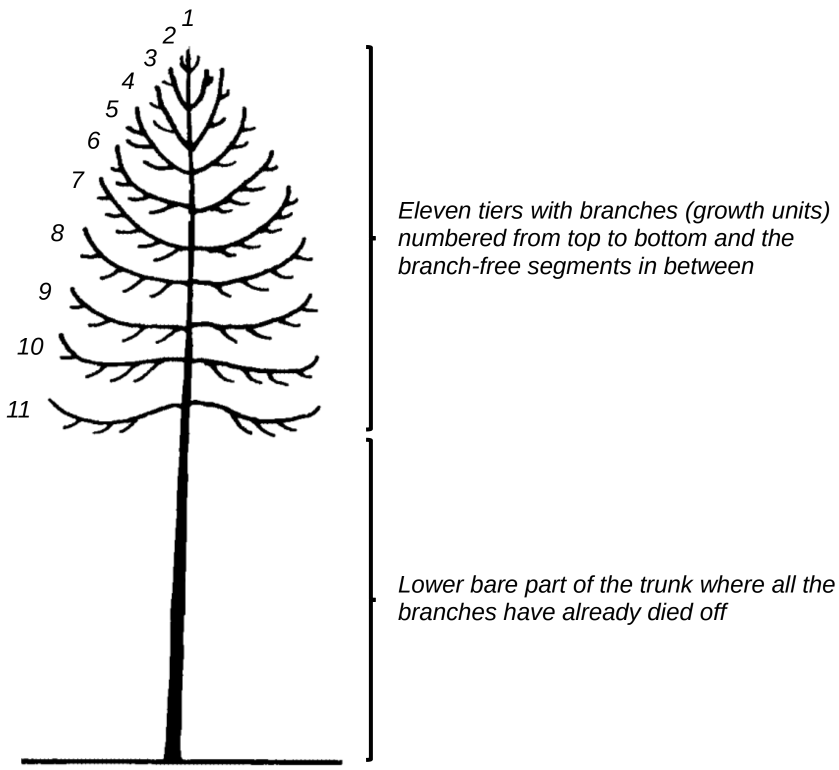

Figure 2.11: Growth units and branch-free segments of a 17 year old pine tree [22]

At the levels where the branches are located are clusters of knots in the wood structure of the trunk. Locally, these segments have a lot of disruptions in the main longitudinal fibre direction of the trunk. Often it turns out that the segment with a cluster of knots has a significant lower compressive resistance in comparison to the branch-free segments right next to it. Thus, if a timber pile made from a coniferous tree fails in compression, it is generally because of a failure at the section where the knots are clustered in the wood structure.

The amounts of sapwood, heartwood, juvenile wood and mature wood in the trunk depend on the height of the tree, see Figure 2.12. The triangles represent the tapered shape of a longitudinal section of the tree trunk and the shaded zones represent the different wood structures. Sapwood is positioned on the external part of the trunk and the linear change of heartwood over the height is a result of the conical shape of the trunk. The juvenile wood is present over the first few growth rings in the wood structure and the conical shape of the trunk causes a varying distribution of mature wood on the outside of the trunk.

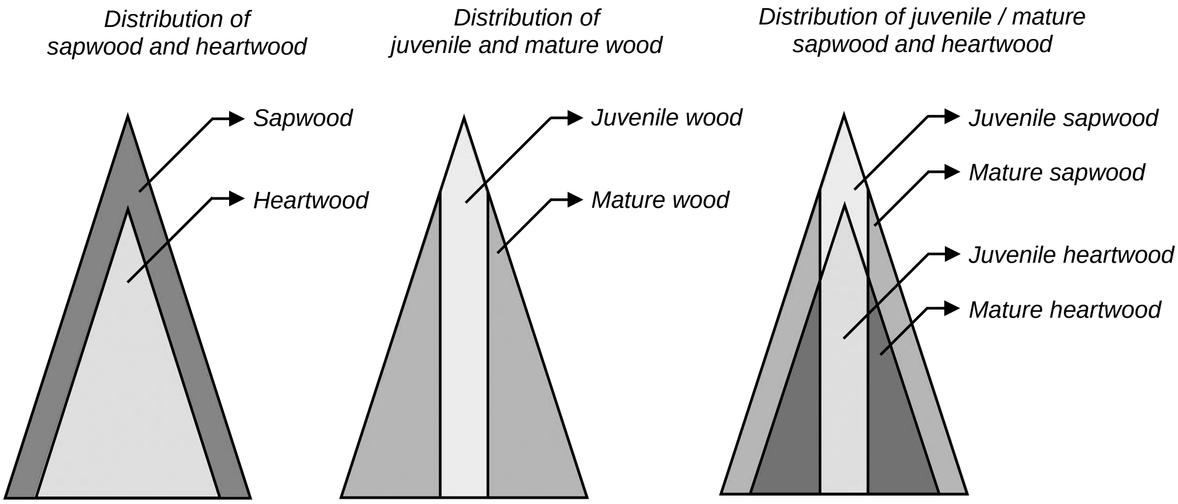

Figure 2.12: Vertical distribution of wood structures in the tree trunk [23]

The indicated zones with the different wood structures do not all extend toward the top of the triangle due to the tapered representation of the trunk. The transition between the juvenile wood and the mature wood is in reality a gradual shift instead of a hard boundary. Also, the dividing lines are shown as linear, but in reality this is not the case due to the deviating shape of the trunk. [23]

2.3 Wood properties

Features and properties of timber piles.

2.3.1 Visible features

Among the visible features, a distinction is made between the characterisation of the knots and the growth rings. The size and the location of a simple knot or a knot group can be evaluated by the knot area ratio and the knot ratio. The aim is to get an unambiguous value so the timber can be classified on the basis of knot-dependent wood properties.

The knot area ratio is widely used in practice as a part of the visual grading process of timber boards. According to the German standard DIN 4074-5, the knot area ratio can be calculated by taking the cumulative area of the knots projected on the cross-section and divide it by the total cross-sectional area. The knot area ratio is used in combination with the slope of the grain to allocate the timber to a structural grade.

The knot ratio for boards is used to determine whether a timber element complies with certain quality requirements so that it can be used for structural applications. According to the Dutch standard NEN 5493, the knot ratio for boards can be calculated by dividing the sum of the knot diameters with the width of the board. There are limit values in the standard for the maximum allowed knot ratio for boards made from (sub)tropical hardwood and European hardwood.

The knot ratio for round wood can be derived from the knot area ratio for round wood, under the assumption that the cross-section is perfectly circular with a centered pith and all the projected knot areas are the shape of an isosceles triangle which originate from the pith. The small-angle approximation is used so the projected knot area can easily be related to the knot surface width. After applying these assumptions and simplifying the formula, it is possible to calculate the knot ratio for round wood by just measuring some dimensions on the exterior of the segment without having to cut the section, see Figure 2.13.

Parameters:

a	:	*Projected area of the knot*
A	:	*Cross-sectional area*
C	:	*Circumference of the section*
d	:	*Surface width of the knot*
R	:	*Radius of the section*

Cross-section round wood:

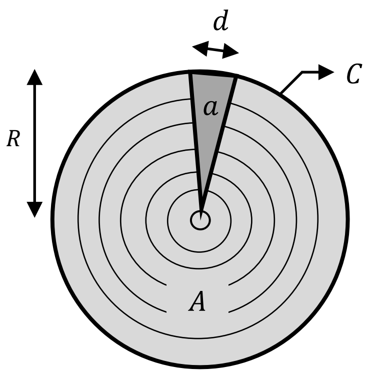

Formula knot area ratio (KAR):

$$KAR = \frac{\sum_{i=1}^{n} a_i}{A}$$

Formula knot ratio (KR):

$$KR = \frac{\sum_{i=1}^{n} d_i}{C}$$

Basic formulas:

$$a = 0.5 * R * d$$
$$A = R^2 * \pi$$
$$C = 2 * R * \pi$$

Derivation of the KR from the KAR:

$$\frac{\sum_{i=1}^{n} a_i}{A} = \frac{0.5 * R * \sum_{i=1}^{n} d_i}{R^2 * \pi}$$
$$= \frac{\sum_{i=1}^{n} d_i}{2 * R * \pi} = \frac{\sum_{i=1}^{n} d_i}{C}$$

Figure 2.13: Comparison of the knot area ratio and the knot ratio for round segments

The knot ratio for round wood is often used for the examination of timber piles and will hereinafter be referred to simply as the knot ratio.

Knot ratio is the quotient between the sum of the knot widths and the circumference:

$$KR = \frac{\sum_{i=1}^{n} d_i}{C} \qquad (2.1)$$

Where:

KR	$[-]$	:	Knot ratio
d_i	$[mm]$	:	Surface width of the knot
n	$[-]$	:	Amount of knots in one segment
C	$[mm]$	:	Circumference of the section

The standard NEN 5461 mentions that the measuring equipment must meet certain requirements. The knot dimensions should be measured using a calibrated calliper with an accuracy of at least 0.1 millimeter and the found decimal value is rounded to the nearest whole millimeter. The circumference needs to be determined on a segment without the bark by using a calibrated tape measure with an accuracy of at least 0.1 millimeter and the found value is also rounded to the nearest whole millimeter.

The surface width of each knot should be measured in perpendicular direction to the length axis of the round wood, regardless of the shape or size of the knot. Do not include the surrounding callus. Observe whether knot clusters are present and if there is an overlap make sure that the same width is not included twice. Take note of any visible covered or overgrown knots but do not include them in the calculation. Some examples of how the knot surface width can be measured are shown in Figure 2.14.

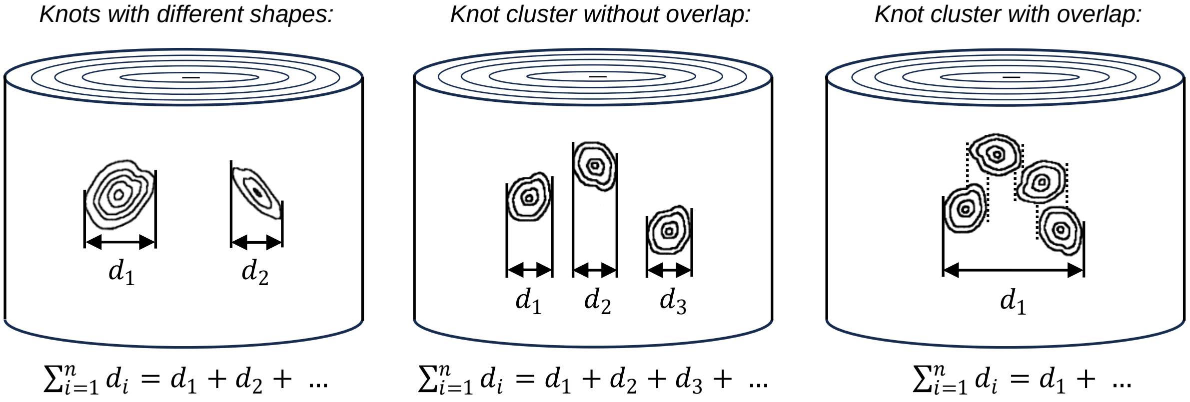

Figure 2.14: Examples of how to measure the knot surface width

All the knot widths along the outside of a segment should be added in the calculation of the knot ratio. Note that the summation of the knot surface width in the figure is not complete yet because there may be other knots present on the back side of the segment. The knot ratio is generally calculated for the section that results in the highest value.

Knots can be classified depending on their overall size. According to the standard NEN 5461, a pin knot has a diameter up to 5 millimeters, a small knot is between 5 and 20 millimeters, a medium knot has a size of 20 to 35 millimeters, a large knot measures 35 to 60 millimeters and very large knot has a diameter of at least 60 millimeters.

Growth rings are important features that provide information about the growth process of the tree and the structure of the wood. The rings are visible in the cross-section of a timber pile. In particular, the age of the tree when it was felled can be determined by counting the number of growth rings. The amount of growth rings along the radius of the section represents the tree's age in years.

The rate of growth is a measure for the extent to which the tree has increased in width during the growing process. The standard NEN-EN 1309-3 describes a way of determining the rate of growth by taking the outer 75% of the radius and dividing it by the amount of growth rings along this distance. If a long section of wood is examined then the rate of growth needs to be determined for both ends. The values from both ends need to be compared and they should both be noted in case there is a clear difference. In general, it is easier to count the rings when the wood is dry.

Rate of growth is described as the radius divided by the number of growth rings:

$$RoG = \frac{0.75 * R}{n_{gr}} \tag{2.2}$$

Where:

RoG	$[mm/year]$	:	Rate of growth
R	$[mm]$	:	Radius of the section
n_{gr}	$[years]$	:	Amount of growth rings

An example for the number of growth rings is shown in Figure 2.15.

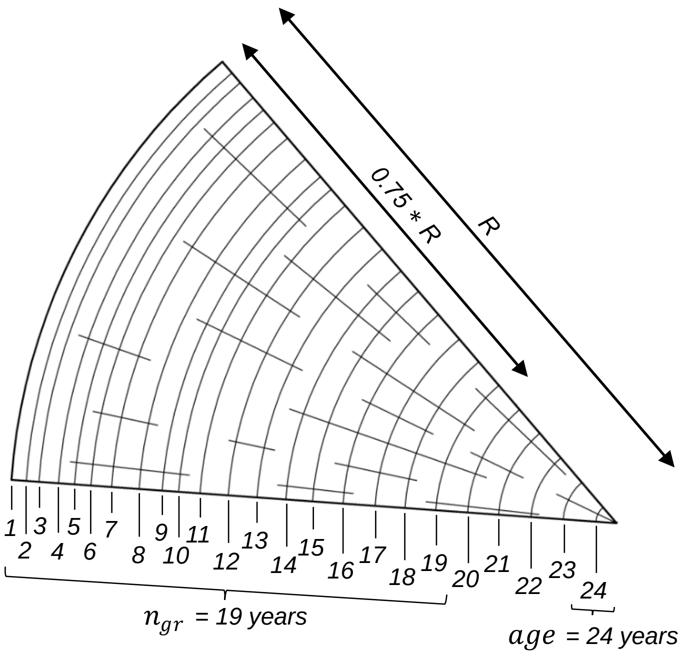

Figure 2.15: Example of determining the amount of growth rings [24]

The rate of growth of the outer 75% of the section provides insight into the development of mature wood and juvenile wood. It is also possible to apply the same calculation to the inner 25% to gain more insight in the quality of the pith. Additionally, the calculation can be made over the entire radius to quantify the growth process of the entire tree.

2.3.2 Physical properties

The most important physical properties, such as density and moisture content, are discussed and the formulas are given where necessary.

There is a difference in density throughout the section of a pile depending on the wood structure. In general, juvenile wood has a lower density than mature wood and the density becomes higher as the position of the wood increases towards the bark. A timber pile from a grown tree trunk can be divided into three zones with a variation in density, see Figure 2.16. The tapered shape of a longitudinal section of a timber pile is exaggeratedly depicted as an elongated trapezium. [23]

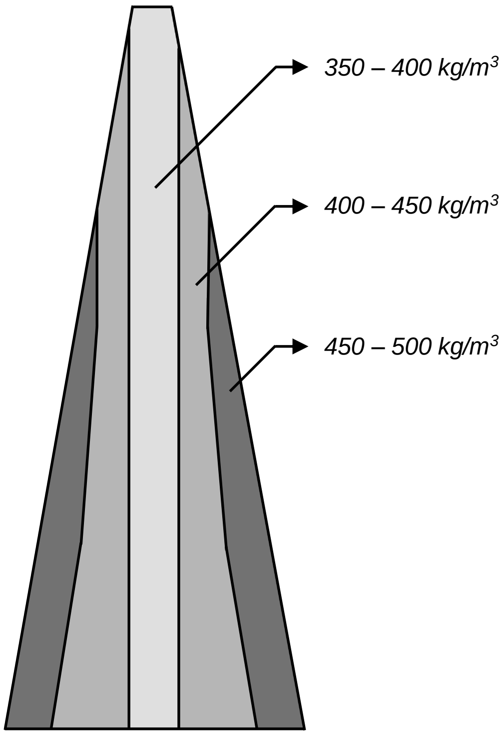

Figure 2.16: Density of an oven-dry timber pile made from a grown radiata pine tree [23]

The density of a specimen taken from a timber pile generally represents a mean value and it is obtained by measuring the total mass of the specimen and divide it by the total volume of the specimen.

Density is defined as the mass of a specimen per unit volume:

$$\rho = \frac{m}{V} \qquad (2.3)$$

Where:

ρ	$[g/mm^3]$	:	Density
m	$[g]$	:	Mass
V	$[mm^3]$	:	Volume

An electric scale can be used to determine the mass of the timber. The standard NEN 5461 states that the scale needs to be calibrated and the mass has to be measured with an accuracy of 0.1 grams.

A segment of a timber pile is approximately the shape of a cylinder and the volume can be determined by using the diameter, radius or circumference of the section. The circumference is often the easiest to measure and it is also needed for the calculation of the knot ratio.

Volume of a cylinder by using the height and circumference:

$$V = \frac{h * C^2}{4 * \pi} \quad (2.4)$$

Where:

V	$[mm^3]$	:	Volume
h	$[mm]$	:	Height of the segment
C	$[mm]$	:	Circumference of the section

It is necessary to pay attention to the amount of moisture in the wood at the time the density is taken because the mass and the volume of the wood are closely related to the humidity of the wood. Wood has a cavity system that is capable of absorbing moisture when it comes in contact with a liquid or humid air and it can release moisture when it is seasoning. A higher moisture content can results in a greater mass and an increased volume due to swelling.

A distinction is made between two types of absorbed water in the wood structure, namely the free water and the bound water. The free water is located in the capillary pores and it is the easiest to be released from the wood structure during the drying process. The bound water is harder to take out because it is positioned between the cell walls and it is connected with hydrogen bonds to the hydroxyl groups of the cellulose [3].

The moisture content represents the total amount of absorbed water in the wood structure. An easy way to determine the moisture content is by weighing the wood when it is wet and when it is dry, the method is explained in the standard NEN-EN 13183-1.

Moisture content is the ratio between the mass of absorbed water and the mass of dry wood:

$$u = \frac{m_{wet} - m_{dry}}{m_{dry}} * 100 \quad (2.5)$$

Where:

u	$[\%]$	:	Moisture content
m_{wet}	$[g]$	:	Mass of the wet wood
m_{dry}	$[g]$	:	Mass of the dry wood

In order to determine the moisture content of a piece of wood, the specimen needs to be weighed so that the current mass of the wet wood can be noted. Then the wood must be dried in an oven with an internal air circulation and a constant temperature of 103 °C (± 2). The specimen has reached the oven-dry point if the mass does not deviate more than 0.1% on two measurements, with an interval of at least 2 hours between the measurements. The mass of the oven-dry specimen can be used as the reference value in the calculation of the moisture content. If the specimen cannot be weighed immediately to record the wet or dry mass, it can be stored in a sealed container for a maximum of 2 hours so that it can still be weighed afterwards.

There are three limit values for the amount of moisture that are important for the properties of the wood. The first boundary is called the water saturation point and the wood in this state has absorbed the maximum amount of water. All pores are filled with water and the moisture content can be higher than 100% if the wood has a high porosity. When the wood is dried, the free water is the first to escape from the wood structure. The second boundary is the fibre saturation point whereby all the free water evaporated and all the bound water is still present. This point generally has a moisture content between 25% and 35% depending on the tree species. The third boundary is the oven-dry point and it is reached after all the free water and bound water is released, therefore the moisture content of an oven-dried specimen is 0%. [3]

The mechanical properties, such as strength and stiffness, usually change a lot as the amount of bound water is altered. The bound water is positioned between the cellulose and if there is a higher amount of bound water it means that the cellulose is separated, resulting in a decrease of molecular binding forces and a reduction of the mechanical properties. An alteration in the amount of free water brings about relatively little change in the mechanical properties, so most of the deviations in the mechanical properties take place between the oven-dry point and the fibre saturation point. In general, wood with a moisture content below the fibre saturation point is more stiff and brittle compared to wood with a higher moisture content. [3]

Swelling of the wood occurs when the cells move slightly apart from each other due to the infiltration of bound water between the cell walls. Shrinking occurs when the bound water is released and the cells in the wood structure come closer together. A difference in the amount of free water does not bring about much change in size because the dimensions of the pores remain the same. Most of the dimensional changes occur between the oven-dry point and the fibre saturation point. [3]

The dimensional changes of the wood due to the swelling/shrinking will differ depending on the direction of the wood fibres. Most fibres are orientated in the longitudinal direction which means that the exchange of bound water between the cell walls mainly takes place in a perpendicular direction and the dimensional changes are most pronounced in the tangential and radial direction. With the same reasoning it can be stated that the wood will experience almost no change of the length in the longitudinal direction. The swelling/shrinking in perpendicular direction of the grain is generally 10 to 20 times larger than the changes in longitudinal direction. The size of the segment determines how quickly moisture can be exchanged with the environment and affects the rate of swelling/shrinking. Other factors that influence the amount of swelling/shrinking are the wood structure, the amount of latewood and the amount of lignin. [3]

The standard EN 14544 provides a guideline for the extent to which a segment of round wood can swell/shrink. For a moisture content of 30% or less, the diameter of round wood decreases by 0.25% for every decrease in moisture content of 1.0%. It also applies the other way around so that the diameter can be estimated as the moisture content increases. It is assumed that the diameter of the round wood remains unchanged when the moisture content exceeds 30%.

2.3.3 Mechanical properties

The main mechanical properties that apply to timber piles will be discussed.

Wood is a anisotropic material which means that the properties depend on the direction that is considered. The strength of a timber pile is linked to the direction in which the fibres are oriented. There is a distinction between two directions, a direction parallel to the grain which is the case for the longitudinal orientation and a direction perpendicular to the grain such as the radial and tangential orientations. Generally the strength is greater in the parallel direction as opposed to the perpendicular direction. The characteristic stress-strain curves for the tensile and compressive resistance is presented in Figure 2.17.

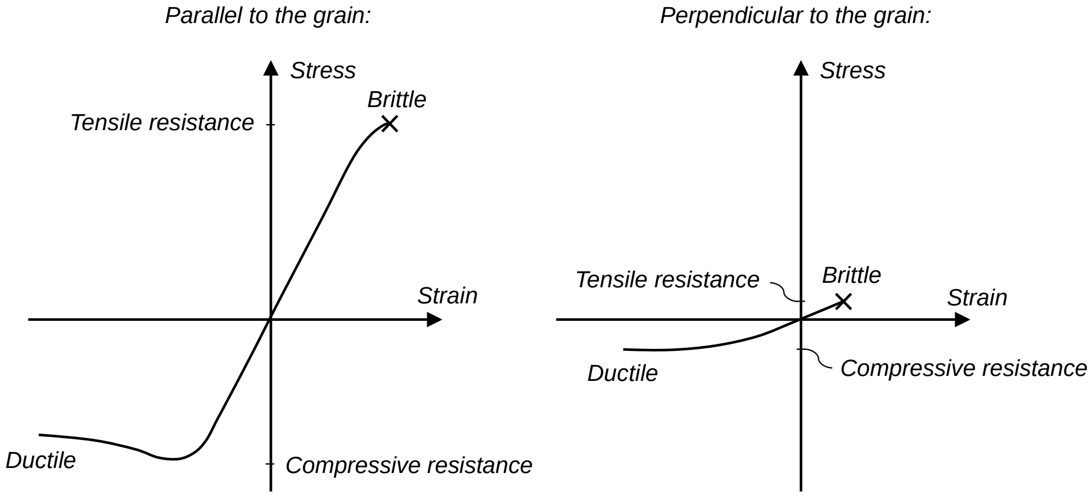

Figure 2.17: Typical stress-strain curves for wood loaded in different directions [3]

Tensile forces and stresses parallel to the grain can be handled well by the fibres in the wood structure. The failure in parallel direction is governed by the local fracture of wood fibres. Tension in perpendicular direction should be avoided because the resistance is very low, especially if cracks and defects are present. The failure occurs by pulling the fibres apart, which has a low resistance due to the absence of transverse fibres. Wood that breaks due to a lack in tensile strength is characterized by a brittle failure. [3]

Compressive failure in longitudinal direction is the result of a local stability issue due to buckling of the wood fibres. The buckling of the fibres is influenced by the amount of bound water in the wood structure. In general, more bound water means that the strength of the hydrogen bonds between the fibres decrease and the buckling of the fibres is more likely to occur. Compression in perpendicular direction causes the fibres to be squeezed until the squash limit is reached. Wood that is loaded in compression can reach high strain levels which result in a more ductile failure. [3]

The physical and mechanical properties are related. A lower density often means a reduced strength and a lower moisture content generally results in a higher strength. For example, juvenile wood has a lower density and a lower strength in comparison to mature wood.

Timber piles are mainly loaded in compression parallel to the grain and therefore the focus is on the compressive resistance in the longitudinal direction. Any eccentricities and defects can result in a non-linear internal stress distribution but the effect of bending, torsion and shear are considered irrelevant since the compressive force is by far the largest component.

The compressive strength can be derived from performing compression tests, where the test results are usually converted to a mean value and a fifth percentile value. The mean value represents the overall strength of the all the samples. The fifth percentile represents the point at which 95% of the samples are expected to have a higher value. Characteristic design values from the standards are derived from the fifth percentile values in order to control the reliability of the material behaviour. The method for the calculation of the characteristic values is explained in standard NEN-EN 14358. [25]

The standard NEN-EN 338 mentions the characteristic values for the compressive strength of coniferous wood, with values in longitudinal direction that range between 16 and 29 newtons per square millimeter depending on the strength class. These values are based on the fifth percentile values from tests that are performed in a so-called standard environment with a temperature of 20 °C (± 2) and a relative humidity of 65% (± 5). The reference point for the moisture content of the wood is set as 20% which is below the fibre saturation point. This means that the values from the standard are not representative for wet timber.

There are two leading studies available on the wet mechanical properties of timber. The first study was carried out by J.W.G. van de Kuilen in 1994 [7]. A total of 93 samples were tested of which 57 spruce (picea abies), 17 douglas fir (pseudotsuga) and 19 larch (larix decidua). The samples were undamaged with a mean moisture content of 100% and a mean wet strength of 20.0 newtons per square millimeter. The fifth percentile value of the wet strength turned out to be 16.3 newtons per square millimeter. This value is used in the Dutch National Annex of Eurocode 5 as a basis for the characteristic design value of new timber piles.

The second study was conducted by S. Aiker and G. Stapf in 2016 [8]. Here a total of 17 spruce (picea abies) samples without degradation were investigated. The mean moisture content turned out to be 89%, with a mean wet strength of 17.6 newtons per square millimeter and a fifth percentile wet strength of 13.4 newtons per square millimeter.

The procedure for performing compression tests on round timber is described in the standard EN 14251. An example of a test set up is shown in Figure 2.18.

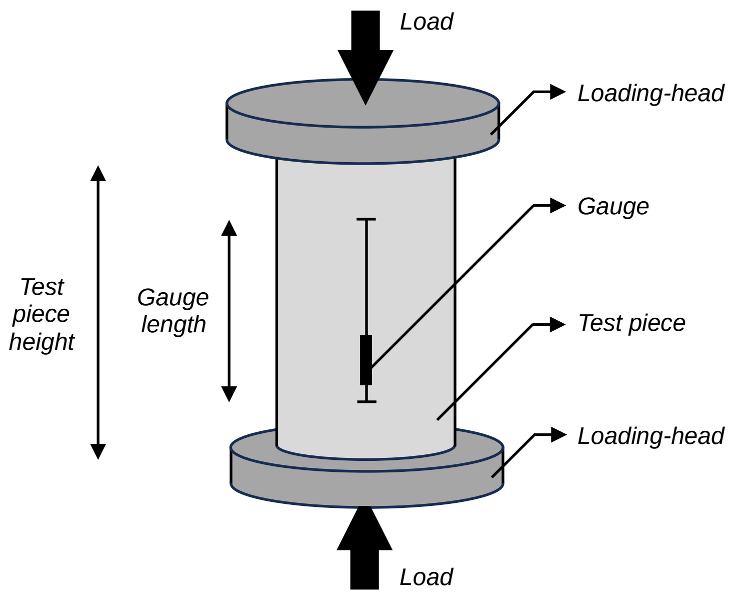

Figure 2.18: Set up for compression test parallel to the grain

A timber test piece is placed between two loading-heads and an increasing load with a constant rate is applied until failure occurs. The rate at which the load increases should be chosen so that failure occurs within 300 seconds (± 120) and the time to failure must be recorded for each test. Both ends of the test piece need to be parallel to each other and perpendicular to the centroidal axis. A gauge can be used to measure the deformation of the test piece during the increasing of the load. The loading-heads need to be locked to hinder any rotations and to prevent the inducing of bending stresses. The load increase and the deformation have to be recorded with an accuracy of at least 1%.

The compressive strength of the test piece can be determined by dividing the maximum load and the cross-sectional area. The cross-sectional area is calculated by multiplying two diameters, both at right angles to each other, in order to take any deviations in roundness into account.

Compressive strength parallel to the grain:

$$f_{c,0} = \frac{4 * F_{max}}{\pi * d_1 * d_2} \qquad (2.6)$$

Where:

$f_{c,0}$	$[N/mm^2]$	:	Compressive strength
F_{max}	$[N]$	:	Maximum load
d_1 and d_2	$[mm]$	:	Two diameters perpendicular to each other

The wood has an elastic behaviour for moderate load levels, meaning that the wood can return to its former state after the load is removed. The wood fibres start to buckle once the load level exceeds the so-called proportional limit which results in a plastic deformation that remains after the load has been removed.

The behaviour of the wood can be presented in a diagram by plotting the load against the deformation. An example of a load deformation curve is shown in Figure 2.19.

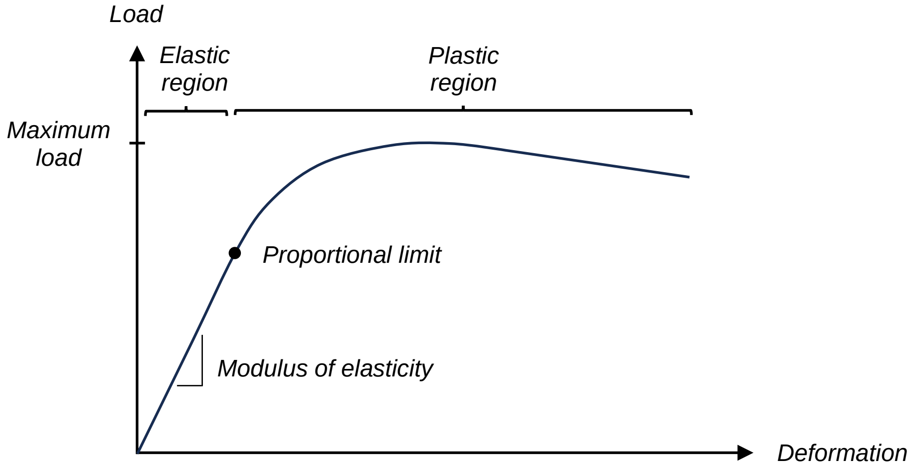

Figure 2.19: Load deformation curve for compression parallel to the grain

An important design stiffness value for timber is the modulus of elasticity (MOE), which represents the resistance of the wood to shorten under the influence of load levels in the elastic region. The modulus of elasticity in compression, also referred to as the Young's modulus, is defined as the slope of the elastic region in the load deformation curve [2].

The method for finding the modulus of elasticity by using the findings of the compression test is described in the standard EN 14251.

Modulus of elasticity in compression parallel to the grain:

$$E_{c,0} = \frac{h_0 * (F_2 - F_1)}{A * (w_2 - w_1)} \qquad (2.7)$$

Where:

$E_{c,0}$	$[N/mm^2]$	:	Modulus of elasticity
$F_2 - F_1$	$[N]$	:	Increment of the load
$w_2 - w_1$	$[mm]$	:	Increment of the deformation
h_0	$[mm]$	:	Gauge length
A	$[mm^2]$	:	Cross-sectional area

The load increment and deformation increment need to be taken from the same section of the slope. Generally, the increments are taken from 10% to 40% of the slope to exclude any measurement uncertainties associated with the start-up of the test and the transition to the plastic region.

The stiffness of wood with fibres in perpendicular direction is considerably lower than for wood with fibres in parallel direction. The modulus of elasticity for wood perpendicular to the grain is about 3% of the value that is obtained for wood parallel to the grain [3].

2.3.4 Time-dependent behaviour

Wood is a viscoelastic material which means that the behaviour of the wood can change under long-term loading. The viscoelastic behaviour is characterised by the effect of relaxation and creep in the wood structure.

Relaxation is described as a decrease in stress over time under the influence of a constant deformation. The relaxation of wood is an effect that limits the functioning of prestressed elements which often means that retensioning is needed to maintain a certain stress level. Creep is known as an increase in deformation over time caused by a constant load. The effect of creep is often the most significant regarding the time-dependent behaviour of timber elements. [3]

The amount of creep is dependent on the direction of the load and the angle of the grain. The creep deformation of wood in tension is generally lower than the deformation of wood in compression. Also, a load perpendicular to the grain results in a much higher creep deformation compared to the deformation that occurs with a load parallel to the grain. [26]

The environmental conditions have a major influence on the rate and the amount of the creep deformation. For example, the amount of creep increases as the temperature rises above the 35 °C. In addition to that, changes in temperature and humidity affect the moisture content and therefore also the creep. The rate at which creep develops accelerates much faster when the moisture content frequently fluctuates from high to low. This phenomenon is known as mechano-absorptive creep and it arises when an internal stress interacts with the alternating swelling and shrinking of the wood. The environmental conditions have been incorporated in the Eurocode 5 with different service classes. [26]

The development of creep deformation over time can be roughly divided into 3 phases. First comes the primary phase which is characterized by a rapid increase in deformation and then stabilizes. The secondary phase has a fairly constant creep rate and that is why this phase is also known as the stable creep or steady-state creep. Finally, there is the tertiary phase where the creep deformation accelerates until failure occurs [26]. The phases and two examples of different creep curves are displayed in Figure 2.20.

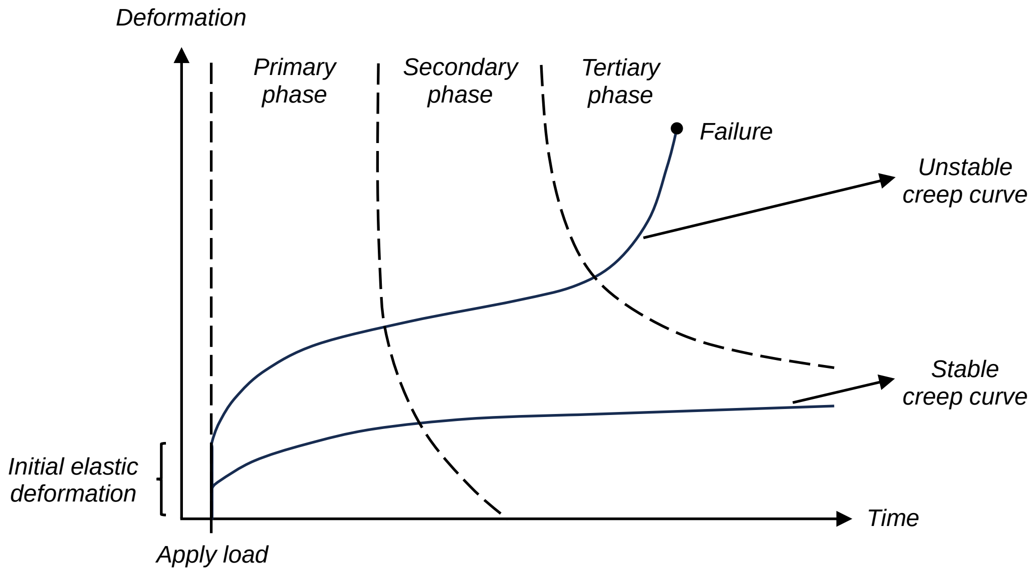

Figure 2.20: Different phases for the development of creep deformation over time [26]

Whether or not the creep deformation develops into the tertiary phase depends on the stress level, the duration of the load and the rate of creep deformation [26]. If the load is removed before creep failure, then the wood can mostly return to its original state over time. However, some permanent creep deformation remains due to damage to the wood microstructure [3].

Creep not only causes deformations, but also a reduction in strength and stiffness. The strength will gradually decrease as the duration of the load increases or the amount of moisture gets higher, this phenomenon is known as the load-duration effect of wood. Also, the stiffness will gradually decrease as the moisture content increases. [26]

The Eurocode 5 has reduction factors for strength and stiffness so that the load-duration effect and environmental conditions can be taken into account. The reduction factors are used during the design process of timber structures to prevent creep from progressing into the tertiary phase [26]. Timber piles are solid timber with a permanent load and wet environmental conditions. The reduction factors for solid timber elements are described in standard EN 14081-1. The allowable stress is reduced by a factor k_{mod} and the value for foundation piles corresponds to 0.5 which symbolizes a reduction of 50% for the strength. The stiffness is reduced by a factor $1/(1+k_{def})$ and the value of k_{def} for foundation piles is equal to 2 which means a reduction of 66% is applied for the modulus of elasticity.

Timber foundation piles have a high permanent load and are therefore subjected to creep, which may ultimately lead to material failure. The creep reduces the elastic response of the foundation piles and the pile will fail in creep when the elastic response is gone. It is often hard to predict the creep deformation of old timber foundation piles because the load history is not known. As a result, it is difficult to estimate when creep failure occurs.

2.4 Degradation

The changes in the structure and the properties of wood due to degradation mechanisms.

2.4.1 Different mechanisms

There are different mechanisms that can cause the breakdown of the wood structure and result in a loss of physical or mechanical properties. The degradation of hundreds of timber pile foundations throughout the Netherlands have been studied and the main three reasons for degraded timber piles were discovered to be wood-destroying fungi, bacterial attack and too high loading [14]. Note that these degradation mechanisms can be present individually, but can also occur at the same time.

Both the wood-destroying fungi and the bacterial attack are a form of biological degradation. The biological degradation is a destructive process by organisms which causes the wood structure to lose its strength [5]. The old timber foundation piles can be sensitive to biological degradation and the effects of the biological degradation often prove to be a significant problem. The following sections are devoted to the various forms of biological degradation and the way in which its effect can be evaluated.

The loads that timber foundation piles endure have been increasing in the past century and the higher loads are one of the major reasons for degrading timber piles. This load increase mainly comes from settlements in the subsoil, where the soil causes a negative skin friction along the length of the pile and attaches to the pile which results in a higher load. The parts of the subsoil that contribute most to this negative skin friction are the upper sand layers that were often applied in the past as a backfill to flatten the working surface before the timber foundations were installed. [14]

In addition to the extra loading from the negative skin friction, there are also higher loads on the foundations of bridges and quay walls from traffic. The amount and the weight of vehicles on public roads have increased, especially over the past 100 years. However, the traffic loads are variable and they are less relevant for the long-term failure processes of 100 to 300 year old piles [27].

The combination of the high permanent loads and the long service life can result in a mechanical degradation of the timber piles. Mechanical degradation is caused by the effects of creep and load duration. A higher load and a longer load duration increases the effect of creep. The creep subsequently causes deformations, a reduction in strength and a reduction in stiffness [26].

Besides the aforementioned forms of degradation, there are also some other types of degradation that can affect timber foundations. The physical and chemical degradation are briefly explained. Physical degradation is often initiated from changes in the environment. The most common type of physical damage is due to elevated temperatures and fire [2]. Other examples are damage due to wind, ultraviolet rays or drying. Chemical degradation occurs, for example, by exposure to acids, alkaline or natrium chloride. The chemical substances can cause discoloration and damage to the wood cells [2]. The physical and chemical degradation are considered not significant for aged timber piles and are therefore not further elaborated.

2.4.2 Biological degradation

The biological degradation occurs due to parasites and microbes that settle in the wood structure. There are basically four types of organisms that damage the wood structure: insects, marine borers, fungi and bacteria.

The insects that cause damage are mainly woodworms and termites. The woodworms are the larvae of certain beetle species that infest the wood and use it as food. Larvae generally prefer warm and humid conditions, while some larvae can already develop in wood with a moisture content as low as 8% [3]. Termites live in colonies, primarily nest in the ground and feed on wood. The termites prefer high temperatures and are attracted to moist areas with wooden components. In addition to insects, marine borers can also cause a lot of damage to timber elements. Marine borers is a collective term for worms and crustaceans that live in salt water and infiltrate the timber of marine structures. The marine borers practically occur all over the world but the attack rate is higher for regions with warmer water and for locations where simultaneously erosion occurs due to water currents. [2]

Insects and marine borers attack the wood and leave tunnels in the wood structure, see Figure 2.21. The damage is often difficult to detect and it is usually at an advanced stage by the time it becomes visually evident. The presence of holes and burrows in the wood result in a reduction of material in the cross-section and a decrease in the resistance of the wood. [5]

Figure 2.21: Examples of damaged wood due to insects and marine borers [2]

The fungi that attack wood can be categorized into wood-staining and wood-destroying fungi. Wood-staining fungi, like moulds and blue-stain fungi, inhabit the wood structure without breaking it down so there is no reduction in strength. These fungal species are mainly found only in the sapwood. The moulds do not penetrate the wood and leave a discoloration on the surface. The blue-stain fungi grow from the inside of the wood and tend to spread fast radially in the wood structure through the rays. [3]

Wood-destroying fungi can be subdivided into white rot, brown rot and soft rot. They reduce the weight and strength of wood by breaking down cell walls for nutrients. The wood-destroying fungi occur in both sapwood and heartwood, there are even species that only affect the heartwood which makes them difficult to detect [2]. In general, fungal decay can develop in an environment with temperatures ranging from -2.5 to +40 °C, a humidity from 30 to 60% and a wood moisture content of at least 20% [3].

White rot fungi break down all major components of the wood structure such as cellulose, hemicellulose and lignin. There is less weight loss during the beginning of the decay and the weight loss becomes progressively worse in later stages when the fungal mycelium is spread throughout the wood structure [28]. This makes the wood more fragile and spongy with a typical whiter colour [2].

Brown rot fungi break down cellulose and hemicellulose but do not affect the lignin. The fungi affect the wood in such a way, causing it to get a browner colour and a crumbly structure with numerous cracks perpendicular to the grain [28]. The brown rot is more common with softwoods and the white rot is more common with hardwoods, but they can appear in both types of wood [2].

Soft rot fungi break down the cellulose and hemicellulose, mainly in wood structures with a high moisture content. The mycelium of the fungi cause characteristic microscopic diamond shaped cavities in the secondary cell walls [28]. Wood that is affected by soft rot gets a greyish colour and the surface can crack in a similar way as happens with brown rot.

The brown rot and white rot attack wood with a moisture content of about 25-100%. They both have a similar velocity of degradation that can reach up to 100 mm/year. The soft rot breaks down wood that is saturated with water. The maximum velocity of degradation of soft rot is about 10 mm/year [1]. The effects of different kinds of fungi are shown in Figure 2.22.

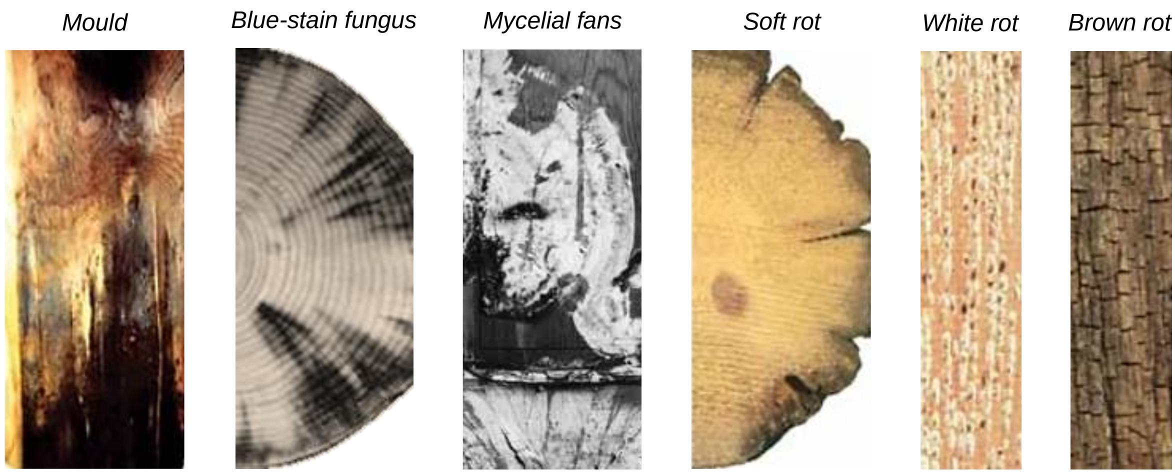

Figure 2.22: Examples of damaged wood due to fungi [2]

Bacterial decay can occur in timber that is kept wet over a longer period of time, for example wood that is submerged or sprayed with water. There are generally two types of bacterial degradation, namely tunnelling attack and erosion attack. In both cases the bacteria break down the lignin in the secondary cell wall of the wood structure and the names are based on the microscopic decay patterns they leave behind. The tunnelling attack causes a very thin decay pattern on the cell wall that radially branches outwards. The erosion attack is recognizable by the presence of channels that turn into a striped decay pattern. The microscopic channels they produce expand progressively and mark the way along which the bacterial colony moves. The bacteria that cause the tunnelling attack mainly occur in aerobic situations where degradation by fungi is limited. On the other hand, the bacteria of erosion attack can cause degradation in low oxygen situations. [29]

When all different types of biological degradation are considered, the erosion attack bacteria are identified as the only type of biological degradation that can cause serious problems for aged timber piles [29]. The erosion attack bacteria can, unlike the other types of degradation, propagate in situations where there is limited oxygen. The timber foundation piles are mainly submerged and are thus located in anaerobic environments where only the bacteria can cause degradation.

Note that degradation of timber foundation piles due to insects and/or fungi can still occur. However, the insects and fungi require oxygen to live [4]. For this, the wood needs to be exposed to the air and that often only happens when the groundwater level drops. This also means that the decay due to insects and fungi is exclusively limited to the pile head that is in direct contact with the oxygen.

The bacterial decay of round wood generally starts from the outside and spreads towards the inside over time which causes the outer layer of the wood to turn into a soft shell. The sapwood degrades faster than the heartwood and the rate of degradation will slow down as the soft shell reaches the heartwood [5]. This can be explained by the characteristic trait that the erosion attack bacteria are unable to break down cell walls from the outside and rely on intercellular cavities and pits to penetrate the wood structure [29]. It is known that the pits in the sapwood will close during the heartwood formation process [3]. So, there are less possibilities for the bacteria to enter the neighbouring cells in the heartwood which slows down the bacterial attack.

The effects of the bacterial degradation for wood in anaerobic environments is characterized by its slow progression [2]. The bacteria attack individual wood cells, soften the structure of the wood and cause a reduction of the strength. Generally, the velocity of degradation from bacteria ranges between the 0 and 1.1 mm/year. This values is a bit lower for piles with an already high level of degradation and ranges between the 0 and 0.8 mm/year. The velocity of degradation of the bacteria is quite slow in comparison to the velocity of the wood-destroying fungi. [4]

The bacterial decay occurs over the full length of the pile and over a longer period of time can result in significant damage [4]. Some examples of timber foundation elements with bacterial decay are pictured in Figure 2.23.

Foundation beam

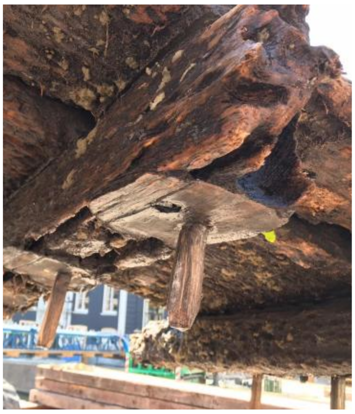

Cross-section with soft shell

Foundation pile

Figure 2.23: Examples of damage to foundation wood due to bacteria [5]

Damage from biodegradation mainly becomes apparent due to the presence of large chunks of the wood structure with a reduction in mechanical and physical properties. In order to take the damage into account, the degraded area of the cross-section is determined and subtracted from the whole cross-sectional area. [5].

There are some interactions between biological degradation and other forms of degradation. For example, some bacteria can make the wood overly adsorptive which makes the wood more susceptible to chemical decay such as alkaline attack [2]. Also, the biological degradation results in a smaller effective cross-section, higher internal stresses and it can cause an increase in the mechanical degradation due to the effect of creep. There is generally not enough information available to do a detailed report on these interactions and it is difficult to demonstrate the significance of these interactions on timber foundation elements.

The durability of timber is practically the way in which it can withstand biological degradation, also referred to as the resistance against decay [2]. In general, heartwood is considered to be more durable than sapwood because the heartwood has closed pits and the pests can less easily penetrate into the wood microstructure. The natural durability of the heartwood from different wood species is described in the standard EN 350. There are many ways to treat wood against biological attack if its natural durability is not high enough. The standard EN 15228 mentions some requirements for the preservative-treatment of structural timber.

2.4.3 Damage detection

The damage of wood degradation often becomes visually detectable when the deterioration has reached an advanced stage. However, it is desirable to be able to determine whether degradation is occurring, even if it is not immediately visible. The condition of the wood can be determined with non-destructive testing methods, also known as integrity testing.

One of the simplest ways to find out if there is some decayed wood is to insert a piercer. It is often possible to penetrate the decayed parts with a piercer by hand because these are much softer than the remaining sound wood. The extent to which the piercer sinks into the wood tells something about the size of the damaged area and the thickness of the soft shell. Although working with a piercer can give a good impression whether there has been any degradation, it is not equivocal evidence to describe the condition of the wood. An example of a piercer is shown in Figure 2.24, but in practice a screwdriver is often used as well.

Figure 2.24: Example of a piercer used to investigate damaged wood

A more precise method to evaluate the condition of wood is by applying micro-drilling measurements. While performing the micro-drilling, a long slender drill bit is pushed into the wood structure and the resistance is measured. The micro-drilling only shows the local resistance of the wood and the drilling has to be repeated on different locations in order to get a good indication of the condition of the whole element. The micro-drilling can be performed in situ and under water by divers.

The results of micro-drilling are presented in a graph by plotting the resistance against the distance, see Figure 2.25. In general, two measurements are taken per section with each about 90 degrees apart. Avoid drilling in areas with knots and defects to make sure that the obtained data is also representative for the surrounding wood. It is good to keep track of the direction in which the micro-drilling is performed. The drill bit goes through the section and comes out on the other side. The device can still detect some resistance after the drill bit came out of the section. For this reason it is necessary to measure the diameter of the pile and compare it to the depth presented on the graph.

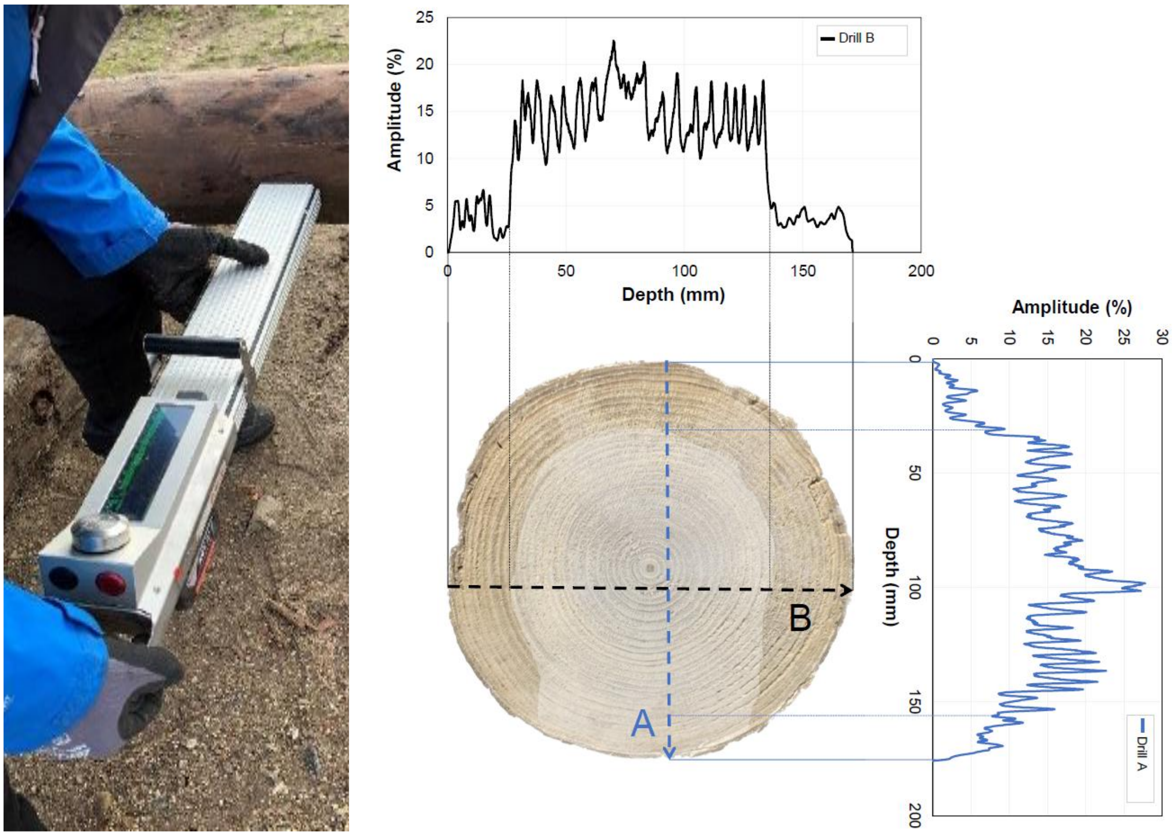

Figure 2.25: Micro-drilling test and a cross-section with corresponding resistance graph [24]

The features of the wood macrostructure can be recognized in the graph. It is possible to distinguish the growth rings of the wood by investigating the small changes in the graph, where the small peaks represent latewood and the small valleys represent earlywood. Other varieties of the resistance can come from the presence of reaction wood, pith, degradation, knots and other irregularities.

Wood that has been attacked by bacteria often has an outside layer with a lower strength and this soft shell can be recognized in the graph because it has a lower resistance. The Delft University of Technology has developed a software program named “soft shell calculator” that can be used to differentiate between the decayed part and the sound part of the section [30]. From this, the cross-sectional area of the decayed part and the cross-sectional area of the sound part can be determined. The level of decay can be expressed in the ratio between the amount of remaining sound wood in comparison to the total cross-section [24].

Level of decay as a ratio between the amount of sound wood and the total amount of wood:

$$p\ A_{sound} = \frac{A_{sound}}{A_{tot}} * 100 \tag{2.8}$$

Where:

$p\ A_{sound}$	$[\%]$	:	Percentage of sound cross-sectional area
A_{sound}	$[mm^2]$	:	Crosss-sectional area of the sound part
A_{tot}	$[mm^2]$	:	Total cross-sectional area

The pile can be classified based on the level of decay. A pile is considered to have a low level of decay when the remaining sound section is higher than 85%. The level of decay is regarded to be weak/moderate when the sound part takes up between 65% and 85% of the section. The pile is having a severe level of decay if the section consists of less than 65% residual sound wood. [24]

A practical way to determine the remaining capacity of the pile is by assuming zero residual strength for the degraded wood. This implies that the internal forces of the pile are transferred only by the remaining sound section. The maximum force, as determined during the compression test, can be divided with the area of the remaining sound section to get the equivalent compressive strength of the pile.

Equivalent compressive strength of the remaining sound wood:

$$EQ\ f_{c,0} = \frac{F_{max}}{A_{sound}} \tag{2.9}$$

Where:

$EQ\ f_{c,0}$	$[N/mm^2]$	:	Equivalent compressive strength
F_{max}	$[N]$	:	Maximum load
A_{sound}	$[mm^2]$	:	Cross-sectional area of the sound part

The equivalent compressive strength gives a good representation of the amount of stress that can be transferred by the pile.

2.5 Preceding research TU Delft

The researchers from the TU Delft's department of Biobased Structures and Materials have conducted experiments and tests on old timber piles. The researches provide an important view on how the age and decay influence the mechanical properties. Key information from a number of relevant studies is described in this section.

2.5.1 Compression tests on large segments

The most extensive research on timber foundation piles is performed mainly by Dr. Ir. G. Pagella as a part of his doctorate, which started in 2021 and was finalised in 2025 [10]. In addition, an interim of findings have been published by G. Pagella in multiple reports and articles which form an important source of information for this section [24] [31]. The findings elaborate on the relationships between biological degradation, building years, physical and mechanical properties of timber foundation piles. This is done by performing numerous tests, including large-scale compressions tests, on segments taken from timber foundation piles.

A total of 60 timber foundation piles were retrieved from Amsterdam, only 5 piles come from fir (abies) trees and the other 55 piles are made from spruce (picea abies) trees. The piles were used as a part of the foundation of bridges and originate from the building years 1727, 1886 and 1922. These piles are cut into smaller pieces and a total of 201 segments were selected for large-scale compression tests. The segments have a uniform length of either 900 mm, 1350 mm or 1800 mm and the length for each segment is chosen to be the value that is closest to 6 times the smallest diameter, as prescribed by the standards EN 408 and EN 14251. The level of decay is measured using a micro-drill and the moisture content is determined using the oven-drying method.

The compression tests were carried out at a constant speed of 0.02 mm/s until failure occurred. All segments were saturated before testing to mimic the conditions of being in the ground. The strain during the test is measured by a total of 10 linear potentiometers positioned around the pile, see Figure 2.26.

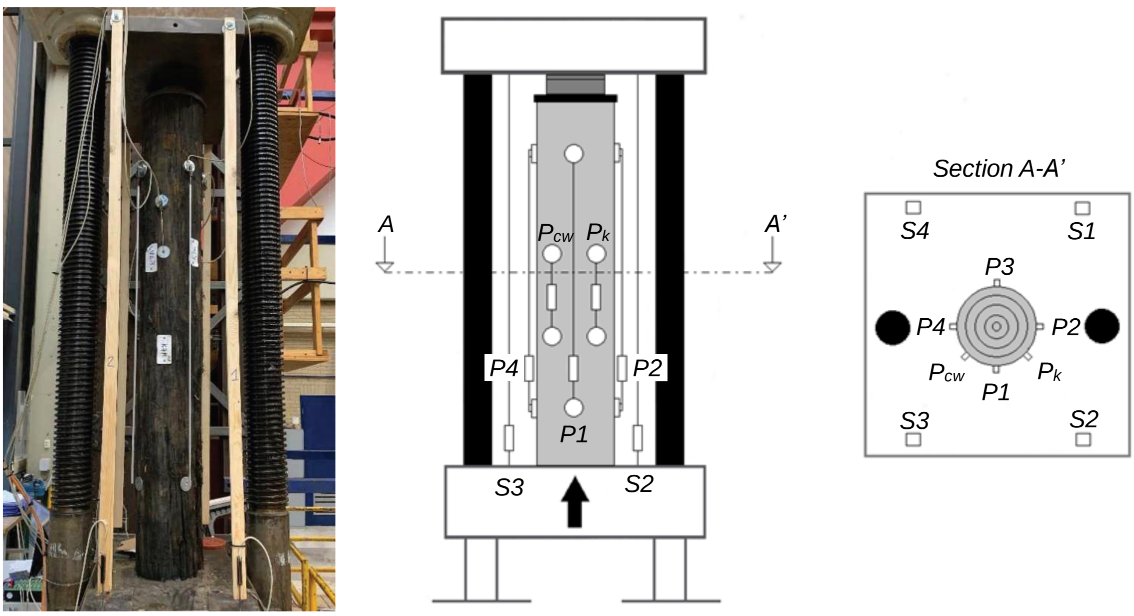

Figure 2.26: Schematic set up for compression testing of large segments

There are 6 potentiometers attached directly to the surface of the pile to measure the deformation. The 4 potentiometers P1, P2, P3 and P4 are located all around the outside of the pile and measure the strain over a height of 2/3 of the segment length. The P_{cw} and P_k linear potentiometer measure the strain over a height of 200 mm. The P_{cw} is located at a section with clear wood and the P_k is placed over a section with knots. Finally, there are the linear potentiometers S1, S2, S3 and S4 that measure the displacement between the bottom and top loading-head.

The results from the large-scale compression tests are used to determine mechanical properties such as the wet compressive strength and the static modulus of elasticity. The data can be divided according to the different wood species, locations along the pile and the different building years, as presented in Table 2.1.

Table 2.1: Overview of physical and mechanical properties from large-scale tests [31]

Segments (No.)	Dry density [kg/m^3]		Moisture content [%]		$f_{c,0,wet}$ [MPa]		MOE_{stat} [MPa]	
	avg	SD	avg	SD	avg	SD	avg	SD
All segments (201)	330	57	130	83	10.4	4.0	7500	2850
Divided according to different wood species:								
Spruce (180)	360	61	130	86	10.2	3.9	7400	2870
Fir (21)	390	47	100	25	13.6	2.6	9300	1660
Divided according to different locations along the pile:								
Head (65)	370	60	130	114	11.2	3.8	8000	2660
Middle (66)	370	58	120	54	11.0	4.0	7900	2990
Tip (70)	350	63	140	70	9.1	3.7	6600	2710
Divided according to different building years:								
1922 (49)	370	34	80	18	13.6	2.5	9800	1860
1886 (56)	360	40	95	26	13.1	2.4	9200	1600
1727 (96)	292	49	175	98	7.2	2.6	5300	2050

It is noteworthy to mention that only a few fir piles were tested and they were all from building year 1886. A lot more spruce piles were investigated and they originate from the years 1727, 1886 and 1922. It is not fair to compare the results of the fir piles and the spruce piles directly.

When looking at the different locations along the pile it can be noticed that the data for the head and middle parts show non-significant differences, meaning that they have a difference within about 5%. However, when a comparison is made with the tip part it can be seen that the average values for the strength and modulus of elasticity are approximately 15%-20% lower than the head and middle parts. This can be explained by the fact that the tip part contains more juvenile wood which generally has a lower strength and stiffness.

The comparison between the different building years also gives some interesting results. The data of the piles from 1922 and 1886 give no significant difference and the mechanical properties are within a difference of approximately 5%. But when it is compared to the strength and stiffness of the piles from 1727 it can be concluded that the values are about 45%-50% lower than the piles from 1922 and 1886. The reason why the mechanical properties of the piles from 1727 are lower is because a lot of the piles from 1727 are affected by biological degradation. This explanation is confirmed by the low dry density and the high moisture content, which also indicate the presence of biological degradation.

The relation between the wet compressive strength and the wet static modulus of elasticity is pictured in Figure 2.27. The data is divided by the different building years of the piles from 1922, 1886 and 1727.

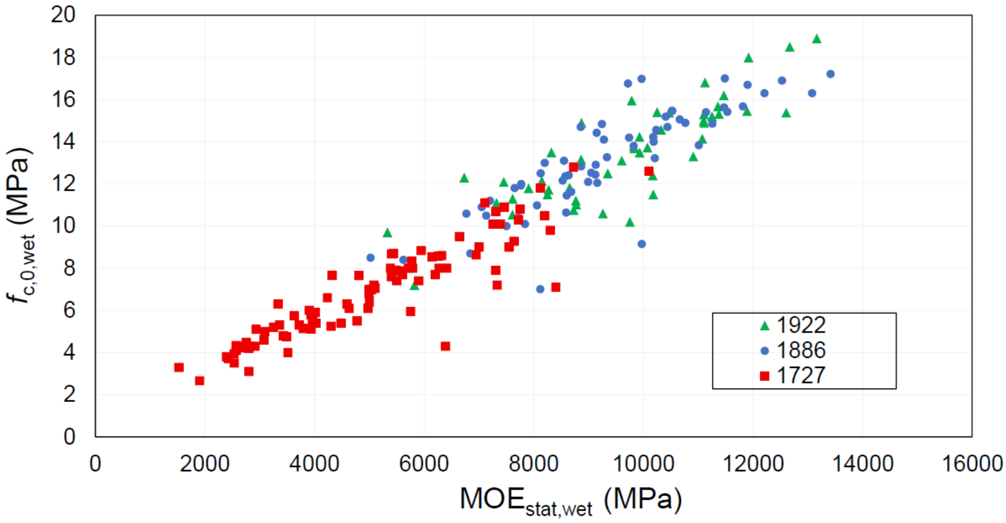

Figure 2.27: Relation between wet strength and modulus of elasticity of segments [24]

The graph indicates a good correlation for the strength and the stiffness of the piles. The modulus of elasticity seems to be directly related to the strength of the pile. Also, both the strength and stiffness for the piles from 1727 are lower than is the case for the other building years. The mechanical properties seem to be influenced by the biological degradation and the level of decay for each segment is introduced in order to highlight the differences.

The level of decay is based on the soft shell thickness and the remaining sound cross-sectional area. A segment has a low level of decay when the remaining sound area is higher than 85%. The segment is classified as moderately decayed when the sound area lies between the 65% and the 85%. A low level of decay occurs when a segments has less than 65% of remaining sound area left. An overview of the mechanical properties separated on the different levels of decay can be found in Table 2.2.

Table 2.2: Overview of the segment properties ordered by the level of degradation [24]

Segments (No.)		Dry density [kg/m^3]		Moisture content [%]		$f_{c,0,wet}$ [MPa]		MOE_{stat} [MPa]		Sound c-s area [%]		EQ $f_{c,0,wet}$ [MPa]	EQ MOE_{stat} [MPa]
		avg	SD	avg	SD	avg	SD	avg	SD	avg	SD	avg	avg
Low decay	Head (30)	400	40	80	14	13.9	2.4	9900	1730	95	5	14.7	10400
	Middle (37)	410	39	90	29	14.0	2.2	10100	1580	96	4	14.6	10500
	Tip (28)	400	47	90	21	12.4	2.4	8900	1590	94	4	13.1	9500
Moderate decay	Head (21)	350	44	130	42	10.3	3.1	7500	1810	76	6	13.5	9900
	Middle (14)	340	36	130	31	8.9	2.1	6700	1490	78	7	11.5	8600
	Tip (17)	370	45	120	31	9.2	2.1	6700	1580	78	6	11.8	8600
Severe decay	Head (14)	330	62	180	48	6.5	2.4	4800	1960	55	10	11.8	8700
	Middle (16)	300	32	180	56	6.0	1.6	3900	1040	50	12	11.9	7800
	Tip (24)	300	36	210	50	5.5	1.9	3900	1490	47	12	11.7	8300

It turns out that 95 from the 201 segments have a low level of decay and originate mainly from the building years 1886 and 1922. Then 52 of the 201 segments showed a moderate level of decay with 34 segments from 1727, 12 segments from 1886 and 6 segments from 1922. The remaining 54 from the 201 segments were all severely decayed, almost all of the segments originated from 1727 and consisting of mainly pile tips.

Based on all the information so far it is possible to differentiate between the segments with a similar wet compressive strength, see Table 2.3. A distinction is made between the different building years, biological degradation and the location along the pile. Hereby the head and middle parts of the piles from 1922 and 1886 are grouped together.

Table 2.3: Classification of the segments based on average wet compressive strength [24]

Building year	Biological degradation	Location	$f_{c,0,wet}$ avg [MPa]
1922 and 1886	Low decay	Head and middle	14.2
		Tip	12.4
	Moderate decay	Head and middle	*
		Tip	10.5
1727	Moderate and severe decay	Head	8.9
		Middle	8.2
		Tip	7.5

* It is not possible to determine the average wet compressive strength of moderately decayed head and middle parts from 1922 and 1886 because there is not enough data available.

The average wet static modulus of elasticity can also be categorized in the same ways as the wet compressive strength. The head and middle parts with low decay from 1922 and 1886 have an average MOE_{stat} of 10000 MPa and the average value for the tip parts is 10% lower. The piles from 1727 with a moderate to severe level of decay have an average MOE_{stat} of 6300 MPa, which varies from 6700 MPa at the head to 5800 MPa at the tip.

The equivalent strength and equivalent modulus of elasticity are adapted values that only use the remaining sound cross-sectional area and do not take the soft shell into account. The equivalent mechanical properties of the segments from 1922 and 1886 show a similar value as the values with a low level of decay. This indicates that the remaining sound cross-sectional area of the segments from 1922 and 1886 still performs good.

The equivalent strength and modulus of elasticity of the segments from 1727 show values that are below the values with a low level of decay. This means that the remaining sound part of the segments from 1727 is no longer in optimal condition. An explanation can be that the piles from 1727 are subject to mechanical degradation after being in service for almost 300 years. The mechanical degradation has not been investigated.

2.5.2 Compression tests on small rectangular prisms

The research consists of a cross-sectional analysis of spruce foundation piles and was carried out by Ir. M. Lee as his master thesis project [32]. The thesis was finalised in 2023 and covers the effect of biological degradation on the mechanical and physical properties of spruce piles. This is done, among other things, by performing compression tests on small rectangular prisms that are sawn from certain locations along the pile.

A total of 6 spruce (picea abies) foundation piles from different building years were selected for the research. There are 3 piles chosen from 1727 and 1 pile from the building years 2019, 1922 and 1886. The piles are stored underwater to get a moisture content above fibre saturation point. A disc is sawn from the head, middle and tip part of each pile which results in 18 discs. The biological degradation is investigated with a micro-drill and the drill path is carefully chosen right through the middle of the section.

The small rectangular prisms are sawn from different positions along the drill path of the previous micro-drill measurement. Each disc is used for the production of 5 small prisms, resulting in a total of 90 prisms. The small prisms have a length of 120 mm and a square section with sides of 20 mm. The length of the prisms are 6 times the width, which is in compliance with the standard EN 408. They are kept in a sealed bag to maintain the same moisture content during for the compression tests. The dry density and moisture content of the prisms are determined with the oven-dry method.

The small rectangular prisms have been tested in compression until failure occurred. On top of the specimen is a hinge which ensures a good force transfer without any buckling. The strain of the prisms is measured with 2 linear potentiometers, see Figure 2.28.

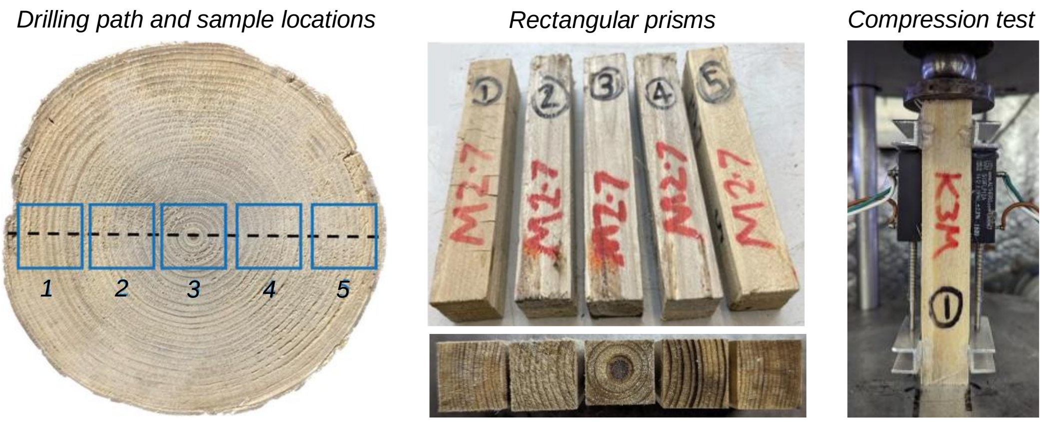

Figure 2.28: Sample selection and compression tests of small rectangular prisms [32]

The results from the tests give a good indication on the distribution of the properties over the width of the pile section. Prisms 1 & 5 are taken from the outside perimeter at the location of the soft shell. Prism 3 is taken from the center with the pith and juvenile wood. Prisms 2 & 4 are positioned at the location of the highest drilling amplitude on each side of the pith.

The drilling amplitude from the micro-drilling measurement is a measure for the resistance of the drill. The soft shell has a low drilling amplitude and a low drilling resistance in comparison to the sound part in the middle of the section. The drilling amplitude is compared to the physical and mechanical properties of the prisms.

In general, a low drilling resistance indicates the presence of degraded wood which has a high moisture content. The results show a good relation between the drilling resistance and the moisture content, as presented in Figure 2.29. The moisture content gradient is drawn based on the five measurements from the tested prisms.

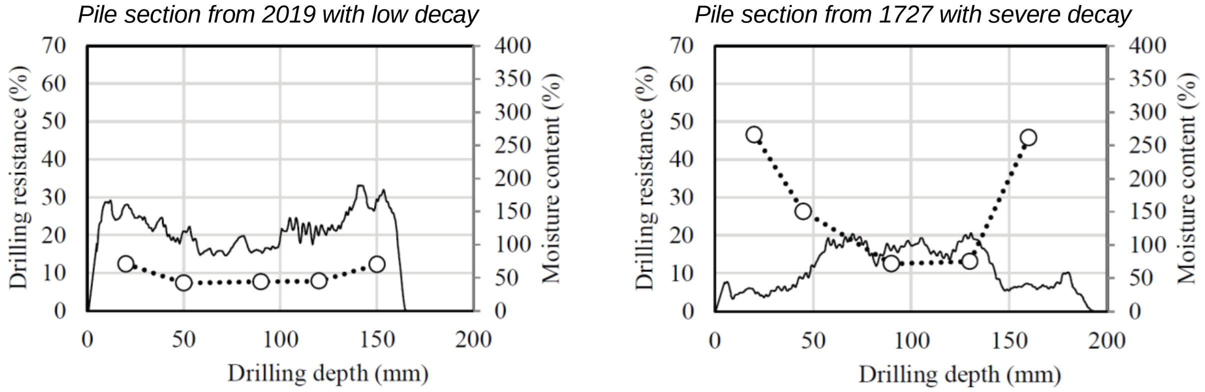

Figure 2.29: Relation between drilling resistance and moisture content gradient [33]

The section from 2019 with no biological degradation shows a fairly uniform moisture content gradient. The moisture content of the peripheral samples 1 & 5 are a bit higher because they contain sapwood. A section from 1727 with severe biological degradation shows a lot of variety in the moisture content gradient. The peripheral samples 1 & 5 are taken from the soft shell and have a moisture content that is about 3 times higher than the sound inner part.

When wood is degraded it also has a lower dry density which results in a lower compressive strength. The relation between the drilling resistance and the wet compressive strength seem to be correlated quite well. An example of this relation can be seen in Figure 2.30, where the location and wet compressive strength of the five samples are compared with the drilling resistance.

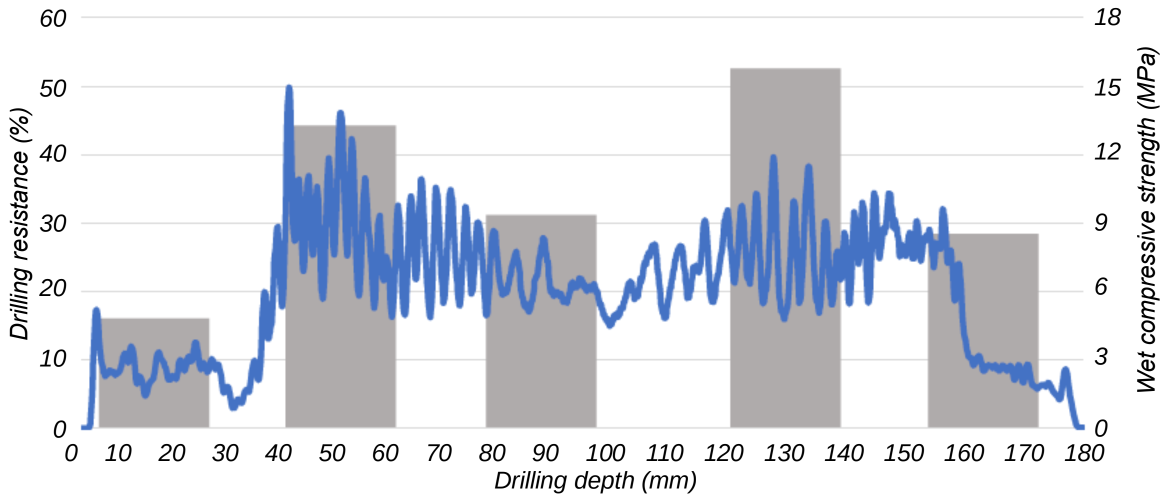

Figure 2.30: Relation between drilling resistance and wet compressive strength [32]

The peripheral samples 1 & 5 are located in the soft shell region which can be recognized by the low drilling resistance and the low wet compressive strength. The samples 2 & 4 have the highest drilling resistance and also the highest wet compressive strength.

The average values regarding the most important physical and mechanical properties of the small rectangular prisms are listed in Table 2.4. The table gives a good indication on how the properties change in a section of a spruce foundation pile.

Table 2.4: Overview of physical and mechanical properties from small-scale prism tests [32]

Prisms (No.)		Dry density [kg/m^3] avg	Dry density [kg/m^3] SD	Moisture content [%] avg	Moisture content [%] SD	$f_{c,0,wet}$ [MPa] avg	$f_{c,0,wet}$ [MPa] SD	MOE [MPa] avg	MOE [MPa] SD
Degraded section	Soft shell periphery (18) Samples 1 & 5	278	46	233	61	5	3	2239	1398
	Interior and center (27) Samples 2, 3 & 4	399	13	70	19	11	2	5894	1382
Non-degraded section	Sound periphery (18) Samples 1 & 5	472	46	132	22	17	3	9297	1919
	Sound interior (18) Samples 2 & 4	514	48	54	23	22	3	12217	2342
	Sound center (9) Sample 3	438	48	45	12	13	2	6795	839

First the values in the degraded section are compared to get a good idea of how these relate to each other. The soft shell has, on average, a moisture content that is 232% higher and a dry density that is 30% lower than the sound inner part. Especially the really high moisture content seem to be a good indicator for the presence of biological degradation. The wet compressive strength and wet modulus of elasticity of the soft shell is about half the value of the sound inner part. The stiffness is of the soft shell has a large variability but still remains very low compared to the rest of the section.

Second the non-degraded samples are compared. A distinction can be made between the periphery, the interior and the center of the section. The part that consistently has the lowest values for the physical and mechanical properties turns out to be the center. The dry density and strength are the lowest, despite the fact that the moisture content is also the lowest. An explanation for the low values is the presence of the pith and juvenile wood in the center of the section. The sound periphery shows a dry density and wet compressive strength that are quite high but also with a very high moisture content because it contains sapwood. The highest strength and stiffness can be found between the periphery and the center, containing mature heartwood.

When the values of the degraded and non-degraded sections are compared, it can be seen that the interior of the degraded section has lower properties than the interior of the non-degraded section. This difference is not because there is biological degradation because the samples are taken away from the soft shell. However, the difference can be explained by the fact that the degraded sections are older and probably have more mechanical degradation.

2.5.3 Compression tests on small discs

The research addresses the effect of knots on the compressive strength of timber foundation piles. The study was completed in 2022 and it was carried out as a master thesis project by Ir. C. Gambarin [12]. Many tests have been conducted, including compression tests on small discs from a timber foundation pile.

A total of 6 discs were sawn from one timber foundation pile from 2019 with no biological degradation. Each of the head, middle and tip segments of the pile resulted in the production of two discs: one disc with the highest knot ratio and one clear wood disc without any knots. The discs are cut with a height of approximately 100 mm and both sides are cut as parallel as possible. The whole lot is kept in water to make sure that the moisture content is above fibre saturation point.

Each disc was tested in compression until failure occurred. The compression test was done at a constant speed of 0.02 mm/s and the strain of the disc is measured with 4 linear potentiometers located on the sides, see Figure 2.31.

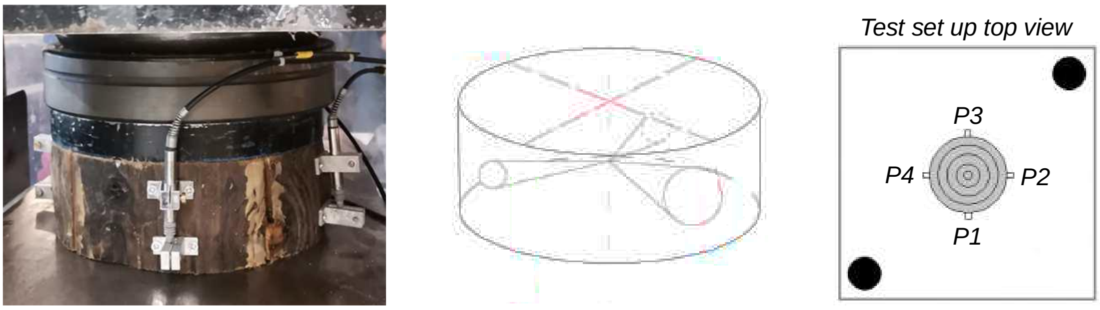

Figure 2.31: Schematic set up for compression testing of small discs [12]

The discs were taken from pile segments which have previously been tested in compression, as mentioned in section "2.5.1 Compression tests on large segments". It is possible to directly compare the strength of the discs with the strength of the segments because they represent the same part of the pile. The wet compressive strength of the discs and segments is presented in Table 2.5.

Table 2.5: Overview of wet strength of small discs and corresponding segments [11]

Element type			Knot ratio [-]	$f_{c,0,wet}$ [MPa]
Segments	1		0.27	15.5
	2		0.31	15.5
	3		0.27	13.3
Discs	1a	Clear wood	0	22.8
	1b	High knot ratio	0.27	14.3
	2a	Clear wood	0	21.4
	2b	High knot ratio	0.31	14.0
	3a	Clear wood	0	20.6
	3b	High knot ratio	0.27	13.8

The discs and segments from the same part of the pile are indicated with the same number. By comparing the results, it becomes apparent that the discs with knots have a similar strength as the segments with the same knots. For example, disc 1b has a wet strength of 14.3 MPa and segment 1 has a wet strength of 15.5 MPa. These values differ a bit but seem to be very close and this trend also occurs with the other discs and segments. A good correlation can be found between the wet compressive strength of segments and discs.

Something else to note is the difference in strength between the disc with knots and the clear wood disc without knots. For example, disc 1b has a high knot ratio and lower strength than the clear wood disc 1a. The principle also holds for the other discs and segments, which indicates that the presence of knots can govern the wet compressive strength of timber piles. Note that only 6 discs were tested. Although these are promising outcomes, more results are needed to properly document these relations.

In addition to the compression tests on discs, the thesis also looked at where along the pile the highest knot ratios occur. The distribution of the knot ratio over the length of one the pile is presented in Figure 2.32.

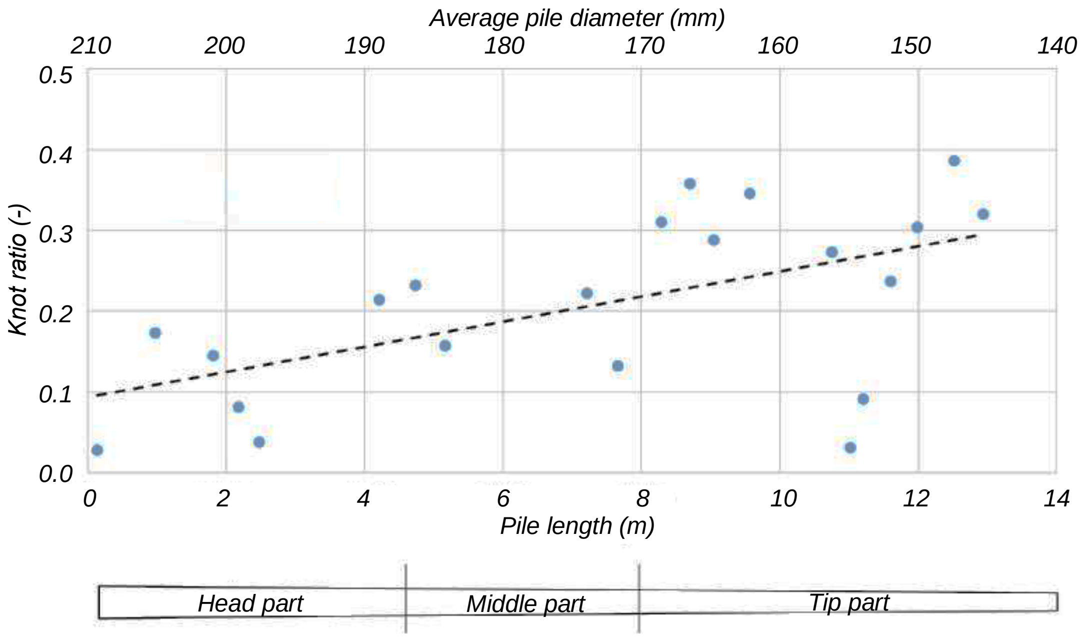

Figure 2.32: Knot ratio distribution of a timber foundation pile [12]

This specific timber pile had relatively low knot ratios at the pile head and the knot ratio got gradually higher towards the pile tip. Similar relations are mapped out for 5 other piles and it turns out that they all show the same distribution. In general it can be said that the knot ratio is higher at the pile tip in comparison to the pile head.

3. Materials

Selection of the timber foundation piles and their properties according to previous tests.

3.1 Origin of the piles

For the research, samples were taken from timber foundation piles with a variety of different conditions. All the piles originate from a total of 3 locations in Amsterdam, see Figure 3.1

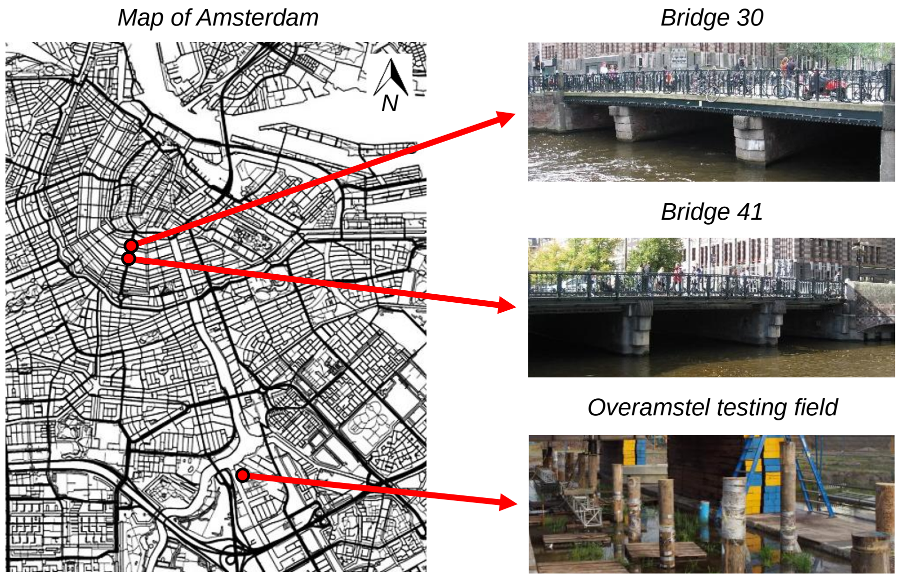

Figure 3.1: Map of Amsterdam with bridge 30, bridge 41 and Overamstel testing field

Bridge 30 and bridge 41 are located at the ‘Vijzelstraat’ in the city center of Amsterdam. They are both solid fixed bridges with two bridge piers and two abutments made out of brick along with stone. Bridge 30 (also known as the Isa van Eeghenbridge) spans the ‘Herengracht’ and bridge 41 (also known as the Johanna Borskibridge) spans the ‘Keizersgracht’.

The plan to construct bridges at these locations originates from 1662 and the bridges were finalised around 1727. After this the bridges were modified around 1886 through lowering and widening of the bridge decks. Then in 1911 the ‘Vijzelstraat’ was widened and arrangements were made to make the bridges more uniform. The structure of bridge 30 remained mostly original and a virtually new design was used for bridge 41, this reconstruction was completed around 1922. The bridges were redesigned in the 1950s to meet the changing traffic requirements and around 1968 a new bridge deck was built for bridge 30. In 2018 it was determined that the bridges were in need of major maintenance because of damage and settlements due to heavy traffic from trams and trucks. The bridges were renovated and the work was completed around 2023. [34]

A total of 60 timber foundation piles were mechanically extracted from bridges 30 and 41 during the last reconstruction in 2021. These piles can be traced back to three different construction years: 1727, 1886 and 1922. Consequently, the piles have been in service for different time durations which may contribute to a variability in the mechanical and biological degradation of the wood structure. The piles are made from two distinct tree species, there are 55 spruce (picea abies) piles and 5 fir (abies) piles. The pile length varies from 9500 mm to 13500 mm, the average diameter of the pile head is 230 mm and the average diameter of the pile tip is 145 mm. [24]

In addition to these relatively old piles, there are a total of 27 new timber piles which were used for a research performed by S. Honardar at the TU Delft in 2019 [35]. There are 18 spruce (picea abies) piles and 9 pine (pinus) piles. The pile length varies from 12250 mm to 15500 mm, the average diameter of the pile head is 250 mm and the diameter of the pile tip varies from 125 mm to 150 mm. A total of 16 of these piles have been used for a load test in Amsterdam soil at the Overamstel testing field. The results from this research are considered to be of limited relevance for this thesis. However, the piles from the Overamstel testing field were mechanically extracted after they had been in the ground for approximately 2 years and later they were made available for further research.

3.2 Pile segmentation and coding system

The piles are cut into segments to make it easier to transport and store. Each pile was sawn into three main parts after the extraction at its location of origin: the head (K), the middle (M) or the tip (V). For example, a 12 meter timber pile is divided into three main parts (K, M & V) of approximately 4 meters each. The parts were then transported to the TU Delft research location.

All the main parts were examined and subjected to large-scale compression tests as part of the research conducted mainly by Dr. Ir. G. Pagella at the TU Delft research location [10], see section “2.5 Preceding research TU Delft” for further information. The large-scale compression tests were done on sub-parts with a length of approximately six times the pile diameter, as prescribed by standard EN 14251. For this purpose, each main part is sawn into smaller sub-parts to create a segment that meets this requirement. The head and middle part were often divided into three sub-parts and the tip was divided into three, four or even five sub-parts, depending on what was practical during execution.

Each segment has a unique code so they can be kept apart and identified at the storage location. The coding system consists of three parts, see Figure 3.2.

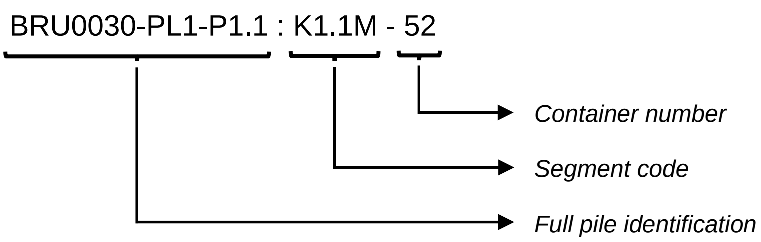

Figure 3.2: Example of the coding system used for the pile segments

The full pile identification code provides information about the former location of the pile such as the number of the bridge and the row position in the foundation layout. The segment code holds information about the part where the segment is sawn from. The container number gives the current location where the pile segment is stored.

The denotation of the segment code will be explained in more detail. The first letter of the segment represents the location of the main part compared to the whole pile: the head (K), the middle part (M) or the tip (V). The digits indicate the pile code which is taken from the full pile identification number. The last letter represents the location of the sub-part in relation to the main part.

In Figure 3.3 it can be seen that the piles were first divided into three main parts and then each main part was divided into sub-parts.

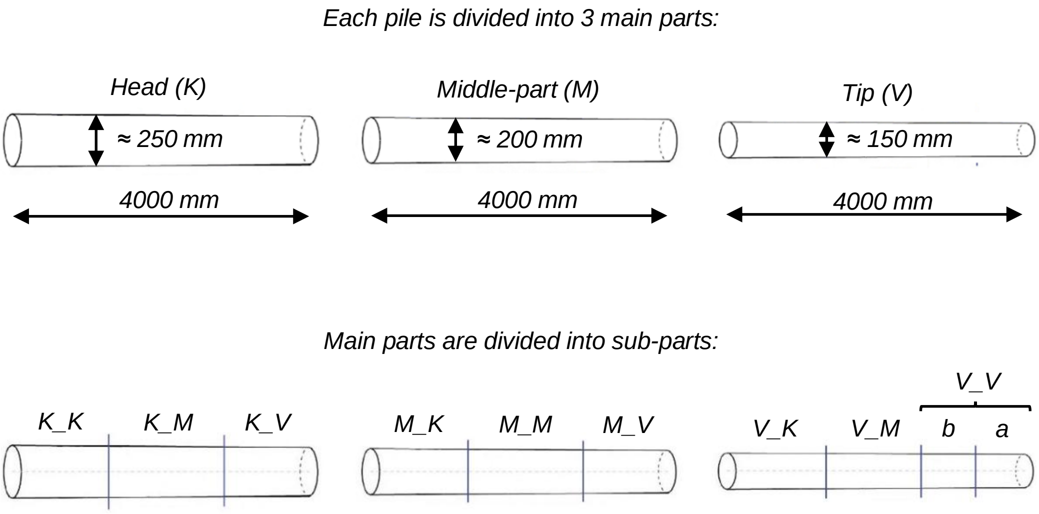

Figure 3.3: Dividing a pile into segments with corresponding segment codes

After the segmentation and the large-scale compression tests, a number of other smaller experiments were carried out by researchers Ir. M. Lee [32] and Ir. C. Gambarin [12] of the TU Delft. Their research involved experiments on small discs and rectangular prisms taken from the segments, see section “2.5 Preceding research TU Delft” for a brief description.

3.3 Selection and sample size

Overall there were 87 timber piles available to be tested for this study. Unfortunately it was not possible to perform tests on all available piles within the time frame of this research and a total of six piles were selected.

It was decided to test piles of the same tree species in order to make the results better suitable to be compared afterwards. Only spruce (picea abies) piles are included in this research as this is the most common species used for timber foundation piles. The aim is to gain insight into the effect of service life and degradation on the mechanical properties of the piles. The chosen six piles have a different service life and different levels of decay.

Discs were taken from these six piles to perform small-scale compression tests. The discs come from different locations over the length of the pile to get an impression of the properties along the pile. Also, discs were sawn from sections with a high knot ratio and from sections without knots so it is possible to examine the differences. A minimum of six discs were taken from each pile, see Figure 3.4.

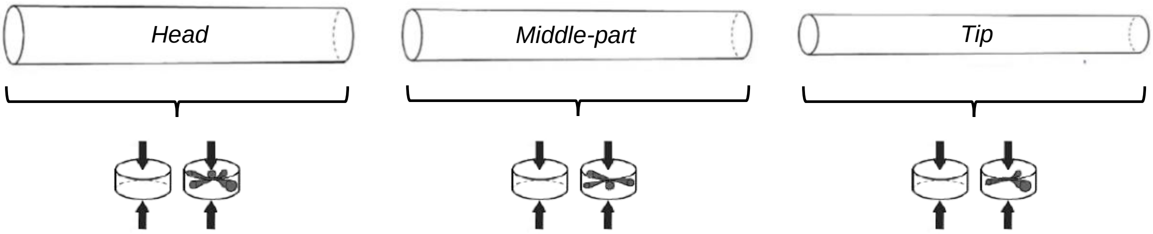

Figure 3.4: Illustration of discs sawn from one timber pile

The results from the small-scale compression tests performed on discs will be compared with the results from the large-scale compression tests performed on segments, as conducted by Dr. Ir. G. Pagella [24]. In this way, it can be investigated whether the results from the small-scale compression tests provide a good approximation of the pile properties. The focus is on the segments that were previously tested during the large-scale compression tests and to take discs from these segments. A total of 20 segments were selected for this research. Close attention is paid to where the segment had previously failed during the segment compression test. The discs have been taken from locations away from the failed and damaged areas to ensure that the wood structure has remained intact.

A total of 45 discs were sawn and tested for this research. If a disc does not contain knots, it is called a clear wood specimen which is indicated with the letters CW. If a disc does contain knots, it is indicated with the letter K. An overview of the selected spruce piles and all discs that were extracted can be found in Table 3.1.

Table 3.1: Run-through of spruce piles, segments and discs selected for the research [24]

Full pile identification	Pile code and container no.	Building year	Service life	Segment	Remaining sound section	Level of decay*	Discs taken from segment
BRU0030-PL2-P2.19	5-228	1727	294 years	K5M	78%	Moderate	CW and K
				M5M	76%	Moderate	CW, K1 and K2
				V5M	49%	Severe	CW, K1 and K2
BRU0030-PL2-P2.21	6-228	1727	294 years	K6M	74%	Moderate	CW and K
				M6M	51%	Severe	CW and K
				V6M	46%	Severe	CW and K
BRU0030-PL1-P3.18	3.18-115	1886	135 years	K3.18M	88%	Low	CW and K
				M3.18M	100%	Low	CW and K
				V3.18M	99%	Low	CW and K
BRU0030-PL1-P5.1	5.1-52	1886	135 years	K5.1M	79%	Moderate	CW, K1 and K2
				M5.1M	92%	Low	CW, K1 and K2
				V5.1M	77%	Moderate	CW, K1 and K2
BRU0041-PL2-P1.13	1.13-52	1922	99 years	K1.13M	76%	Moderate	CW and K
				M1.13M	95%	Low	CW and K
				V1.13M	83%	Moderate	CW and K
OAM-P1.4	1.4-235	2019	2 years	K1.4M	100%	Low	CW and K
				M1.4K	100%	Low	CW and K
				V1.4K	100%	Low	CW and K
				V1.4Vc	100%	Low	CW and K
				V1.4Vb	100%	Low	CW and K

** Level of decay: Low level of decay if remaining sound section is higher than 85%*
Moderate level of decay if remaining sound section is between 65% and 85%
Severe level of decay if remaining sound section is lower than 65%

There are 2 piles from 1727: pile 5-228 with a moderate level of decay and pile 6-228 with a severe level of decay. Also, there are 2 piles from 1886: pile 3.18-115 with a low level of decay and pile 5.1-52 with a moderate level of decay. In addition there are pile 1.13-52 from 1922 and pile 1.4-235 from 2019, both with a low level of decay. Note that there are no piles from 1727 available with a low level of decay and there are no piles from either 1886 or 1922 with a severe level of decay, therefore this could not be included in this research.

As far as is known, these piles have only remained below the water level, which means that no fungal degradation could have occurred. It is assumed that all degradation that is present is due to bacterial attack.

Piles 5-228, 6-228, 3.18-115 and 5.1-52 were extracted from the foundation of bridge 30 and pile 1.13-52 comes from the foundation of bridge 41. These piles have been exposed to compressive loads from the bridge and the passing traffic for different service lives.

Pile 1.4-235 originates from the Overamstel testing field where it was subjected to a compressive force of about 350 kN for less than a day and the pile was positioned in the ground for just under two years.

Most segments account for two discs: one CW and one K. However, three discs have been sawn from the segments M5M, V5M, K5.1M, M5.1M and V5.1M: one CW and two K.

Previous small-scale compression tests have been carried out by Ir. C. Gambarin [12] on discs with a height of 100 millimeters. After consideration it seemed better to choose a value that is a bit higher. A height of 150 millimeters is chosen for this research because then it is sufficiently high to allow all the knots and surrounding deviations of the grain to be captured in the specimen.

3.4 Relevant data from preceding research

The selected 20 segments have all been tested in large-scale compression, as performed by Dr. Ir. G. Pagella [24]. The results of these tests are relevant and can be used to analyse the results of the small-scale compression tests.

A distinction is made between physical properties and mechanical properties. The physical properties of the segments are presented in Table 3.2.

Table 3.2: Physical properties of the selected segments [24]

Pile	Segment	Length segment L [mm]	Average diameter D_{avg} [mm]	Average soft shell SS_{avg} [mm]	Age [years]	Rate of growth RoG [mm/year]	Wet density ρ_{wet} [kg/m^3]	Dry density ρ_{dry} [kg/m^3]	Moisture content u [%]
5-228	K5M	1350	198.4	11.6	58	1.49	680	339	121
	M5M	1350	184.1	12.0	49	1.69	701	354	118
	V5M	1355	149.6	22.3	39	1.70	768	336	151
6-228	K6M	1350	211.7	15.0	56	1.73	648	362	97
	M6M	1350	183.6	26.0	48	1.68	671	335	120
	V6M	900	145.3	23.3	38	1.65	716	337	133
3.18-115	K3.18M	1350	240.9	7.3	84	1.22	582	411	56
	M3.18M	1350	221.8	0.0	71	1.32	595	429	52
	V3.18M	1350	182.5	0.6	55	1.40	668	400	84
5.1-52	K5.1M	1800	270.6	15.4	76	1.51	784	479	80
	M5.1M	1800	254.6	4.9	66	1.62	933	366	181
	V5.1M	1350	193.1	12.1	58	1.39	771	351	141
1.13-52	K1.13M	1800	255.7	16.6	98	1.10	659	451	61
	M1.13M	1350	228.1	2.9	77	1.26	689	470	61
	V1.13M	1350	205.3	9.2	68	1.25	644	425	67
1.4-235	K1.4M	1800	281.7	0.0	42	3.03	779	495	74
	M1.4K	1350	259.4	0.0	37	3.44	716	380	109
	V1.4K	1350	221.2	0.0	28	3.54	709	402	104
	V1.4Vc	1350	200.5	0.0	24	3.98	657	390	85
	V1.4Vb	1350	174.5	0.0	21	3.93	619	391	75

Generally there are three different lengths for the segments: 900 mm, 1350 mm or 1800 mm. The length is chosen to be approximately six times the average diameter. The thickness of the soft shell of each segment is measured by using a micro-drill. This value of the soft shell was used to determine the level of decay as presented in Table 3.1.

The density and moisture content of each segment is determined by cutting a disc from both sides, weighing it and taking the average value. The discs were 30 mm thick and contained no defects.

The mechanical properties of the segments are shown in Table 3.3.

Table 3.3: Mechanical properties of the selected segments [24]

Pile	Segment	Failure at section with knots?	Matching knot ratio KR [-]	Maximum force F_{max} [kN]	Max stress section $f_{c,0\ wet}$ [N/mm²]	Max stress sound part EQ $f_{c,0\ wet}$ [N/mm²]	MOE static $E_{c,0\ stat}$ [N/mm²]	MOE dynamic $E_{c,0\ dyn}$ [N/mm²]
5-228	K5M	Yes	0.114	333.9	10.8	13.8	7750	7862
	M5M	Yes	0.068	228.9	8.6	11.4	6323	6668
	V5M	Yes	0.273	130.1	7.4	15.0	5495	5928
6-228	K6M	Yes	0.074	344.9	9.8	13.3	8299	8639
	M6M	No	-	166.7	6.3	12.3	4591	5691
	V6M	Yes	0.266	109.4	6.6	14.3	4230	4680
3.18-115	K3.18M	No	-	678.9	14.9	16.9	10766	11398
	M3.18M	No	-	549.2	14.2	14.2	10179	10935
	V3.18M	No	-	316.5	12.1	12.2	8990	10434
5.1-52	K5.1M	Yes	0.115	678.4	11.8	15.0	7650	7918
	M5.1M	Yes	0.202	559.2	11.0	11.9	8058	8327
	V5.1M	Yes	0.244	295.8	10.1	13.2	7836	7334
1.13-52	K1.13M	Yes	0.069	924.4	18.0	23.8	11917	12213
	M1.13M	Yes	0.040	756.1	18.5	19.5	12672	12470
	V1.13M	Yes	0.072	509.8	15.4	18.6	10250	10137
1.4-235	K1.4M	No	-	963.1	15.5	15.5	9198	9916
	M1.4K	Yes	0.150	800.3	15.1	15.1	8718	9124
	V1.4K	Yes	0.221	530.2	13.8	13.8	7563	8325
	V1.4Vc	Yes	0.196	433.4	13.7	13.7	6889	8003
	V1.4Vb	Yes	0.278	332.9	13.9	13.9	6874	8069

Most of the segments failed at a section with knots which indicates that the defects govern the strength. The corresponding knot ratio of the failed sections are given in the table.

The highest force occurs at the head of the pile and this gradually decreases towards the pile tip, due to the change in size and surface area. Here the maximum stress of the section is determined by taking the whole cross-sectional area into account. The maximum stress of the sound part is calculated by assuming that the soft shell has zero strength and all of the force is carried by only the remaining sound part. The highest stress of the sound part lies between the 11.4 and 23.8 N/mm^2.

The static modulus of elasticity (static MOE) is derived from the results of the large-scale compression test. The dynamic modulus of elasticity (dynamic MOE) was determined in-situ with the frequency response method, by using a timber grader (MTG) tool on the full length of the pile. Both represent the short-term response of the pile and they show a similar trend which means that the values are a reliable estimate for the MOE.

4. Methodology

Procedures and equipment for testing the timber foundation piles.

4.1 Collecting and sawing

During this research, discs are sawn from timber foundation pile segments after which they are subjected to tests. The segments that were selected for this study are listed in section “3.3 Selection and sample size”. Most of the segments had to be found and sorted at the storage location in Vlaardingen, see Figure 4.1. The required segments were transported to the TU Delft Macro laboratory, also known as the Stevin laboratory, located at Stevinweg 1 in Delft. All relevant segments are stored together in the basement of the Stevin laboratory from where they are available for sawing and testing.

Storage location in Vlaardingen *Storage basement at Stevin laboratory in Delft*

Figure 4.1: Storage location Vlaardingen and storage basement at Stevin laboratory Delft

The segments are investigated in order to find out its orientation in comparison to the entire foundation pile. This is done by looking at the pictures of the piles taken during the different stages of segmentation and comparing them to the segments that are present in the basement. In some cases it was difficult to determine which side of the segment was top or bottom because some of the labels were removed and turned around.

After the orientation is known, the focus shifts to mapping the positions and sizes of all the knots. The surface width of each knot is measured with a calliper perpendicular to the axis of the pile, see Figure 4.2. Only the width of the actual knot is measured and the deviations of the fibres around the knot are not considered. The circumference of the pile is measured with a tape measure by pulling it tight around the pile. In general there are some bumps on the pile due to the presence of the knots, therefore the circumference is measured just next to the knot in question to get a more consistent value.

Finding the knot width with a calliper *Finding the circumference with a tape measure*

Figure 4.2: Measuring with a calliper and a measuring tape

The measurements of the knot width and the circumference are rounded to the nearest whole millimeter. They are used to calculate the knot ratio:

$$KR = \frac{\sum_{i=1}^{n} d_i}{C} \qquad (4.1)$$

Where:

KR	$[-]$	:	Knot ratio
d_i	$[mm]$	:	Surface width of the knot
n	$[-]$	:	Amount of knots in one segment
C	$[mm]$	:	Circumference of the section

Note that during this phase the wood is kept at an indoor climate in the basement. The moisture content of the wood is not known at this point but it is somewhere between the oven-dry point and the fibre saturation point. The measurements taken are only used for the calculation of the knot ratio. The values of the knot ratios are compared with each other which can be done because all the segments are kept in the same indoor climate at the same humidity level.

Now that the knot ratios are known, it can be decided where to saw the discs. The discs are sawn from segments that are previously subjected to large-scale compression tests. During the compression tests the failure mainly occurred at a location with knots and most of the cracks formed just above or below the actual knots. When searching for suitable locations for the discs, the location of the damaged parts are taken into account and the discs are cut away from the damaged parts.

All discs will have a height of 150 millimeters. A distinction is made between clear wood discs without knots (CW) and discs with knots (K). An overview of the locations of the knots, the knot ratios and the locations of the discs can be found in Appendix A.

The clear wood discs (CW) are sawn as far away from all the knots as possible. However, sometimes the knots are so close together that it is not possible to get a disc of 150 mm without any knots. In these cases it was decided to keep the center of the disc without knots as much as possible, while there may be some defects in the wood structure on the top or bottom of the disc. In this way, the fibre deviations caused by the knots have the least influence on the potentiometers that measure the strain in the middle of the disc during the small-scale compression tests.

The knotted discs (K) are sawn from the sections with the highest knot ratios. The group of knots is captured in the middle of the 150 mm disc height. The distance from the last knot to the end of the disc is approximately the same at the bottom and the top of the disc. In some cases, a second disc with knots has been cut from the segment. The second knotted disc is sawn from a section with an intermediate knot ratio, not too close to the highest knot ratio, in order to see how it behaves during the small-scale compression test.

First all of the discs are sawn with a height just above the 150 mm, this rough cut is done with an electric chainsaw. Because every disc has the same height, it is decided to build a sawing jig to keep every cut uniform and to keep it stable during handling, see Figure 4.3.

Each segment is consecutively placed in the jig, the pith is aligned horizontally on both ends, the segment is fixed in the jig with F-clamps and the chainsaw cuts vertically downwards. There is a laser to make sure that the chainsaw makes the cut perpendicular to the axis of the pith. After the first cut, the chainsaw is moved backwards just over 150 mm along a horizontal rail while the segment remains fixed. Then the second cut is made, exactly parallel to the first cut and perpendicular to the pith. All the discs are close to the needed height after doing all the rough cuts. A thickness planer is used on one side of the discs to give all the discs the exact correct height of 150 mm.

Sawing jig *Cutting the discs* *Thickness planer*

Figure 4.3: Process of sawing the discs from the segments

After the sawing process, each disc looks fresh and the growth rings are clearly visible, especially on the side that has been worked on by the thickness planer. Also all the knots and other defects can be seen. Some photographs and physical properties of the individual discs can be found in Appendix B.

A permanent marker is used to draw two axes A and B on the top side of each disc. These axes have their origin in the pith and run perpendicular from each other. These axes are used later on for the micro-drilling measurements and as a grid to measure the radii.

4.2 Submerging the discs

Now that all discs are sawn, they are labelled and stored in a black tub. The tub is filled with water and clamps are needed to hold the discs underwater, see Figure 4.4.

Labelled discs in tub *Tub filled with water and clamps*

Figure 4.4: Discs are labelled and submerged in water

The discs are stored submerged in water to mimic the same conditions like when they were in the soil. The aim is to keep the moisture content way above the fibre saturation point to prevent any changes in the wood structure during the following tests. It takes approximately 2 weeks for the discs to get to their maximum mass and thus to reach the water saturation point. The discs are weighed using an electric scale and the mass is recorded with an accuracy of 0.1 g.

The radius of each disc is measured in four directions from the pith to the perimeter, along the axes of A and B. Two transparent triangular rulers are put on the top cross-section of the disc and the center point is put on the pith, see Figure 4.5. The measurements of the radii are taken in whole millimeters and are only used for the calculation of the radial shrinkage.

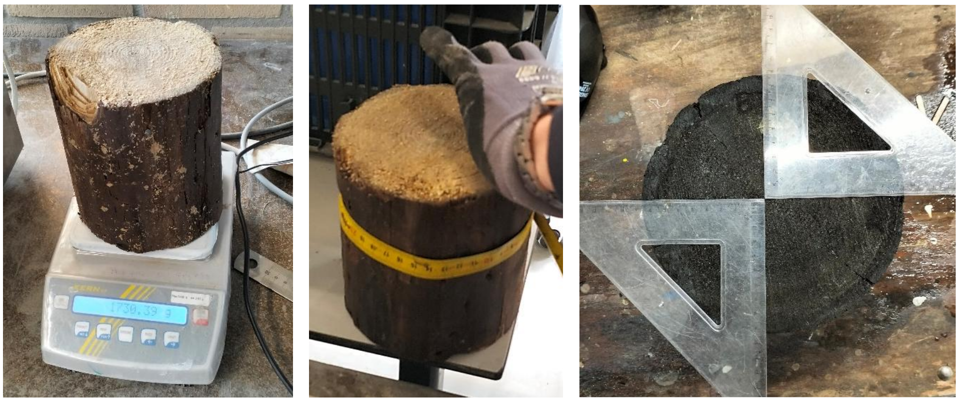

Figure 4.5: Measuring the weight and the dimensions of the saturated discs

The other wet dimensions of the discs are quantified using a measuring tape and all values are rounded off to the nearest millimeter. Measuring the circumference in the middle of the disc does not always give a representative value, especially for the discs with knots where the remnants of the branches make the surface irregular. Therefore, the circumference is measured on the top side and on the bottom side of each disc. A measuring tape is used and pulled tight around the disc to get a precise measurement. Both of the values for the top and bottom circumference are converted to an average circumference.

The formulas for the average diameter, the cross-sectional area and the volume of each disc:

$$D_{avg,\ wet} = \frac{C_{avg,\ wet}}{\pi} \tag{4.2}$$

$$A_{wet} = \frac{{C_{avg,\ wet}}^2}{4 * \pi} \tag{4.3}$$

$$V_{wet} = \frac{h_{wet} * {C_{avg,\ wet}}^2}{4 * \pi} \tag{4.4}$$

Where:

$D_{avg,\ wet}$	$[mm]$	:	Average wet diameter
$C_{avg,\ wet}$	$[mm]$	:	Average wet circumference
A_{wet}	$[mm^2]$	:	Wet cross-sectional area
V_{wet}	$[mm^3]$	:	Wet volume
h_{wet}	$[mm]$	:	Wet height

When the shape of a disc is non-circular, the diameter of the disc will change depending to where it is measured. However, the circumference still gives a good representative value for the section. So even though the shapes of the discs are not perfectly circular, the formulas still give a good value because the average circumference is used as the main input.

The wet density of the disc can be calculated by dividing the weight of the saturated disc with the wet volume of the disc:

$$\rho_{wet} = \frac{m_{wet}}{V_{wet}} \tag{4.5}$$

Where:

ρ_{wet}	$[g/mm^3]$	:	Wet density
m_{wet}	$[g]$	:	Wet mass
V_{wet}	$[mm^3]$	:	Wet volume

The values regarding the dimensions of the discs are listed in Appendix B. The information regarding the radii and the weight of the discs are presented in Appendix E.

4.3 Integrity testing

Integrity tests are done to find the thickness of the soft shell and to detect any potential defects in the wood structure of the discs. The way this is examined is by applying micro-drilling measurements. In addition, a handheld piercer tool is used to investigate the thickness of the soft shell and to compare it with the data from the micro-drilling measurements, see Figure 4.6.

Test with micro-drill *Transfer micro-drill data to laptop* *Test with piercer tool*

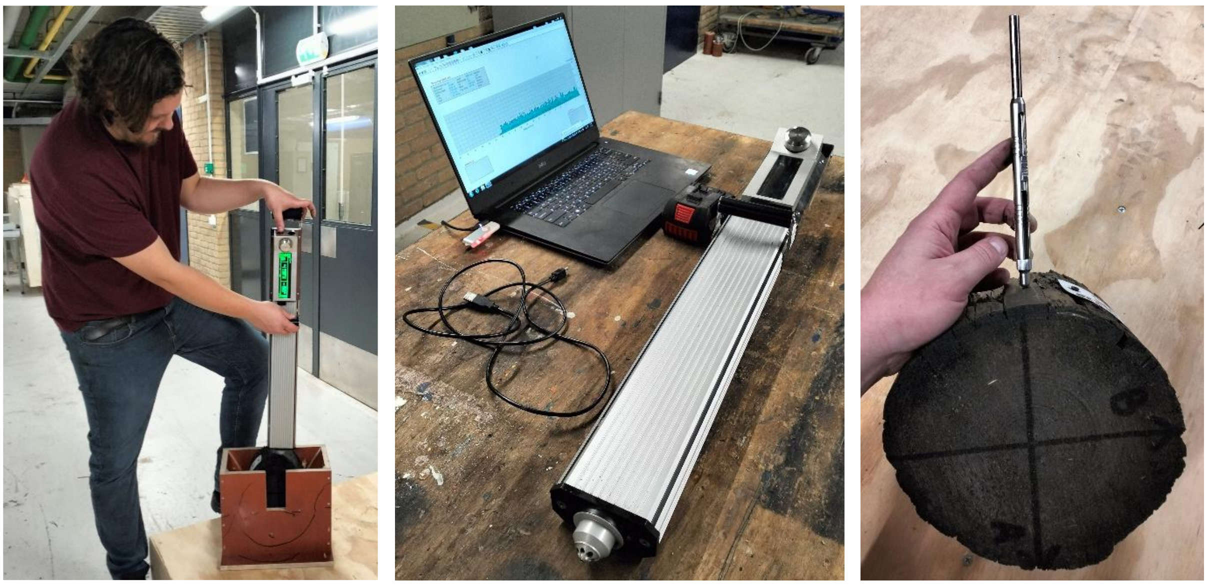

Figure 4.6: Integrity testing of the discs

Only the clea rwood discs will undergo integrity tests because these are most representative for the rest of the segment. The knots in the other discs cause differences in fibre direction and density which can locally deviate a lot and may lead to abnormal results during the integrity tests. It is assumed that the results of the clear wood disc are also relevant for the corresponding disc with knots and the same data is used for both.

The type of micro-drill that is used is the IML-RESI PowerDrill 400 which is produced by the German company Instrumenta Mechanik Labor System (IML). Each drill bit has a hard chrome coating with a length of 400 mm, a diameter of 1.5 mm and a 3.1 mm wide triangular shaped drill point. The drill is set to rotate at 2500 r/min and to penetrate the wood at 150 cm/min, while recording the wood resistance at every 0.1 mm along the depth.

The tests are performed on wet discs at water saturation point. Each disc is drilled vertically down through the middle while the disc sits stable in a small jig. After the first measurement, the disc is rotated 90 degrees and the disc is drilled a second time. This results in a total of two micro-drilling measurements A and B for each CW disc, both taken approximately perpendicular to each other.

The piercer tool is made from stainless steel, has a 1.5 mm wide probe with a rounded tip and a maximum penetration depth of 85 mm. It is used right next to the entry hole and the exit hole of each micro-drilling measurement. The probe is gently pushed into the wood structure until it is no longer able to go in and the penetration depth can be read from the ruler on the back. This results in a total of four measured values for the soft shell thickness taken around the surface of the disc.

The data from the micro-drill is transferred to a computer and loaded into the “soft shell calculator” software for further analysis, see Figure 4.7. This software uses a series of steps to determine the thickness of the soft shell layer [30]. First, the resistance of the drill is plotted against the drilling distance. The length of the drill path is entered manually so the graph is cut off at the left and right threshold (LT and RT). It draws a line at the center of the graph and it assumes that the wood structure near the center is sound. Then, it determines an incremental outwards moving average (IOMA or drill_MA) of the drill resistance by going from the center to the left and right side. The maximum value of the IOMA on each side is used to divide the corresponding half of the graph into four zones. Zones 1, 2, 3 and 4 correspond respectively to 20%, 40%, 60% and 80% of the resistance in comparison to the maximum IOMA on that side. Lastly, the thickness of the soft shell is defined as the width of zone 1 and zone 2 together. Each micro-drilling measurement results in two values for the soft shell thickness, one upon entering the wood and one when it leaves the wood, so a total of four values per disc.

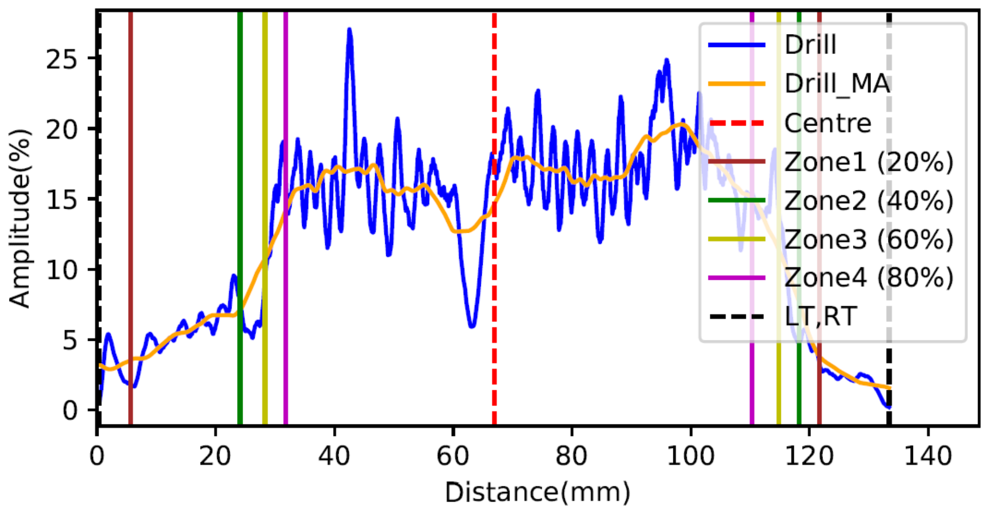

Figure 4.7: Example of output from the "soft shell calculator" software for disc V6M A

Because the IOMA uses the variances of the signal instead of looking at the absolute values, it can provide good values for the soft shell thickness even when some deviations are present in the wood structure. For example, in disc V6M there is a small heart shake at the center of the disc which is visible in the graph of path A as a lower signal around 62 mm of the distance. By using the IOMA the brief lower signal does not influence the location of the zones and thus the calculation of the soft shell thickness.

All the graphs from the micro-drill and the corresponding data is presented in Appendix C.

The micro-drilling method and the piercer tool method each result in four values for the thickness of the soft shell. The four values are turned into an average value, so each method has its own average soft shell thickness.

The area of the sound inner part is considered to be circular and can be found by subtracting the soft shell from the whole cross-sectional area. This is done by taking the diameter of the sound inner part and then calculate the area:

$$A_{sound} = \frac{\pi * (D_{avg,\ wet} - 2 * SS_{avg})^2}{4} \tag{4.6}$$

Where:

A_{sound}	$[mm^2]$	:	Crosss-sectional area of the sound part
$D_{avg,\ wet}$	$[mm]$	:	Average wet diameter
SS_{avg}	$[mm]$	:	Average thickness of the soft shell

The level of decay can be determined by looking at the ratio between the area of the sound inner part and the total area of the disc:

$$p\ A_{sound} = \frac{A_{sound}}{A_{tot}} * 100 \tag{4.7}$$

Where:

$p\ A_{sound}$	$[\%]$	:	Percentage of sound cross-sectional area
A_{sound}	$[mm^2]$	:	Crosss-sectional area of the sound part
A_{tot}	$[mm^2]$	:	Total cross-sectional area

There are three different levels of decay that are considered [24]:

$p\ A_{sound} > 85\%$	Low level of decay
$65\% \leq p\ A_{sound} \leq 85\%$	Moderate level of decay
$p\ A_{sound} < 65\%$	Severe level of decay

The values from the micro-drill are the most accurate and these are used in further calculations. Only the clear wood discs were tested with the micro-drill but the same values for the thickness of the soft shell are also used to describe the decay on the knotted discs of the same segment. The values from the piercer tool are solely used for comparisons and will not be used in further calculations.

4.4 Compression testing

Compression tests are carried out to investigate the mechanical properties of the discs. This is done by putting the discs in a compression bank and measure the strain while increasing the load until failure occurs.

The compression bank is made by the German company Toni Technik and is located at the concrete section of the Macro laboratory, see Figure 4.8. The machine has a height-adjustable top plate and applies pressure with a hydraulic jack positioned under the bottom plate. It has a closed cabinet around the testing area, which means that it is not possible to open the cabinet when the loading-heads are moving. The top plate is hinged and is able to rotate during the compression tests to make sure that the compressive force is distributed evenly. A computer is used to control the compression test and to record the data. The data is recorded with an accuracy of 0.1 N for the load increase and 1 ms for the time.

Compression bank and computer *Cabinet and testing area* *Specimen before a test*

Figure 4.8: Compression testing of the discs

The strain is measured with linear potentiometers, also known as linear variable differential transformers (LVDT). A total of four linear potentiometers, numbered from D1 to D4, are attached to the sides of each disc approximately 90 degrees apart from each other. They are positioned between the knots as much as possible to prevent any irregular results. A schematic representation of the test set up is presented in Figure 4.9.

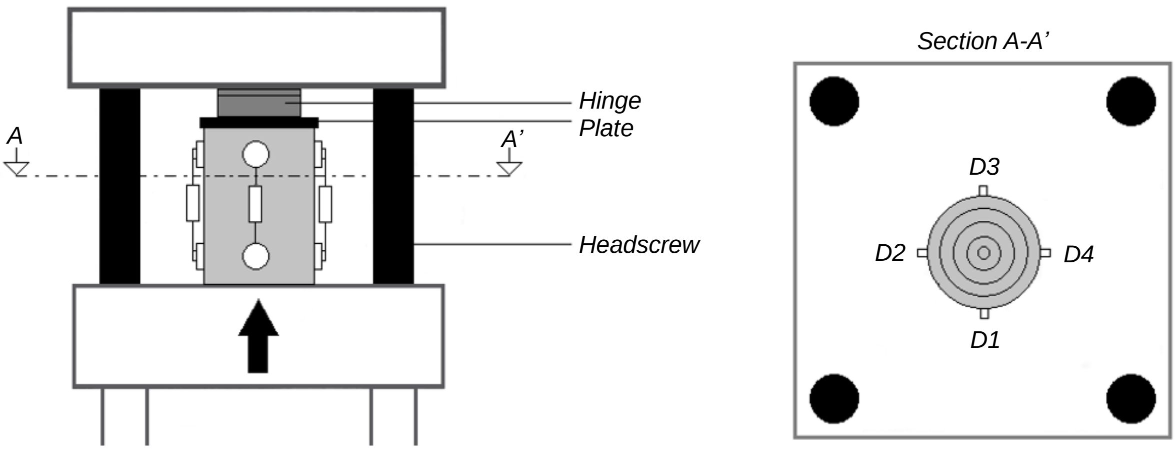

Figure 4.9: Schematic set up for compression testing of the discs

Each linear potentiometer is positioned so it only measures the strain in the middle of the disc. In this way, the deformations that occur due to the introduction of the compressive force near the top plate and bottom plate are not included in the measurements. The linear potentiometers have a stroke of only 2 mm and in some cases it was needed to remove them during the test to prevent damages when they run out of range. However, in all cases the stroke was sufficient to measure the strain in the elastic region which is needed to determine the elasticity of the specimen. Note that there were other linear potentiometers available with a larger stroke but it was not possible to use them because their housing did not fit between the loading plates.

The linear potentiometers are attached to the side of the discs with brackets and screws. Two metal brackets are needed for each potentiometer, one on the top to hold the potentiometer in place and one on the bottom as a barrier to measure the strain. Each bracket is secured with two screws and the screws have a size of 3.5 x 45 mm which is long enough to get the brackets fixed through the soft shell. The gauge length is considered to be the distance between the center of the screws of the two bracket, because that is where the constraints of the linear potentiometer are physically attached to the structure of the wood. In case of the linear potentiometers the gauge length is 60 mm, see Figure 4.10.

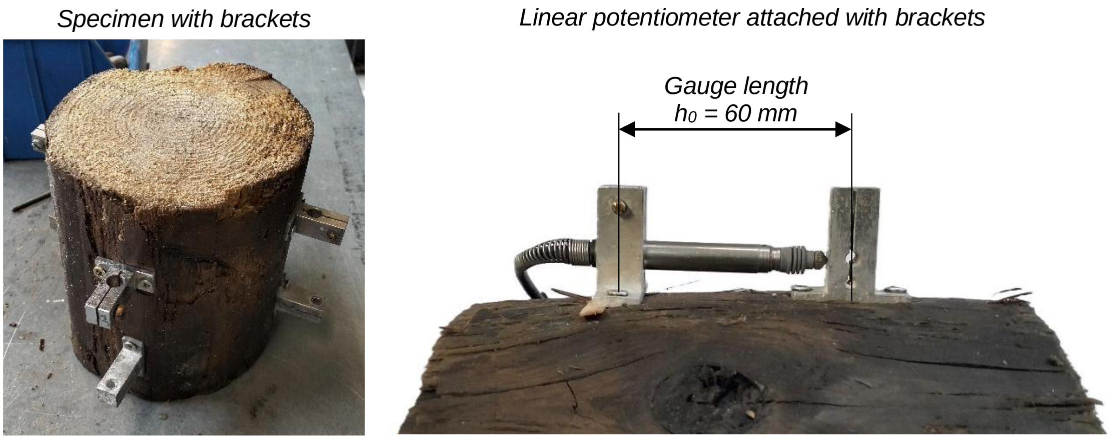

Figure 4.10: Linear potentiometer mounted to the side of the discs

A preloading is applied two times at the beginning of each disc compression test. This is done to get a better response from the disc that is more representative to the conditions when they are in use. The discs are part of a foundation pile that was loaded for a long time. Now that it is kept out of the ground and soaked in water it could be that the wood structure loosened up a bit. The preloading is used to get rid of the slack at the beginning of the test.

For the first preload, the compression bank goes on until about 25% of the maximum load that was present during the previous segment compression test. After this, the first preload is lowered until approximately 10 kN remains. Then the second preload is applied, again compressing up to about 25% of the maximum load and releasing it to approximately 10 kN. Now the specimen is ready for the compression test until failure occurs.

The speed of the compression machine needs to be chosen so the failure occurs between 180 and 420 seconds, as explained in standard EN 14251. The tests that were run first had a speed of 0.015 mm/s. After testing four specimens (discs V5M K2, K5.1M K2, V5.1M K2 and V1.4Vc CW) it turned out that the failure occurred a bit too fast. The following remaining 41 discs are tested with a speed of 0.010 mm/s and the failure occurred within the set time limit.

The moment of failure is considered to be the point when the maximum load is reached. After that, the deformations increase while the force drops and cracks occur. The test will continue for a while to make sure that it was indeed the highest force and to see the development of the cracks. The maximum load is divided by the wet cross-sectional area to get the value for the wet compressive strength:

$$f_{c,0\,wet} = \frac{F_{max}}{A_{wet}} \tag{4.8}$$

Where:

$f_{c,0\,wet}$	$[N/mm^2]$	:	Wet compressive strength
F_{max}	$[N]$	:	Maximum load
A_{wet}	$[mm^2]$	:	Wet cross-sectional area

The wet cross-sectional area also includes the soft shell of the disc. Generally, the soft shell has a lower density and a lower strength in comparison with the remaining sound section. When it is assumed that the soft shell does not carry any load, then the equivalent wet compressive strength of the remaining sound wood is calculated:

$$EQ\ f_{c,0\,wet} = \frac{F_{max}}{A_{sound}} \tag{4.9}$$

Where:

$EQ\ f_{c,0\,wet}$	$[N/mm^2]$	:	Equivalent wet compressive strength
F_{max}	$[N]$	:	Maximum load
A_{sound}	$[mm^2]$	:	Cross-sectional area of the sound part

The results of each disc compression test is presented in a load deformation diagram where all the preloads and the maximum loads are made visible. Also the elastic and plastic regions can be distinguished. All the data and the graphs from the disc compression tests are presented in Appendix D.

The slope of the load deformation curve in the elastic region is used to determine the modulus of elasticity. The slope is considered between 10% and 40% of the maximum force, which excludes the plastic region and also irregularities from the beginning of the test. A linear regression line is plotted over each data set to get a representative value for the slope. The modulus of elasticity can be calculated with the following formula:

$$E_{c,0} = \frac{m * h_0}{A_{wet}} \tag{4.10}$$

Where:

$E_{c,0}$	$[N/mm^2]$	:	Modulus of elasticity
m	$[N/mm]$	:	Slope of load deformation curve
h_0	$[mm]$	:	Gauge length
A_{wet}	$[mm^2]$	:	Wet cross-sectional area

Two methods are considered to determine the modulus of elasticity, the first one is by looking at the displacement of the jack and the second one is by examining the average strain of the linear potentiometers. When the displacement of the jack is considered, the length over which the deformation is measured is the full height of the 150 mm disc. When the strain of the linear potentiometers is investigated, the gauge length is 60 mm.

Only the average strain from the linear potentiometers is used in the calculation of the modulus of elasticity. Because the disc is compressed with a hinged top plate, the disc can deform which causes elongation on one side and shortening on the other side. The data from the individual linear potentiometers are not useful because they describe a very local behaviour. But by looking at the average strain measured on all sides it is a representative value for the disc.

4.5 Oven-drying the discs

The last part for obtaining the data for the research consists of drying the discs, taking the dry weight and dimensions. The discs are dried in a big industrial oven at a constant temperature of 103 °C (± 2), as described in the standard NEN-EN 13183-1. There is enough free space around the discs and the trays are perforated to make sure the hot air can circulate and the moisture can evaporate more efficiently, see Figure 4.11. Some of the discs are weighed during the drying process to check if they are still releasing any moisture. The oven-dry point is reached when the mass does not change more than 0.1% between two measurements that are at least 2 hours apart. The drying time was different for each specimen, because some discs have a larger diameter and other discs contain more resin which takes more time to dry. Eventually all discs reached the oven-dry point after about 3 weeks of drying.

Big oven filled with discs *Discs after oven-drying process*

Figure 4.11: Oven-drying of the discs

The discs are weighed directly after coming out of the oven with an electric scale and the mass is recorded with an accuracy of 0.1 g. The difference in mass between the disc at water saturation point and oven-dry point is considered to be the amount of water loss. This is the amount of water that was present in the disc during the integrity testing and the disc compression testing.

The moisture content is a percentage that represents the amount of water that is present when the disc is at water saturation point. It is calculated by looking at the difference in mass between the wet and dry discs, as described in standard NEN-EN 13183-1. The difference in wet and dry mass is divided with the mass of the oven-dry disc:

$$u = \frac{m_{wet} - m_{dry}}{m_{dry}} * 100 \qquad (4.11)$$

Where:

u	$[\%]$	:	Moisture content
m_{wet}	$[g]$	:	Mass of the wet wood
m_{dry}	$[g]$	:	Mass of the dry wood

The dimensions of the dry discs are measured in the same way as when the discs were wet. Two triangular rulers are used to determine the radii from the pith to the perimeter of each disc as pictured in Figure 4.12. The dimensions are rounded to the nearest whole millimeter.

Weighing discs *Measuring circumference* *Measuring radius*

Figure 4.12: Measuring the weight and the dimensions of the oven-dry discs

The radii of the discs are measured along axes A and B. So the radii of the wet discs and dry discs are taken at the same location and can be compared to determine the radial shrinkage:

$$radial\ shrinkage = \frac{R_{wet} - R_{dry}}{R_{wet}} * 100 \qquad (4.12)$$

Where:

R_{wet}	$[mm]$	:	Radius of disc at water saturation point
R_{dry}	$[mm]$	:	Radius of disc at oven-dry point

The radial shrinkage represents the percentage by which the radius decreases after the drying process. First, the radial shrinkage is calculated four times for each quadrant. After that, the average value of the radial shrinkage is determined for each disc. The average value is representative for each specific disc and can be compared with other discs.

A measuring tape is used to measure the circumference at the top and bottom section. The measuring tape is pulled tight around the outside to get a good reading of the circumference. The values are rounded to the nearest whole millimeter and are converted into an average value. This average circumference is used to determine the average dry diameter, the dry cross-sectional area and the dry volume of each disc:

$$D_{avg,\ dry} = \frac{C_{avg,\ dry}}{\pi} \tag{4.13}$$

$$A_{dry} = \frac{{C_{avg,\ dry}}^2}{4 * \pi} \tag{4.14}$$

$$V_{dry} = \frac{h_{dry} * {C_{avg,\ dry}}^2}{4 * \pi} \tag{4.15}$$

Where:

$D_{avg,\ dry}$	$[mm]$	:	Average dry diameter
$C_{avg,\ dry}$	$[mm]$	:	Average dry circumference
A_{dry}	$[mm^2]$	:	Dry cross-sectional area
V_{dry}	$[mm^3]$	:	Dry volume
h_{dry}	$[mm]$	:	Dry height

Note that the discs have cracks that occurred during the drying process, such as heart shakes and radial shakes. The drying cracks are cavities in the wood structure which makes the calculated values for the cross-sectional area and the volume not completely accurate. However, it is too difficult to take the presence of all the drying cracks into account in the calculations and the used values give a reliable indication.

The volume of the wet disc and dry disc are compared with each other to obtain the volumetric shrinkage:

$$volumetric\ shrinkage = \frac{V_{wet} - V_{dry}}{V_{wet}} * 100 \tag{4.16}$$

Where:

V_{wet}	$[mm]$	:	Volume of disc at water saturation point
V_{dry}	$[mm]$	:	Volume of disc at oven-dry point

It turned out to be hard to map out the longitudinal shrinkage because the height did relatively change very little after the drying process. Also, the height of the dry disc is hard to measure because it can deviate a bit depending on which side is taken into account. The volumetric shrinkage comes mainly from the shrinkage in radial direction.

When the dry weight is divided with the dry volume, the value for the dry density can be calculated. By using the dry volume, there are voids present due to the drying cracks. The value for the dry density becomes less and less representative of the disc in question when the amount and size of the drying cracks increase. That is why also a value for the basic density is calculated. The basic density compares the dry mass with the wet volume because then all the cracks are closed.

The formulas for the dry density and the basic density:

$$\rho_{dry} = \frac{m_{dry}}{V_{dry}} \tag{4.17}$$

$$\rho_b = \frac{m_{dry}}{V_{wet}} \tag{4.18}$$

Where:

ρ_{dry}	$[g/mm^3]$	:	Dry density
m_{dry}	$[g]$	:	Dry mass
V_{dry}	$[mm^3]$	:	Dry volume
V_{wet}	$[mm^3]$	:	Wet volume

The dimensions of the discs are presented in Appendix B. All the information about the weight, the moisture content, the radii and the radial shrinkage is listed in Appendix E.

5. Results

The results of the tests that were performed during the study.

5.1 Assumptions

Before the results and the analysis of the tests are presented, it is important to clarify the assumptions that are done during the processing of the data.

Each disc is a product of nature and there are always some irregularities in the shape and wood structure. The discs have slightly different particulars but they also have a lot of resemblances. Assumptions are made in order to simplify some calculations and to make it easier to analyse the different characteristics of the discs. There are three main assumptions regarding the shape of the discs, the wood structure of the knots and the strength of the soft shell. A schematic overview of the main assumptions are pictured in Figure 5.1.

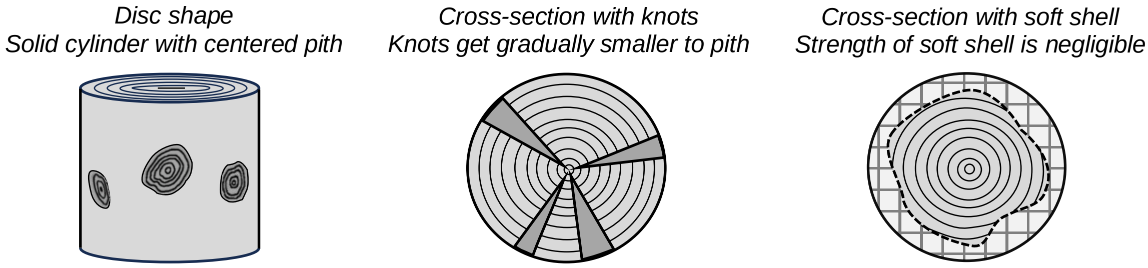

Figure 5.1: Main assumptions regarding disc shape, knots and soft shell

The shape of each disc is assumed to be a solid cylinder with a circular cross-section and a centered pith. This principle is used in the formulas for the cross-sectional area and the volume of the discs. Note that the average circumference is used as the main input for these formulas. The average circumference is a good representative value for the real size of the disc which makes the outcome of the formula a reliable estimate, even when the real shape is not a perfect cylinder.

Saturated discs are considered to be solid because all the cracks are closed due to the swelling of the wood and the cavities are filled with water. However, there are air cavities and empty voids present after the discs went through the oven-drying process. It is too difficult and not feasible to map out all the drying cracks of all the discs. That is why the assumption is made that there are no voids present in the wood structure of the dry discs. It allows for an easy calculation of the dry cross-sectional area and the dry volume. That also means that the value for the dry density is not exactly accurate because the drying cracks are included.

The knot ratio is a characteristic of a section with knots and it represents the percentage of fibres that run in radial direction in contrast to the fibres that normally only run lengthwise. The exact position of how the knots lie inside the wood structure of the discs is not known. However, it is known that they commonly run from the pith to the bark and get wider as they get closer to the bark. That is why it is assumed that each knot is shaped like a isosceles triangle that originate from the pith. This assumption, in combination with a circular cross-section and a centered pith, makes it possible to determine the knot ratio by using only the circumference and the knot surface width.

A piece of decayed wood has a lower strength and elasticity than a piece of undamaged wood. If a section contains both decayed wood and sound wood, then there is an internal redistribution of forces and the stronger sound parts will carry most of the load. After all, the wood will compress due to the load and since the degraded part has a much lower elasticity it will exert hardly any force in comparison to the sound part with a high elasticity. The degraded soft shell will contribute very little to the load-carrying capacity of the wood and that is why it is assumed that the soft shell has zero strength.

The parts of the knots that run through the soft shell layer have a higher density and are often not as degraded as the soft shell itself. Nevertheless, these parts of the knots are located inside the soft shell with low stresses and barely any load transfer. Therefore it is assumed that the part of the knots inside the soft shell layer also have zero strength.

The precise barrier between decayed soft shell and the sound wood is hard to compute. The thickness of the soft shell is measured at four different places around the disc and the values are converted to an average soft shell thickness. Using an average value gives the impression that the thickness of the soft shell is equal around the whole section. When this is combined with the assumption of a circular cross-section, then it can be said that the inner sound part also consists of a circular section.

Level of decay is measured for the clear wood discs only, not for the discs with knots. It is not possible to get a uniform soft shell measurement for a section with knots by using a micro-drill because of all the different wood structures and densities present. However, each segment brought forth a clear wood disc and a knotted disc, which were located not very far apart on the pile. So it is assumed that the level of decay from the clear wood disc is also the same decay that occurs on the discs with knots.

When the previous statements are taken into account, it is possible to make a straightforward visualisation of the load-carrying cross-sectional area for the degraded discs, see Figure 5.2.

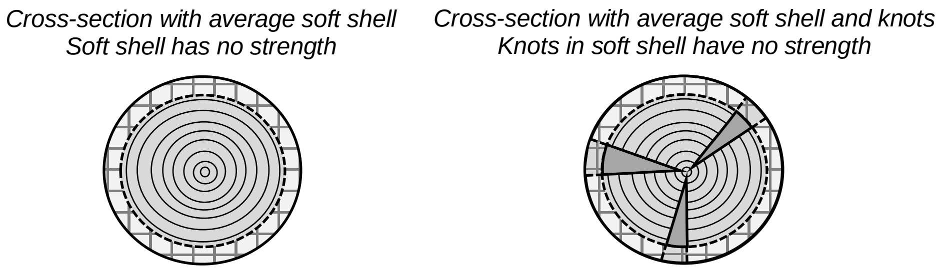

Figure 5.2: Visualisation of the load-bearing cross-sectional area for discs with decay

By using all previous assumptions it can be concluded that the load-bearing cross-sectional area of all discs is assumed to be circular. Here it does not matter if there is any decay and knots present. If there is decay, the remaining sound load-bearing section in the middle of the disc is assumed to be circular. If there are knots, the knot ratio can be calculated by taking the circumference and the knot width which are measured on the outside of the pile. In the case both decay and knots occur at one section, then the sound load-bearing section in the middle is still circular and the value for the knot ratio remains the same.

5.2 Identification and age

There are 45 discs that were used as specimens for the research which were retrieved from a total of six different spruce timber foundation piles. A distinction is made between clear wood discs (CW) and discs with knots (K). The pile identification, service life, age and rate of growth can be found in Table 5.1.

Table 5.1: Pile identification, service life, age and rate of growth

Pile	Full pile identification	Building year	Service life [years]	Segment		Age [years]	Rate of growth RoG [mm/year]	Discs taken from segment
5-228	BRU0030-PL2-P2.19	1727	294	Head	K5M	58	1.49	CW and K
				Middle	M5M	49	1.69	CW, K1 and K2
				Tip	V5M	39	1.70	CW, K1 and K2
6-228	BRU0030-PL2-P2.21	1727	294	Head	K6M	56	1.73	CW and K
				Middle	M6M	48	1.68	CW and K
				Tip	V6M	38	1.65	CW and K
3.18-115	BRU0030-PL1-P3.18	1886	135	Head	K3.18M	84	1.22	CW and K
				Middle	M3.18M	71	1.32	CW and K
				Tip	V3.18M	55	1.40	CW and K
5.1-52	BRU0030-PL1-P5.1	1886	135	Head	K5.1M	76	1.51	CW, K1 and K2
				Middle	M5.1M	66	1.62	CW, K1 and K2
				Tip	V5.1M	58	1.39	CW, K1 and K2
1.13-52	BRU0041-PL2-P1.13	1922	99	Head	K1.13M	98	1.10	CW and K
				Middle	M1.13M	77	1.26	CW and K
				Tip	V1.13M	68	1.25	CW and K
1.4-235	OAM-P1.4	2019	2	Head	K1.4M	42	3.03	CW and K
				Middle	M1.4K	37	3.44	CW and K
				Tip	V1.4K	28	3.54	CW and K
					V1.4Vc	24	3.98	CW and K
					V1.4Vb	21	3.93	CW and K

Among the chosen piles and specimens, pile 1.13-52 has the lowest value for the rate of growth and also happens to be sawn from the oldest tree of 98 years old at the base of the tree. In addition, it is also noteworthy that pile 1.4-235 has the highest rate of growth and comes from the youngest tree of 42 years old.

There seems to be a trend, namely an older tree results in a lower rate of growth. In Figure 5.3 is a graph that shows the age of the trees in comparison to the rate of growth.

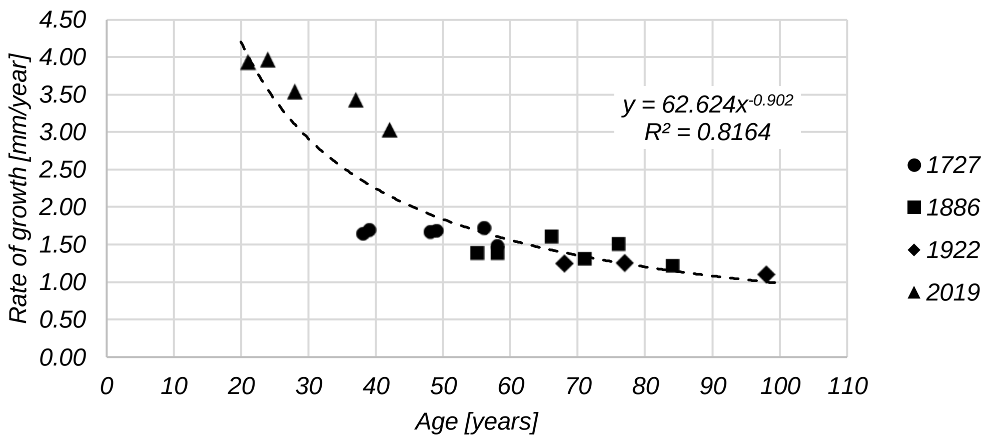

Figure 5.3: Relation between age and rate of growth

The trend between the age and rate of growth can be explained by the difference in the wood structure. In general, older trees have more mature wood which has smaller annual rings than the juvenile wood. The smaller annual rings mean a lower rate of growth. It also indicates that there is less earlywood which results in a higher density.

Note that the gap between the growth rate of the pile from the building year 2019 and the older piles is quite big. This big gap is partly caused by the way the forest management has changed during the 1900s. The older piles from 1727, 1886 and 1922 are made from timber that most likely had been taken from so-called primary old-growth forests. The primary forests developed without human intervention which explains the old age and low rate of growth of the wood. The pile from 2019 on the other hand was probably harvested from a tree farm, which are known for planting trees in a way that allows them to grow quickly and make them ready for harvest within 50 years. This could explain why the growth rate of the pile from 2019 is approximately 2 times higher than the growth rate of the other older piles.

5.3 Knot sizes and distribution

The main findings regarding the knot distribution of the pile and the knot ratio of the discs are presented in Table 5.2. All individual knot diameters and corresponding knot ratios are listed in Appendix A. Only the knots of the indicated segments are considered in this study.

Table 5.2: Knot distribution, discs with knots and knot ratios

	Segment						Disc	
Pile	Tag	Amount of knots [knots/m]	Knot width [mm] avg	Knot width [mm] SD	Failure at section with knots?	Matching knot ratio KR [-]	Tag	Knot ratio KR [-]
5-228	K5M	7.4	15.0	5.6	Yes	0.114	K	0.138
	M5M	14.8	15.9	5.8	Yes	0.068	K1 K2	0.168 0.104
	V5M	8.9	21.1	6.4	Yes	0.273	K1 K2	0.144 0.128
6-228	K6M	8.1	15.4	7.4	Yes	0.074	K	0.136
	M6M	11.1	17.1	7.9	No	-	K	0.121
	V6M	10.0	20.0	8.0	Yes	0.266	K	0.130
3.18-115	K3.18M	3.7	13.8	3.3	No	-	K	0.092
	M3.18M	3.7	14.8	2.4	No	-	K	0.109
	V3.18M	3.0	19.0	7.4	No	-	K	0.080
5.1-52	K5.1M	11.1	29.1	9.9	Yes	0.115	K1 K2	0.175 0.138
	M5.1M	7.8	27.1	6.7	Yes	0.202	K1 K2	0.170 0.113
	V5.1M	11.9	29.3	14.5	Yes	0.244	K1 K2	0.257 0.228
1.13-52	K1.13M	8.3	13.9	3.5	Yes	0.069	K	0.090
	M1.13M	19.3	11.4	5.1	Yes	0.040	K	0.072
	V1.13M	11.9	17.4	7.7	Yes	0.072	K	0.101
1.4-235	K1.4M	7.2	17.9	3.1	No	-	K	0.136
	M1.4K	7.4	22.4	4.5	Yes	0.150	K	0.128
	V1.4K	11.9	28.5	10.9	Yes	0.221	K	0.305
	V1.4Vc	9.6	24.9	10.9	Yes	0.196	K	0.265
	V1.4Vb	6.7	30.6	10.1	Yes	0.278	K	0.235

The amount of knots and the knot sizes for the head, middle and tip segments of each pile can be compared with each other to get a sense of the knot distribution along the length of the pile. The head parts of the investigated piles basically contain the least amount of knots. And, in most cases, it can be noticed that the average knot width is the smallest at the pile head and the largest at the pile tip.

These observations are supported by the boxplots in Figure 5.4. By looking at the median of the knot quantity and the median of the knot sizes it becomes apparent that the pile tip contains the most knots and also the largest knots. However, there is some scatter in the results and there are some outliers for the knot sizes of the head and middle parts. This means that the large knots often occur at, but are not exclusive to, the tip of the pile.

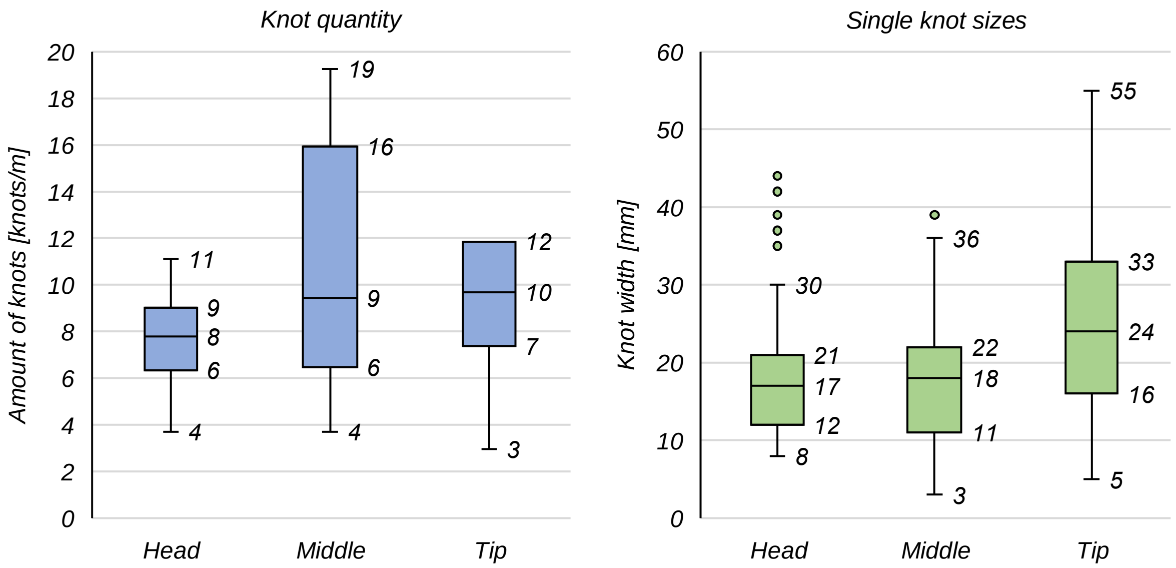

Figure 5.4: Distribution of the knot quantity and knot sizes of the 20 segments considered

The knots that are positioned close together form a knot whorl and the cumulative size of these knots in relation to the circumference of the pile is known as the knot ratio. The discs with knots are taken, as much as possible, from the sections with the highest knot ratios. However, in 6 cases it was not possible to take a disc with the highest knot ratio of the segment.

Each segment has previously been subjected to a large-scale compression test. It turns out that 5 segments (V5M, V6M, M5.1M, M1.4K and V1.4Vb) failed at the section with the highest knot ratio. It is not desirable to isolate and test the knot whorls where failure has occurred due to the presence of cracks and loss of cohesion. That is why in these 5 cases it was decided to cut a disc from the section with the second highest knot ratio.

The other instance where it was not possible to obtain a disc with the highest knot ratio is with segment V1.13M. Here the highest knot ratio occurs at a location that is too close to the end of the segment and it was simply not possible to capture the knot whorl in a disc.

It can be seen that the discs from pile 3.18-115 and pile 1.13-52 have a relatively low knot ratio in comparison to the other discs. The reason why these knot ratios are lower will be explained in more detail.

Pile 3.18-115 has very few knots in comparison to the other piles and only about 4 knots per meter pile length were detected. This is the reason that the observed knot whorls have a relatively low knot ratio. Also, the lack in the amount of knots and the low knot ratios have most likely contributed to the fact that the failure of the segment compression tests occurred at a section without knots.

Pile 1.13-52 turned out to have a lot of knots and the middle segment M1.13M even has approximately 19 knots per meter pile length. However, most of the knots are relatively small and they are spread along the length of the segments. This means that the amount of knots that could be captured in one knot whorl is limited, which is the cause for the low knot ratio.

The distribution of the knot ratios for the head, middle and tip segments are presented in a boxplot in Figure 5.5.

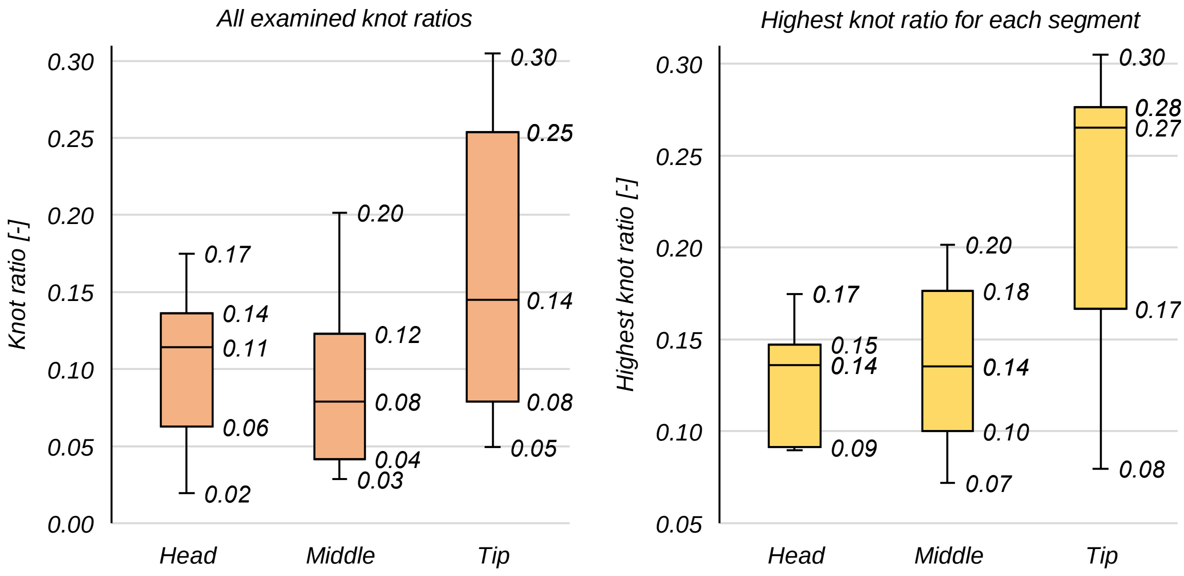

Figure 5.5: Distribution of the knot ratios of the 20 segments considered

The boxplot containing all knot ratios shows that the pile tip generally contains higher knot ratios in comparison to the head and middle of the pile. Note that the knot ratio of the pile head can also be quite high, even though it was stated earlier that the amount of knots and knot sizes at the head are limited.

In addition to the boxplot with all knot ratios, there is also a boxplot that only shows the highest knot ratio of each segment considered. This is done to find the location on the pile where the knots have the biggest influence. It turns out that the highest knot ratio of each pile is located on the pile tip, meaning that the pile tips relatively have the biggest knot whorls in relation to the cross-section.

5.4 Biological degradation

The soft shell of the clear wood discs are evaluated with non-destructive integrity tests using a micro-drill and a handheld piercer tool. The main results are presented in Table 5.3 and the values from all individual measurements are presented in Appendix C.

Table 5.3: Soft shell thickness and level of decay measured for the clear wood discs

		Micro-drill				Piercer tool			
Pile	Segment tag	Soft shell thickness [mm] SS_{avg}	Soft shell thickness [mm] SD	Percentage sound area pA_{sound} [%]	Level of decay *	Average soft shell [mm] SS_{avg}	Average soft shell [mm] SD	Percentage sound area pA_{sound} [%]	Level of decay *
5-228	K5M	13.3	5.1	74	Moderate	19.0	3.7	64	Severe
	M5M	20.3	6.0	61	Severe	20.0	2.7	62	Severe
	V5M	12.4	9.9	70	Moderate	17.8	5.6	59	Severe
6-228	K6M	14.8	9.1	73	Moderate	22.3	6.0	61	Severe
	M6M	25.6	4.5	51	Severe	28.3	2.9	47	Severe
	V6M	17.5	6.2	57	Severe	22.8	3.1	46	Severe
3.18-115	K3.18M	1.6	2.4	97	Low	8.3	3.2	87	Low
	M3.18M	0.2	0.3	100	Low	4.3	1.0	92	Low
	V3.18M	0.9	1.9	98	Low	4.8	2.9	90	Low
5.1-52	K5.1M	12.7	5.5	82	Moderate	18.3	2.6	74	Moderate
	M5.1M	4.0	2.8	93	Low	16.0	2.2	75	Moderate
	V5.1M	8.8	5.4	83	Moderate	15.0	4.8	71	Moderate
1.13-52	K1.13M	0.0	0.1	100	Low	7.3	1.0	89	Low
	M1.13M	0.1	0.3	100	Low	3.3	1.5	94	Low
	V1.13M	6.2	4.8	88	Low	8.5	2.4	84	Moderate
1.4-235	K1.4M	0.0	0.0	100	Low	1.5	1.3	98	Low
	M1.4K	0.0	0.0	100	Low	0.8	0.5	99	Low
	V1.4K	0.0	0.0	100	Low	1.3	0.5	98	Low
	V1.4Vc	0.0	0.0	100	Low	1.0	0.8	98	Low
	V1.4Vb	0.0	0.0	100	Low	1.0	0.0	98	Low

** Level of decay:* *Low level of decay if remaining sound section is higher than 85%*
Moderate level of decay if remaining sound section is between 65% and 85%
Severe level of decay if remaining sound section is lower than 65%

The thickness of the soft shell is measured for the clear wood discs only and not for the discs with knots. Each segment has one clear wood disc which means that the soft shell is examined for one section per segment. The thickness of the soft shell is determined at 4 positions along the perimeter of each disc. The average soft shell thickness from these values, including the standard deviation, is listed in the table.

There is some variation in the thickness of the soft shell. The thickness is measured locally and it may vary depending on the location. Also, it was observed that there was damage on the outside of some discs which means that parts of the soft shell are broken off. The damaged parts measure a lower soft shell thickness which means that the thickness of the soft shell at these locations is not representative for the amount of biological degradation that occurred. Therefore it is principle to measure multiple points and consider the average value.

The overall degradation of the entire pile can be estimated by looking at the degradation of the segments taken from different parts of the pile. Pile 6-228 is mainly severely decayed, while pile 5-228 and pile 5.1-52 are more moderately decayed. Then pile 3.18-115, pile 1.13-52 and pile 1.4-235 show a low level of decay.

The measurements with the micro-drill are the most accurate and the results from the micro-drill are considered to be the correct values that are used for all calculations.

The piercer tool is used in practice as a simple way to estimate the extent to which wood has been damaged. However, the measured values with the piercer tool are not the most reliable because the penetration depth depends on how much force is applied on the piercer which may vary per situation and person. The tests with the piercer tool for this study are performed to get a more hands-on experience and familiarity with the thickness of the soft shell layer. The results from the piercer tool measurements are only used for the comparison with the results from the micro-drill measurements. The measured soft shell of each pile and method of integrity testing is presented in Figure 5.6.

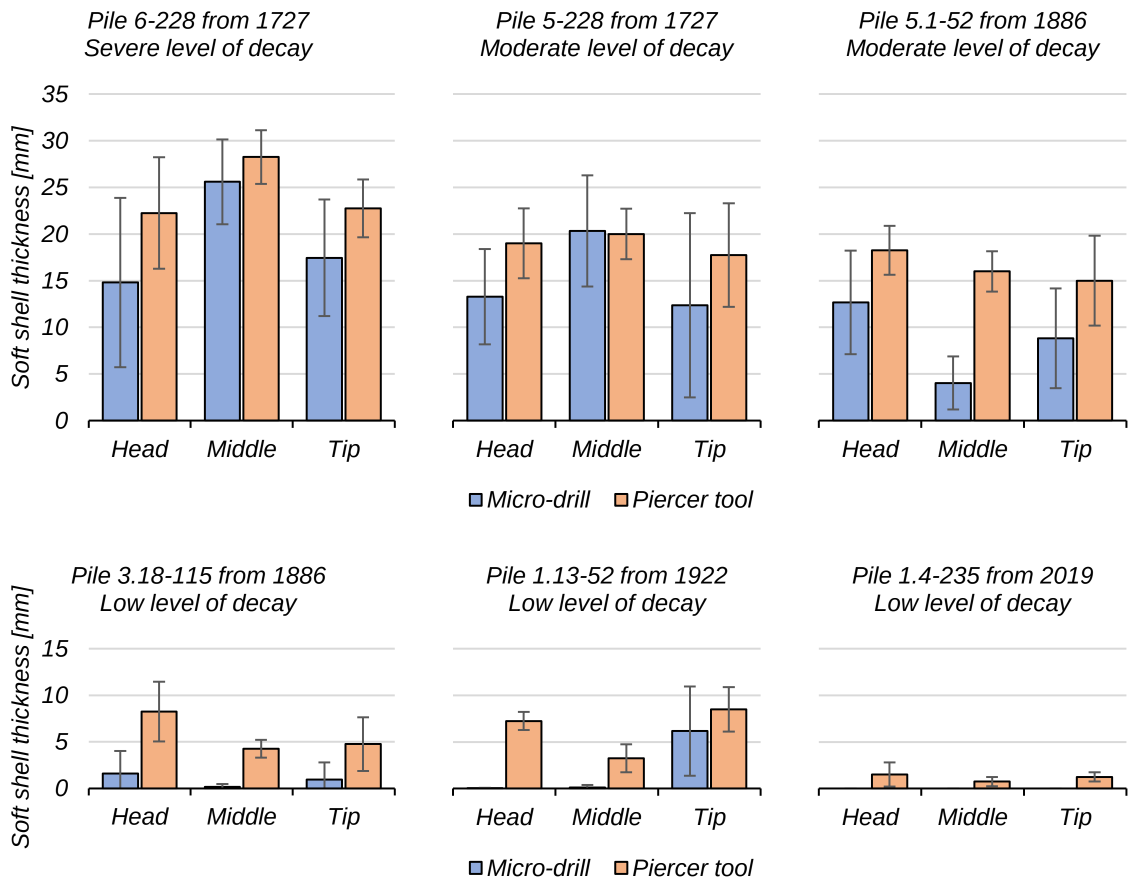

Figure 5.6: Soft shell thickness of each pile measured with micro-drill and piercer tool

By comparing both the results from the micro-drill and piercer tool measurements it can be seen that both show a similar trend. Both results clearly indicate whether the timber is still in good condition or when there is moderate/severe degradation present. The piercer tool seems a good low-tech option to estimate the thickness of the soft shell.

The piercer tool almost always measures a slightly higher value for the thickness of the soft shell. This effect is even noticeable for the new pile 1.4-235 which has not yet been affected by biological degradation and therefore does not have a soft shell. Here the piercer tool can be pressed a few millimeters into the wood structure which means that a value is measured. The measured value is entered in the table as the thickness of the soft shell but in reality this is not entirely correct.

It is clear that the piercer tool can penetrate sound wood for only a few millimeters. This also explains why the results of the piercer tool give a slightly higher soft shell thickness for the parts with biological degradation. The probe is pressed through the soft shell and will sink a few millimeters in the remaining sound wood on the inside which results in a measurement that is slightly higher than the true thickness of the soft shell.

Another reason for the deviation in the results may be due to a difference in the locations of the relative tests. The piercer tool was used at a point right next to the location of the micro-drilling measurement. Even though the differences should be minimal, it can still happen that the soft shell changed a bit over this small distance.

Although the piercer tool generally gives higher values, it is noteworthy to mention that the corresponding standard deviation for the degraded piles is lower in comparison to the values measured with the micro-drill. This indicates that the results from the piercer tool are coherent and form a more decisive representation of the soft shell thickness.

5.5 Density and moisture content

The mass, density and moisture content of all the discs are listed in Table 5.4. All discs are weighed at wet and dry condition which makes it possible to investigate the differences for a distinctive amount of moisture. The mass in wet condition is measured right before the compression tests and the mass in dry condition is determined right after the oven drying process. The wet condition corresponds to the water saturation point and the dry condition is equal to the oven-dry point.

Table 5.4: Mass and density of discs in wet and dry condition including moisture content

Pile	Segment tag	Disc tag	Wet mass m_{wet} [g]	Dry mass m_{dry} [g]	Wet density ρ_{wet} [kg/m^3]	Dry density ρ_{dry} [kg/m^3]	Basic density ρ_b [kg/m^3]	Water loss [g]	Moisture content u [%]
5-228	K5M	CW	3223	1393	744	361	322	1830	131
		K	3339	1494	749	370	335	1845	124
	M5M	CW	3208	1324	779	351	321	1884	142
		K1	3142	1301	798	368	330	1841	142
		K2	2905	1147	800	346	316	1758	153
	V5M	CW	2212	826	821	343	307	1386	168
		K1	2328	900	843	362	326	1428	159
		K2	2355	902	827	352	317	1453	161
6-228	K6M	CW	3887	1652	789	371	335	2235	135
		K	4152	1841	802	395	356	2311	125
	M6M	CW	3090	1174	804	337	305	1916	163
		K	3064	1155	803	333	302	1909	165
	V6M	CW	2017	694	849	324	292	1323	191
		K	1993	712	839	332	300	1281	180
3.18-115	K3.18M	CW	4454	2350	669	389	353	2104	90
		K	4539	2494	686	417	377	2045	82
	M3.18M	CW	3860	2073	687	408	369	1787	86
		K	4036	2225	718	437	396	1811	81
	V3.18M	CW	2868	1548	711	424	383	1320	85
		K	2889	1566	736	436	399	1323	84

Table will continue on the next page

Continuation of Table 5.4

5.1-52	K5.1M	CW	6357	2697	793	374	336	3660	136
		K1	6954	3167	856	426	390	3787	120
		K2	6596	2948	813	406	363	3648	124
	M5.1M	CW	5775	2528	828	396	362	3247	128
		K1	6999	3226	899	463	414	3773	117
		K2	7562	3547	868	451	407	4015	113
	V5.1M	CW	3441	1568	781	397	356	1873	119
		K1	3604	1678	850	444	396	1927	115
		K2	3682	1816	826	457	407	1867	103
1.13-52	K1.13M	CW	5523	2902	769	450	404	2621	90
		K	5885	3203	792	486	431	2682	84
	M1.13M	CW	4970	2559	787	452	405	2411	94
		K	4839	2672	789	477	435	2167	81
	V1.13M	CW	3656	1882	754	426	388	1774	94
		K	3979	2113	770	458	409	1866	88
1.4-235	K1.4M	CW	6516	3311	732	399	372	3205	97
		K	7229	3821	755	424	399	3408	89
	M1.4K	CW	5663	2958	723	408	378	2706	91
		K	6033	3289	727	423	396	2744	83
	V1.4K	CW	3845	2019	720	404	378	1826	90
		K	4317	2398	756	447	420	1919	80
	V1.4Vc	CW	3026	1659	708	414	388	1367	82
		K	3502	1995	752	457	429	1507	76
	V1.4Vb	CW	2501	1396	709	420	396	1105	79
		K	2827	1613	745	454	425	1214	75

The dry density and the basic density are both a measure for the amount of dry matter in the wood structure. However, the dry density uses the dry volume and the basic density uses the wet volume as a reference. It can be seen that the basic density has a lower value than the dry density. This is not surprising because the wet volume is always larger than the dry volume. The dry discs have drying cracks and air pockets which are not taken into account when the dry volume was determined, this makes the value of the dry density less accurate. The wet disc has no voids and all cracks are swollen shut which sometimes makes the wet volume a better value to be related to the amount of dry mass. The difference between the dry density, basic density and how they both relate to the moisture content is in Figure 5.7.

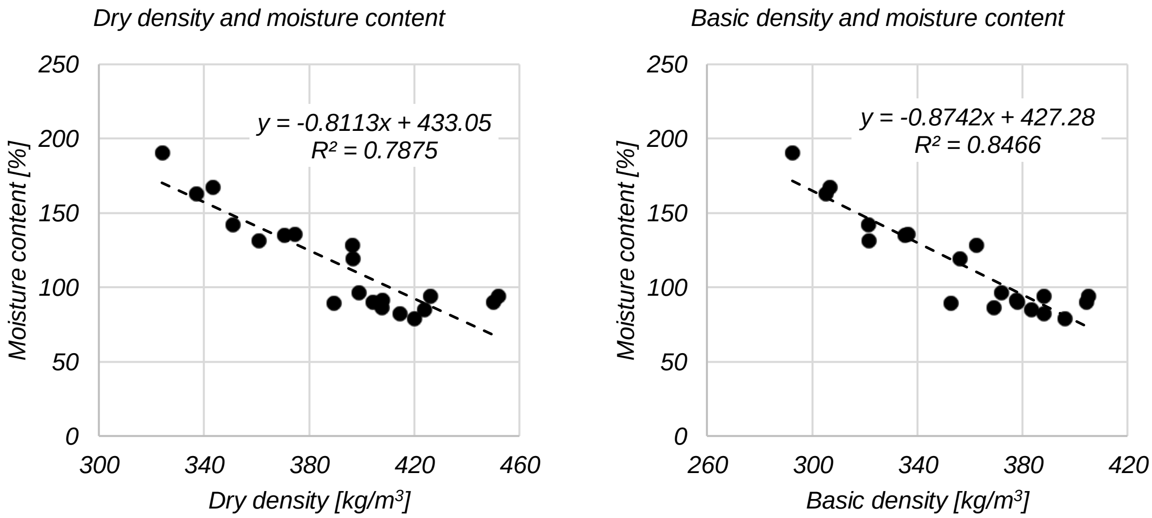

Figure 5.7: Dry density, basic density and moisture content for the 20 clear wood discs

The linear regression model for the basic density has a slightly higher correlation coefficient R^2 in comparison to the model for the dry density. A higher correlation coefficient means that the data has a better fit with the regression model, which can be an indication that the data set is more accurate. However, the model for the dry density shows a correlation coefficient of 0.78 which is still considered to be a very good match with the data. Also the dry density is used more often in practice. This has led to the choice to give preference to the use of the dry density in the remainder of the study.

It is apparent that the dry density and the moisture content have an inverse effect. Meaning that a higher moisture content often results in a lower dry density and vice versa. In addition, the density is also influenced by other factors of which the most important are the rate of growth, the amount of biological degradation and the size of the knots. These different topics will be discussed one after the other.

A higher rate of growth means that the annual rings are wider and that there is more earlywood. The presence of more earlywood is often associated with a lower density. This relation is also noticeable in the results. It is possible to compare the clear wood discs of pile 1.4-235 and pile 1.13-52 because they both lack knots and they both have a low level of decay. Previously it was noted that the rate of growth of pile 1.4-235 is approximately 2 or 3 times higher than that of pile 1.13-52. By comparing the values of the clear wood discs it can be seen that the dry density of pile 1.13-52 is higher than that of pile 1.4-235.

Biologically degraded wood generally has a higher moisture content and a lower dry density in comparison to sound wood. This can be seen by comparing the values of the clear wood discs with each other and to make a distinction between the different levels of decay. The relation between the biological degradation, dry density and moisture content is pictured in Figure 5.8.

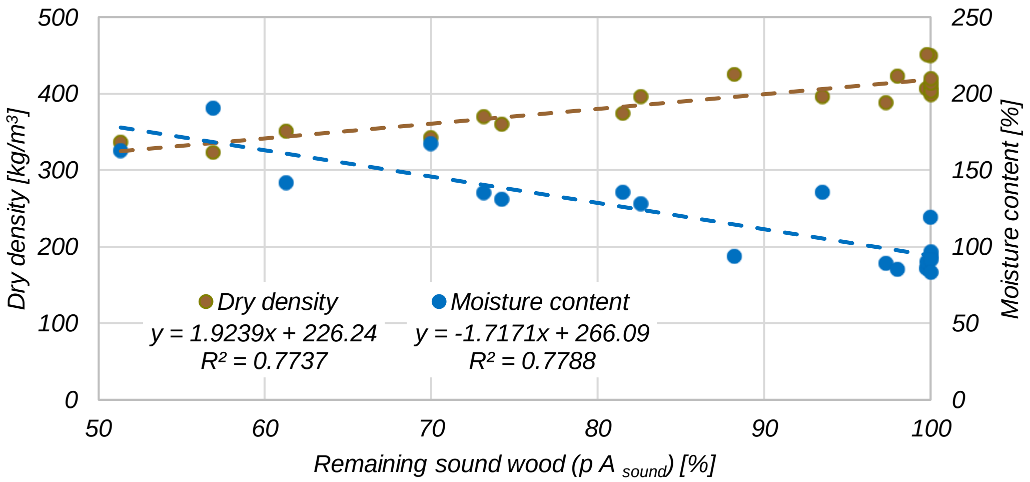

Figure 5.8: Biological decay with density and moisture content for the 20 clear wood discs

The data follows a nice pattern where, as more degradation occurs, the dry density decreases and the moisture content increases. The amount of biological degradation appears to have a greater influence on the dry density than the difference in growth rates. The previously noted difference between the dry densities of pile 1.4-235 and pile 1.13-52 appears to be relatively small because the data points are plotted close together in relation to the other points in the graph.

There is also a relation between the density and the amount of knots in the wood. Generally, the knots have a higher dry density than the surrounding wood structure. This means that the discs with knots should have a higher dry density than the clear wood discs. For this study it is only viable to compare the knotted discs and clear wood discs from the same segments because otherwise a difference in biological degradation is also included.

The dry density of the 25 knotted discs are compared with the dry density of the compatible clear wood discs. A total of 23 of the knotted discs turn out to have a higher dry density than the corresponding clear wood discs. The 2 exceptions are both parts of a pile from 1727 with a severe level of decay which may explain the anomaly.

It has previously been assumed that the soft shell thickness, as measured at the clear wood discs, also applies to the discs with knots. This assumption seems to be supported by the fact that the discs with knots have a slightly higher density than the clear wood discs. After all, if the dry density of the knotted discs had been lower than that of the clear wood discs, then it would indicate that the knotted discs had more biological degradation. It can also be argued from the other side, namely if the knotted discs had a much higher dry density than they have now, then it would have been plausible that the knotted discs had a lot more biological degradation in comparison to the clear wood discs.

5.6 Size and shrinkage

The discs dimensions and the shrinkage after the oven drying process are listed in Table 5.5. All wet and dry dimensions are available in Appendix B and the shrinkage is in Appendix E.

Table 5.5: Disc dimensions with radial shrinkage and volumetric shrinkage

			Wet condition Water saturation point			Dry condition Oven-dry point			Shrinkage	
Pile	Segment tag	Disc tag	Average diameter $D_{avg, wet}$ [mm]	Area section A_{wet} [mm^2]	Volume disc V_{wet} [mm^3]	Average diameter $D_{avg, dry}$ [mm]	Area section A_{dry} [mm^2]	Volume disc V_{dry} [mm^3]	Radial shrinkage [%]	Volumetric shrinkage [%]
5-228	K5M	CW	191.8	28887	4333068	182.9	26265	3860891	4.66	10.90
		K	194.5	29708	4456191	186.4	27280	4037436	6.14	9.40
	M5M	CW	187.0	27467	4119999	180.2	25493	3772982	4.33	8.42
		K1	182.9	26265	3939685	174.3	23854	3530369	4.46	10.39
		K2	175.5	24204	3630550	169.5	22565	3317009	4.39	8.64
	V5M	CW	151.2	17955	2693200	143.9	16258	2406183	5.71	10.66
		K1	153.1	18411	2761669	145.8	16692	2487181	4.66	9.94
		K2	155.5	18990	2848463	148.5	17318	2563039	4.57	10.02
6-228	K6M	CW	204.5	32850	4927512	195.1	29903	4455509	4.67	9.58
		K	209.6	34507	5175984	200.4	31534	4667059	4.21	9.83
	M6M	CW	180.6	25628	3844263	172.5	23377	3483172	5.05	9.39
		K	180.0	25448	3817215	172.7	23420	3466182	4.51	9.20
	V6M	CW	142.0	15829	2374385	135.8	14475	2142348	5.14	9.77
		K	142.0	15829	2374385	135.9	14509	2147374	5.96	9.56
3.18-115	K3.18M	CW	237.8	44405	6660742	227.1	40511	6036210	4.02	9.38
		K	239.4	45001	6615203	230.0	41540	5981751	3.91	9.58
	M3.18M	CW	218.4	37449	5617326	208.5	34141	5086968	4.36	9.44
		K	218.4	37449	5617326	208.7	34193	5094737	4.93	9.30
	V3.18M	CW	185.1	26909	4036276	176.7	24512	3652266	5.38	9.51
		K	182.6	26173	3925981	175.2	24116	3593280	5.02	8.47

Table will continue on the next page

Continuation of Table 5.5

5.1-52	K5.1M	CW	260.9	53443	8016399	248.9	48664	7202203	4.93	10.16
		K1	262.6	54162	8124362	252.9	50232	7434293	5.15	8.49
		K2	262.4	54097	8114518	249.1	48726	7260142	5.11	10.53
	M5.1M	CW	243.3	46510	6976480	232.7	42523	6378465	4.00	8.57
		K1	257.0	51889	7783348	244.0	46754	6966277	4.26	10.50
		K2	272.0	58105	8715765	259.3	52793	7866084	4.19	9.75
	V5.1M	CW	193.4	29369	4405284	184.5	26724	3955112	5.70	10.22
		K1	189.7	28267	4240079	180.8	25674	3774020	4.96	10.99
		K2	194.5	29708	4456191	184.8	26816	3968773	4.34	10.94
1.13-52	K1.13M	CW	246.8	47858	7178687	234.8	43283	6449120	3.69	10.16
		K	251.1	49539	7430797	237.3	44227	6589792	4.85	11.32
	M1.13M	CW	231.6	42117	6317531	220.0	37997	5661513	4.43	10.38
		K	228.2	40910	6136485	218.8	37613	5604306	4.06	8.67
	V1.13M	CW	202.9	32341	4851117	195.0	29854	4418390	4.05	8.92
		K	209.4	34454	5168127	198.6	30986	4616848	5.24	10.67
1.4-235	K1.4M	CW	274.9	59336	8900329	265.5	55351	8302588	3.43	6.72
		K	285.0	63815	9572218	277.4	60440	9005570	4.11	5.92
	M1.4K	CW	257.8	52211	7831617	248.9	48664	7250867	3.97	7.42
		K	265.5	55351	8302588	256.9	51825	7773712	3.93	6.37
	V1.4K	CW	212.9	35616	5342366	205.9	33312	4996777	4.30	6.47
		K	220.1	38052	5707761	213.4	35776	5366350	4.02	5.98
	V1.4Vc	CW	190.5	28505	4275724	184.9	26862	4002475	2.38	6.39
		K	198.8	31035	4655285	192.6	29127	4369102	2.89	6.15
	V1.4Vb	CW	173.0	23507	3525985	168.5	22311	3324362	2.94	5.72
		K	179.5	25313	3796991	174.3	23854	3554223	3.15	6.39

The discs in wet condition are at the water saturation point and the dimensions were measured prior to the compression tests. The dry condition means that the discs are at oven-dry point and the dimensions were measured immediately after the oven drying process. The diameter is an average value retrieved from the circumference at the top and bottom of the discs. There is no standard deviation given as this would not be very useful because it concerns an average of two values that are relatively close to each other.

The top of disc points towards the pile tip and the bottom of the disc points towards the head of the pile. Generally, due to the tapering of the pile, it would be expected that the bottom of the disc is slightly larger than the top of the disc. But the individual measurements show some variation and it regularly arises that the top of the disc is the largest side. It seems that the local defects have a big influence on the dimensions of the discs at this scale. Examples of such local defects that have been observed are the damage to the soft shell and the deviation of the wood grain around the knots.

When the disc dimensions in wet and dry condition are compared, it can be noticed that some shrinkage has occurred. The radial and volumetric shrinkage is presented in the table. A bit of longitudinal shrinkage was also noticeable, however it proved difficult to get a precise measurement because it often only concerned 1 to 2 mm over the total height of the disc. Besides, it turned out that in some cases the height of the disc could vary considerably depending on which side of the disc was measured. For these reasons it must be noted that the shrinkage in longitudinal direction cannot properly be investigated and is therefore not included in the table.

The shrinkage of wood happens when the moisture content becomes lower than the fibre saturation point at a moisture content of approximately 30%. Below that point the bound water between the wood cells will evaporate which causes the dimensional changes. The values from the different discs can be compared to see if there are any relations between the radial shrinkage and other properties.

Note that the evaporation of the free water will not cause any shrinkage. Therefore it would not make sense to compare the amount of shrinkage with the moisture content because it mainly encompasses the free water. However, at this point it seems interesting to see if there is any connection between the radial shrinkage and the biological degradation. Even though the soft shell mainly contains free water, the cells are also affected by bacteria which may cause different behaviour. As an example, a comparison is made between the radial shrinkage of pile 6-228 with severe decay and pile 3.18-115 with low decay. Both of the piles have a radial shrinkage of around 5%. So it can be concluded that there seems to be no real connection between the radial shrinkage and the biological degradation.

The differences between the radial shrinkage and the amount of latewood is checked. From the literature research it is known that latewood generally experiences more radial shrinkage than earlywood. This effect can be investigated by looking at the discs from pile 1.4-235 that have a relatively high rate of growth and a low age, which means that there is less latewood in comparison to the other piles. Here it seems that the values of the radial shrinkage from pile 1.4-235 fluctuates between 2.5% and 4.3%, while the values of the other piles lie between the 3.7% and 6.1% respectively. This difference is even more noticeable for the volumetric shrinkage, which for pile 1.4-235 is somewhere between the 5% and 8% while the other piles have a value between the 8% and 12%. The relation between the shrinkage and the rate of growth is shown in Figure 5.9.

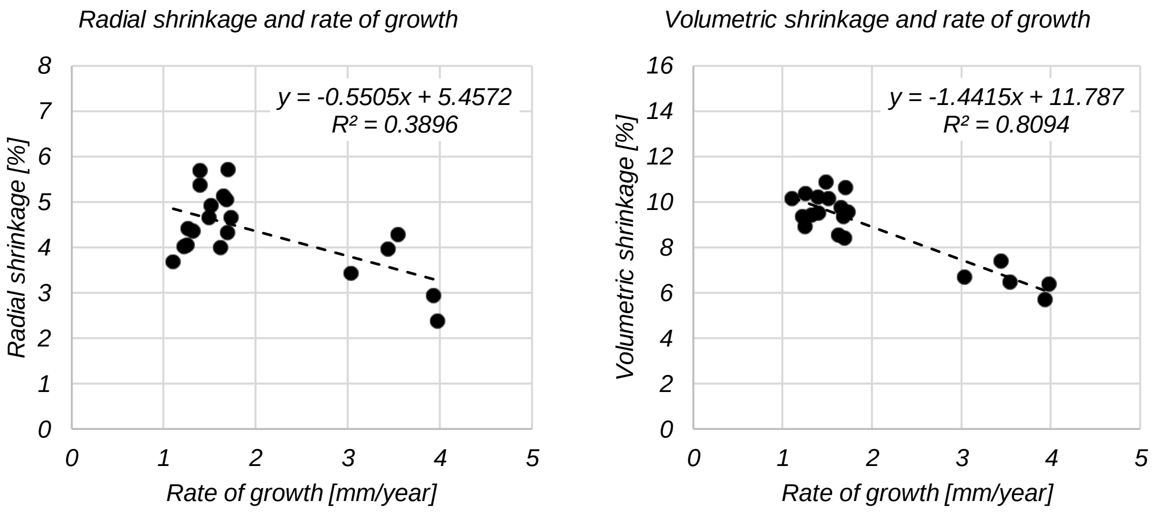

Figure 5.9: Shrinkage and rate of growth for the 20 clear wood discs

It seems that the amount of latewood has a major influence on the shrinkage of the wood. The graphs clearly show two groups, a group with the 5 values from pile 1.4-235 and a group with the other 15 specimens. Two separate groups with data are insufficient to make a good linear regression model, therefore the model shown in the graphs is only meant as an indication.

5.7 Strength and modulus of elasticity

The strength and modulus of elasticity (MOE) are results that follow from the small-scale disc compression tests. All information from the individual compression tests are explained in detail in Appendix D and the main outcomes are listed in Table 5.6.

Table 5.6: Maximum force, strength and modulus of elasticity

Pile	Segment tag	Disc tag	Machine test speed [mm/s]	Duration until failure [s]	Maximum force F_{max} [kN]	Strength section $f_{c,0\ wet}$ [N/mm^2]	Strength sound part EQ $f_{c,0\ wet}$ [N/mm^2]	MOE average sensors [N/mm^2] $E_{c,0\ D}$	MOE average sensors [N/mm^2] SD	MOE jack $E_{c,0\ S}$ [N/mm^2]
5-228	K5M	CW	0.010	212	305.4	10.6	14.2	12946	22261	6233
		K	0.010	319	298.7	10.1	13.5	3686	16199	1825
	M5M	CW	0.010	225	282.0	10.3	16.8	3244	1861	1485
		K1	0.010	200	243.3	9.3	15.1	3948	5346	1728
		K2	0.010	261	222.1	9.2	15.0	1889	166	762
	V5M	CW	0.010	207	157.1	8.7	12.5	6299	36046	1885
		K1	0.010	233	155.0	8.4	12.0	2578	2867	791
		K2	0.015	166	171.6	9.0	12.9	2035	640	644
6-228	K6M	CW	0.010	213	371.0	11.3	15.4	8531	3066	4671
		K	0.010	196	370.7	10.7	14.7	14402	34489	8283
	M6M	CW	0.010	187	210.1	8.2	16.0	7735	6900	3304
		K	0.010	227	187.9	7.4	14.4	3027	2850	1284
	V6M	CW	0.010	238	112.5	7.1	12.5	25593	12996	6752
		K	0.010	276	129.9	8.2	14.4	3309	7941	873
3.18-115	K3.18M	CW	0.010	223	624.8	14.1	14.5	28824	27865	21332
		K	0.010	303	611.5	13.6	14.0	-9404	10147	-7053
	M3.18M	CW	0.010	207	552.5	14.8	14.8	22182	7737	13845
		K	0.010	194	536.5	14.3	14.4	7540	1222	4706
	V3.18M	CW	0.010	198	394.3	14.7	15.0	8426	5620	3779
		K	0.010	219	378.9	14.5	14.8	8436	4718	3680
5.1-52	K5.1M	CW	0.010	187	629.4	11.8	14.4	5610	3839	4997
		K1	0.010	309	587.6	10.8	13.3	22181	10427	20023
		K2	0.015	388	508.2	9.4	11.5	678	3837	611
	M5.1M	CW	0.010	231	575.5	12.4	13.2	2602	1647	2017
		K1	0.010	260	537.5	10.4	11.1	10798	7388	9338
		K2	0.010	229	667.8	11.5	12.3	2836	3158	2746
	V5.1M	CW	0.010	254	367.1	12.5	15.1	5669	4755	2775
		K1	0.010	211	301.9	10.7	12.9	12931	16313	6092
		K2	0.015	157	345.4	11.6	14.1	5366	19260	2657
1.13-52	K1.13M	CW	0.010	253	818.9	17.1	17.1	6647	4851	5302
		K	0.010	284	733.0	14.8	14.8	5908	3169	4878
	M1.13M	CW	0.010	248	651.6	15.5	15.5	7304	8736	5127
		K	0.010	227	673.5	16.5	16.5	32795	55394	22361
	V1.13M	CW	0.010	243	475.1	14.7	16.7	30615	79845	16502
		K	0.010	238	496.4	14.4	16.3	5917	1654	3398
1.4-235	K1.4M	CW	0.010	309	875.3	14.8	14.8	2093	257	2070
		K	0.010	383	837.2	13.1	13.1	2761	7447	2937
	M1.4K	CW	0.010	257	805.2	15.4	15.4	6487	3520	5645
		K	0.010	315	731.3	13.2	13.2	3369	5319	3108
	V1.4K	CW	0.010	248	536.6	15.1	15.1	5239	7123	3110
		K	0.010	319	479.2	12.6	12.6	3190	858	2023
	V1.4Vc	CW	0.015	200	443.7	15.6	15.6	4271	2379	2029
		K	0.010	368	398.0	12.8	12.8	2825	5651	1461
	V1.4Vb	CW	0.010	322	363.3	15.5	15.5	6139	109494	2405
		K	0.010	229	350.4	13.8	13.8	5317	19736	2243

The compression tests are performed with a displacement controlled set-up. All 45 discs were subjected to compression tests, mostly with a machine test speed of 0.010 mm/s and in 4 cases with a speed of 0.015 mm/s. According to the standard EN 14251 the failure should occur within 300 ± 120 seconds, this was successful for all cases except 2 (discs V5M K2 and V5.1M K2) that experienced a slightly shorter time.

The wet compressive strength is determined two times, first for the entire cross-section and then for the sound part whilst assuming that the soft shell does not contribute to the strength. A comparison between the wet compressive strength of the entire cross-section is pictured in Figure 5.10.

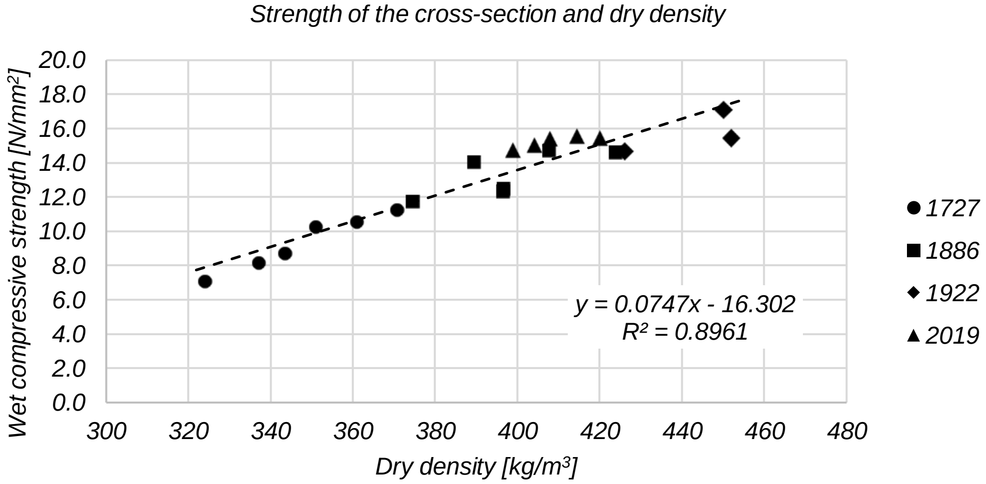

Figure 5.10: Strength of the entire section and dry density of the 20 clear wood discs

There is a very good correlation between the wet compressive strength of the entire cross-section and the dry density. The lowest values are from specimens that originate from 1727 with a moderate or low level of decay. The highest points in the graph are of discs from 1922 and 2019 that have a low level of decay.

If it is assumed that the soft shell has no strength, then the sound part in the middle of the section will carry all the load. A comparison between the wet compressive strength of only the sound part and the dry density is presented in Figure 5.11.

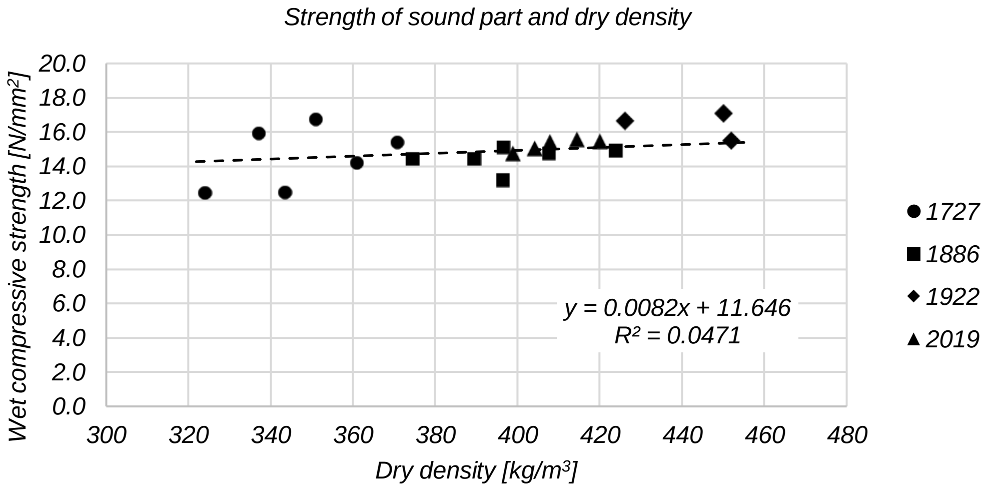

Figure 5.11: Strength of the sound part and dry density of the 20 clear wood discs

The graphs show that the wet compressive strength of the sound part is more uniform in contrast to the wet compressive strength of the entire section. The values that belong to the degraded specimens became higher and the values of the non-degraded discs remained the same.

The linear regression model for the strength of the sound part shows an almost flat line which indicates that the strength of the sound parts from all the piles are similar. A similar strength for all the sound wood is a realistic scenario and this also indicates that the assumption of a soft shell with zero strength is reasonable. The correlation coefficient R^2 is very low which indicates that not all data has a good fit with the linear regression model. However, this is not a problem because the values that occur seem to be quite reasonable and no extreme outliers are observable.

There are many more physical properties that could be interesting to compare with the wet compressive strength. The interaction between the wet compressive strength, the knots and the biological degradation is an important part of this study. Therefore, these relationships will be thoroughly explained in the analysis chapter.

Now the modulus of elasticity is examined. The modulus of elasticity is calculated by the quotient between the stress and the strain in the elastic region of the material. In principle, the strain is derived from 4 individual measurements with separate linear potentiometers that are positioned along the perimeter of each disc. The average value from these 4 sensors is used to calculate the modulus of elasticity.

There is a lot of variation in the values for the modulus of elasticity that are calculated with the strain of the sensors. That is why it was also investigated whether the displacement from the jack might be representative for the deformation of the discs. The relation between the modulus of elasticity and the wet compressive strength of the entire cross-section is pictured in Figure 5.12.

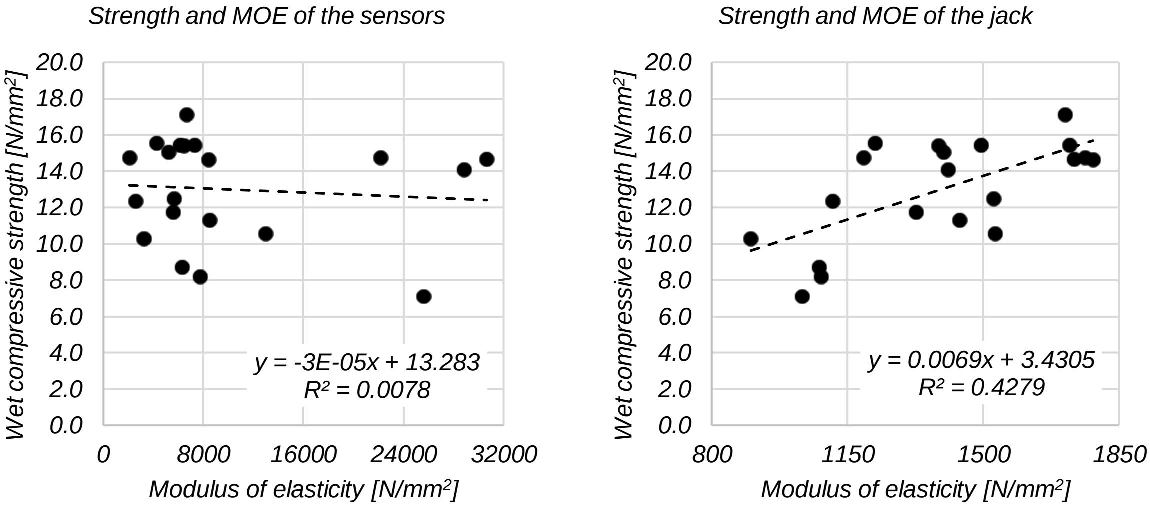

Figure 5.12: Strength of entire section and modulus of elasticity of the 20 clear wood discs

Note that the relation between the stress and the modulus of elasticity should follow a slanting line diagonally towards the top right. An example of such a relation was given in chapter 2 in Figure 2.27.

The calculated average values of the modulus of elasticity of the sensors show a large variation, ranging from negative to values over 30000 N/mm^2. This is in no way correct and it does not match with the values from the segment compression tests. There also appear to be unusual values for the standard deviation. As a rule of thumb, the standard deviation is considered high if it is greater than one-third of the average value. If this principle is applied to the modulus of elasticity of the linear potentiometers, then it turns out that in 39 out of 45 cases have a high standard deviation occurs.

This indicates that something went wrong with the individual measurements of the linear potentiometers. The reason behind the strange results from the linear potentiometers is looked at in more detail and will be further explained in the analysis chapter.

On the other hand, there seems to be a better relation between the strength and the modulus of elasticity which results from the displacement of the jack. The values show a trend in the right direction with a better correlation. However, the moduli of elasticity are much lower than the typical values that occurred during the large-scale tests. The reason for the lower values may be that the displacement of the jack also includes the preloading and the load introduction in the specimen. The modulus of elasticity from the jack displacement is not representative of the foundation piles and are therefore not usable in this study.

6. Analysis

The analysis of the test results with a focus on the mechanical properties of the timber piles.

6.1 Strength and biological degradation

The wet compressive strength of timber foundation piles is mainly determined by the amount of knots and the presence of biological degradation. The relation between the strength and the knots is discussed in the next section. In this section the connection between the strength and the biological degradation is investigated.

A high amount of biological degradation means that there is a smaller sound load-bearing cross-sectional area and a lower strength. This relation is clearly visible when the strength and the amount of biological degradation are plotted in a graph, see Figure 6.1.

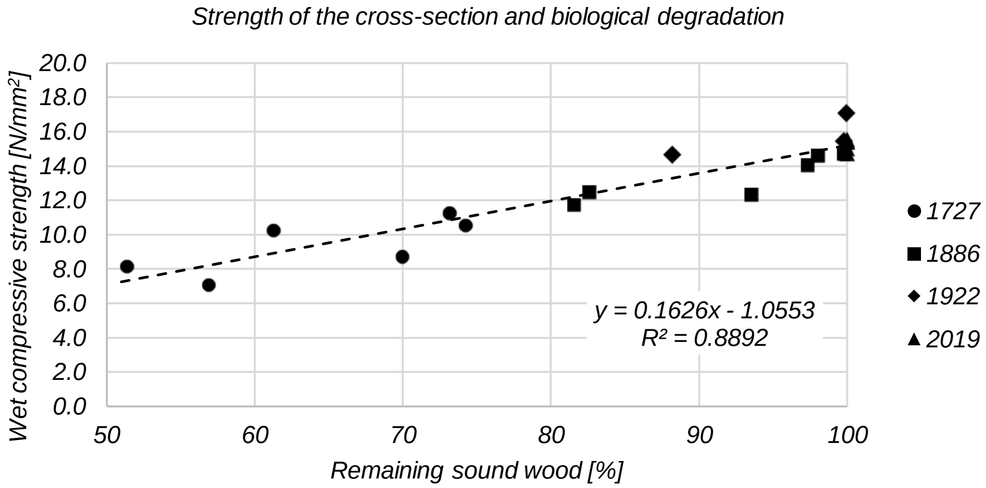

Figure 6.1: Strength of the entire section and biological decay of the 20 clear wood discs

The correlation coefficient R^2 is quite high which means that the data has a very good fit with the linear regression model. There seems to be a clear link between the wet compressive strength and the biological degradation.

Note that the reduction in the load-bearing area due to biological degradation can results in higher stresses which in turn can enhance the effect of the mechanical degradation. This interaction does have a negative effect on the strength, but it is far too complicated to inquire and for this reason it will not be further elaborated in this study.

The different clear wood specimens are compared and divided into groups to get a better understanding of how the properties are distributed. The groups are made based on similar strength, building years and biological degradation.

The results show that the specimens with the most biological degradation also have the oldest building year and the lowest wet compressive strength. This concerns pile 5-228 and pile 6-228 from 1727, which both have a remaining sound cross-sectional area between the 50% and 80%. Therefore pile 5-228 and pile 6-228 are grouped together.

All other specimens are less old and have a remaining sound cross-sectional area that is higher than 80%. However, the strength values differ too much to be able to classify all other specimens into one group. A distinction can be made between a difference in building years. Here it appears that the wet compressive strength of pile 3.18-115 and pile 5.1-52 are similar and both piles come from 1886. This means that they are also considered together as a group.

The two remaining piles are the ones with the shortest service lives of the selected cases. Pile 1.4-235 originates from 2019 and is barely used with no observable biological degradation. Pile 1.13-52 comes from 1922 and it turns out that its strength is closest to that of pile 1.4-235 and therefore it is decided that they are also classified together in a group.

So all the clear wood specimens can be divided into 3 groups with similar properties, see Table 6.1.

Table 6.1: Overview of strength, building year and biological decay of 20 clear wood discs

Remaining sound part	Building year	Piles	Sample size	Dry density ρ_{dry} [kg/m^3]		Moisture content u [%]		Percentage sound area p A_{sound} [%]		Strength section $f_{c,0\ wet}$ [N/mm^2]		Strength sound part EQ $f_{c,0\ wet}$ [N/mm^2]	
				avg	SD	avg	SD	avg	SD	avg	SD	avg	SD
50%-80%	1727	5-228 6-228	6	348	17	155	23	64	9	9.4	1.6	14.6	1.8
80%-100%	1886	3.18-115 5.1-52	6	398	17	107	23	92	8	13.4	1.3	14.5	0.7
	1922 2019	1.13-52 1.4-235	8	422	20	90	6	98	4	15.4	0.8	15.7	0.8

The most interesting values in the table are the wet compressive strength for the different groups. There are clearly big steps between the groups for the values from the strength of the entire section. The specimens from 1886 have an average strength that is 4.0 N/mm^2 higher than the ones from 1727. Sequentially, it turns out that the specimens from 1922 / 2019 have an average strength that is 2.0 N/mm^2 higher than the discs from 1886.

Regarding the standard deviation (SD), it appears that the greatest amount of scatter can be found for the specimens from 1727. This is due to the fact that there is a lot of variation in the amount of biological degradation between the different specimens from 1727. Because of this, it was considered to make another subdivision, but then groups are created with a very small sample size which are overly specific. If the groups get smaller, it also becomes more likely that the values are biased. Taking this into account, it was ultimately decided not to adjust the groups.

It can be noted that the strength of the discs from 1886 have a strength that is about 14% lower in comparison to the strength of the discs from 1922 / 2019. In a similar fashion it can be seen that the strength of the discs from 1727 have a strength that is approximately 39% lower in comparison to the strength of the discs from 1922 / 2019. This shows the destructive effect of biological degradation on the strength.

From the results it can be deduced that the amount of degradation is directly related to a loss in strength. This confirms that the strength of the soft shell is very low compared to the strength of the remaining sound inner part of the pile. The previous assumption that the strength of the soft shell is negligible seems therefore justified.

When the strength of the sound part is considered, and the soft shell is assumed to have zero strength, then the presence of the biological degradation is no longer a deviating factor between the values. Here it can be seen that the specimens from 1727 and 1886 have an average strength that lies close together. The average strength of the sound part for the specimens from 1727 / 1886 is approximately 1.2 N/mm^2 lower in comparison to the average value for the specimens from 1922 / 2019. This difference can be explained by the belief that there is more mechanical degradation for the older piles in comparison to the newer ones.

6.2 Strength and knots

The relation between the wet compressive strength and the presence of the knots is investigated. This is done by comparing the strength of the 20 clear wood discs with the strength of the corresponding 25 discs with knots.

The first thing that stands out is that, for 22 of the 25 knotted discs considered, the strength of the clear wood disc is higher than the strength of the knotted disc from the same segment. This is a clear indication to illustrate that the presence of knots have a big negative effect on the wet compressive strength. The 3 exceptions are discs V5M K2, V6M K and M1.13M K. These exceptions are specimens with varying amounts of biological degradation and different building years, so there seems to be no clear reason why exactly these discs deviate which is why these are considered outliers in this pattern.

The second thing that can be observed is that a higher knot ratio corresponds to a lower wet compressive strength. This relation becomes apparent when the negative effects of the biological degradation are disregarded and only the strength of the sound part is considered. The strength of the sound part and the knot ratio are plotted in Figure 6.2.

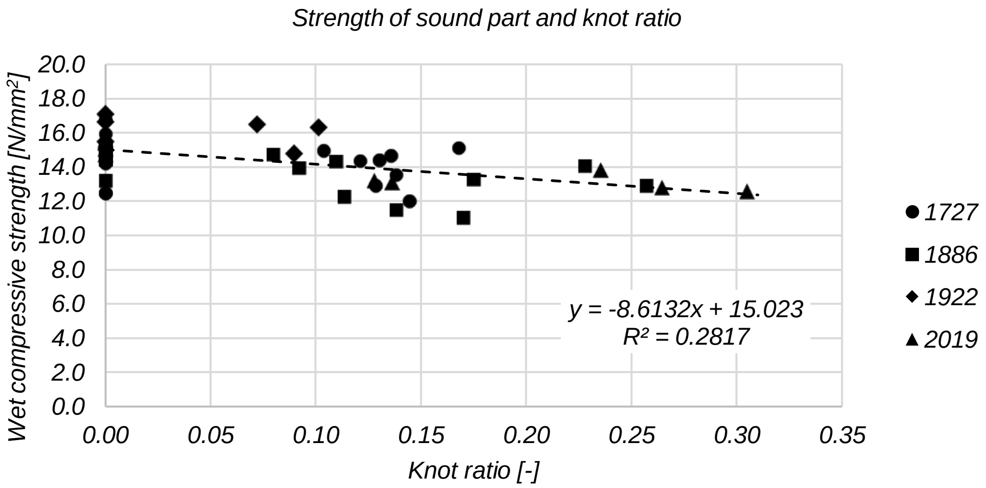

Figure 6.2: Strength of the sound part and knot ratio of all 45 discs

The linear regression model shows a 5.7% decrease of the wet compressive strength for each 0.1 increase of the knot ratio. For the cases with a knot ratio below the 0.10 there is a wet compressive strength that is comparable to the strength of the discs without knots. On the other hand, for the cases where the knot ratio is higher than 0.10, a decrease in the wet compressive strength of up to 30% can be observed.

The correlation coefficient R^2 is quite low which means that the data has a weak fit with the linear regression model. Possible explanations for the lower coherence of the data can come from the assumptions that were made earlier. For example, it has been assumed that the soft shell of the discs with knots is the same as the clear wood discs. However, it may be that the soft shell thickness of the knotted discs is somewhat different which means that the calculated strength of the sound part may be a bit different. In addition, it is also possible that the knots do not run through the wood structure as was assumed during the calculations of the knot ratios. Despite all these uncertainties, the outcome is still quite good and the decrease in strength can be demonstrated well.

In order to further investigate the effect of the knots, a subdivision will be made based on the different building years. The graphs regarding the strength and knot ratios for the different building years are presented in Figure 6.3.

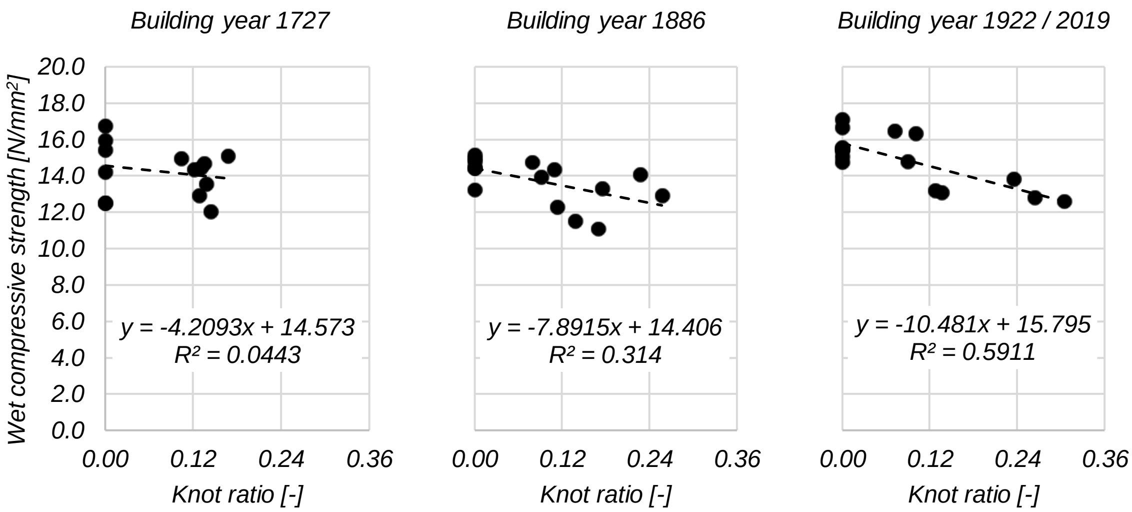

Figure 6.3: Strength of the sound part and knot ratio divided over different building years

Each graph shows a group at a knot ratio of 0.00 that consists of the clear wood specimens. There appears to be not much variation in the knot ratios of the discs from 1727 which results in a data cluster located around a knot ratio of 0.13 . The data points of the other two graphs are more spread out. For the next steps it is chosen to split the data in the middle at a knot ratio of 0.15 .

If the wet compressive strength of the discs are roughly divided based on the knot ratios, then it turns out that the clear wood discs have an average strength of 15.0 ± 1.2 N/mm², the discs with a knot ratio between 0.07 and 0.15 have an average strength of 14.0 ± 1.4 N/mm² and the discs with a knot ratio between 0.15 and 0.32 have an average strength of 13.0 ± 1.0 N/mm². In general it can be said that a knot ratio between the 0.07 and 0.15 causes a 7% decrease in strength and a knot ratio ranging from 0.15 to 0.32 results in a 14% decrease in strength.

A subdivision is made based on the different building years, see Table 6.2.

Table 6.2: Overview of strength of the sound part and knot ratio of all 45 discs

		KR = 0			0.07 < KR < 0.15			0.15 < KR < 0.32		
Building year	Piles	Sample size	Strength sound part EQ f $_{c,0\ wet}$ [N/mm^2] avg	SD	Sample size	Strength sound part EQ f $_{c,0\ wet}$ [N/mm^2] avg	SD	Sample size	Strength sound part EQ f $_{c,0\ wet}$ [N/mm^2] avg	SD
1727	5-228 6-228	6	14.6	1.8	8	13.9	1.1	ND	ND	ND
1886	3.18-115 5.1-52	6	14.5	0.7	5	13.4	1.4	4	12.9	1.3
1922 2019	1.13-52 1.4-235	8	15.7	0.8	5	14.8	1.6	3	13.1	0.7

Here the average values from 1727 and 1886 lie quite close together. When one group from 1727 / 1886 is considered, then the values for the wet compressive strength would be:

14.5	± 1.3	N/mm^2	at	KR = 0
13.7	± 1.2	N/mm^2	at	0.07 < KR < 0.15
12.9	± 1.3	N/mm^2	at	0.15 < KR < 0.32

The strength at “0.07 < KR < 0.15” is compared to the strength at “KR = 0”. For the group from 1727 / 1886 there is a reduction in strength of 6.0% and for the group from 1922 / 2019 there is a reduction of 5.7%. This reduction is quite similar and it also corresponds to the linear regression model of Figure 6.2. Now the strength at “0.15 < KR < 0.32” is compared to the strength at “KR = 0”. Here there are somewhat bigger differences noticeable. The group from 1727 / 1886 has a 11.6% decrease in strength while the group from 1922 / 2019 has a decrease of 16.6%. However, the strength of both groups came closer together with an average value around 13.0 N/mm^2.

6.3 Comparison strength of discs and segments

The wet compressive strength of the discs is compared with the wet compressive strength from the segment compression tests. The strength of the clear wood discs versus the strength of the segments is plotted in Figure 6.4.

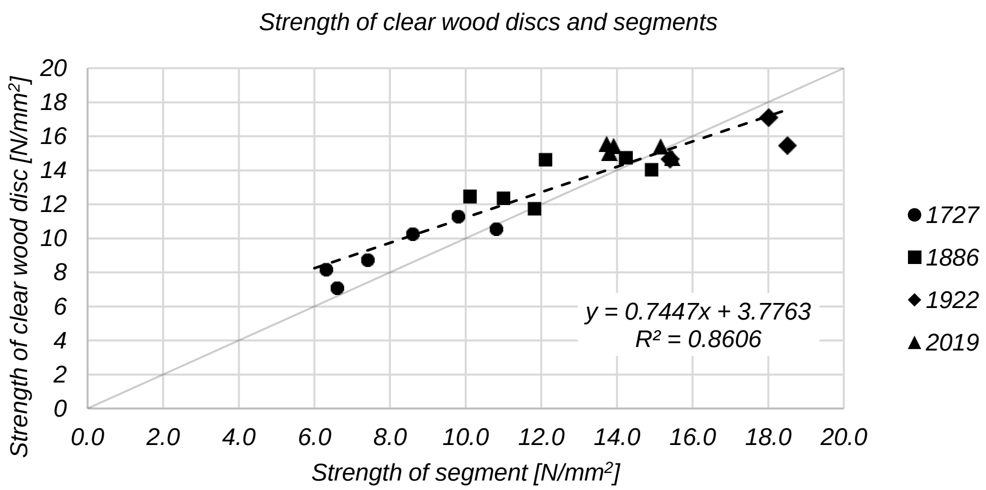

Figure 6.4: Strength of the 20 clear wood discs and segments

More information about how the strength of the segments was determined can be found in previous paragraphs of this thesis. The procedure of the segment compression tests is briefly explained in section “2.5.1 Compression tests on large segments” and the values used for the comparison are listed in section “3.4 Relevant data from preceding research”.

The correlation between the strength of the discs and the segments is very good, which means that the strength of the discs follow a similar pattern as the strength of the segments.

When the strength of all 45 discs are compared with the strength of the 20 segments that they were sawn from, it turns out that 25 discs have a value that remains within the 10% difference of those of the segments. From the remaining 20 discs, a total of 17 have a strength that ranges between the 10% and 20% difference from the segments. The last 3 discs have a strength that deviates between the 20% and 26% and are considered outliers. Note that these discs are not the same sections that failed during the segment compression tests. Also, the discs have different amount of knots and degradation, making it understandable that the values will somewhat deviate.

It is interesting to mention that of the 20 segments considered, a total of 15 segments failed at a section with knots during the large-scale compression tests. Of these it appeared that 5 segments failed at the section with the highest knot ratio (V5M, V6M, M5.1M, M1.4K and V1.4Vb). This clearly shows that the presence of large knots can be governing the strength of a timber pile. Therefore it is interesting to look at the strength of the discs with a high knot ratio and compare this with the strength of the segments.

The wet compressive strength of the discs and the segments are compared, distinguishing between groups with different building years. The strength of the discs is subdivided based on the relevant knot ratios. The bar charts with the wet compressive strength of the discs and the segments are shown in Figure 6.5.

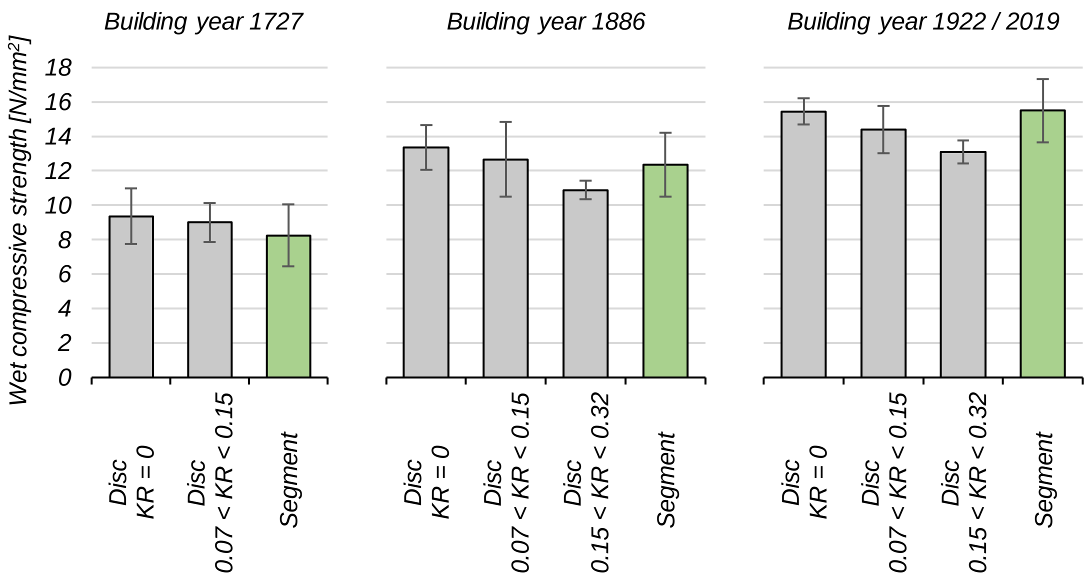

Figure 6.5: Comparison between the strength of the discs and segments

The exact values of the wet compressive strength as presented in these bar charts are listed in Table 6.3.

Table 6.3:Overview of the strength of the entire section of all 45 discs and 20 segments

Building year	Piles	Strength disc KR = 0 [N/mm^2]		Strength disc 0.07 < KR < 0.15 [N/mm^2]		Strength disc 0.15 < KR < 0.32 [N/mm^2]		Strength segment $f_{c,0\ wet}$ [N/mm^2]	
		avg	SD	avg	SD	avg	SD	avg	SD
1727	5-228 6-228	9.4	1.6	9.0	1.1	ND	ND	8.3	1.8
1886	3.18-115 5.1-52	13.4	1.3	12.7	2.2	10.9	0.5	12.4	1.9
1922 2019	1.13-52 1.4-235	15.4	0.8	14.4	1.4	13.1	0.7	15.5	1.9

It can be seen that the wet compressive strength from the segment compression tests is almost identical with the values of the discs and there are only small deviations per group.

The results from the group from 1727 show that the segments have a lower strength than the knotted discs. The group from 1886 has a segment strength that is similar to discs with knots. In the group from 1922 / 2019 the strength of the segments is similar to the strength of the clear wood discs.

The wet compressive strength values from the large-scale segment compression tests are assumed to be the correct values that represent the actual strength of the timber piles. These values can be used to validate the results from the small-scale disc compression tests. From this perspective, it seems that the strength of the discs with a large amount of biological degradation are slightly higher than the actual strength of the pile. On the other hand, the strength of the discs without biological degradation and with knots appear to be a somewhat lower.

The segments and the discs generally experience a completely different failure mechanism in compression. The segments often have a buckling type of failure, while the discs commonly fail due to crushing of the wood. This could be a possible reason for the minor deviations in strength between the degraded discs and segments. After all, it has been shown that a heavily degraded pile has a significantly smaller effective cross-section, which can make the pile more sensitive to a buckling failure mechanism, possibly playing a part in it to fail at a lower force in the large-scale compression test than in the small-scale compression test. Note that the buckling behaviour of the pile is not a subject of this study and is therefore not discussed in more detail.

Despite having different failure mechanisms, it appears that the strength of a segment and the strength of a disc with the largest knots from the same segment are quite similar with a good correlation. This can be explained due to the fact that the section with the highest knot ratio governs the strength of the segment and also the strength of the corresponding disc. This shows that it is possible to accurately assess the wet compressive strength of a segment by performing a compression test on the disc with the highest knot ratio from that segment.

6.4 Inconsistencies regarding the modulus of elasticity

The modulus of elasticity is an important mechanical property that can be determined by looking at the deformation of a specimen during a compression test. In general, the modulus of elasticity is the gradient between the stress and the strain in the elastic region of the material.

The strain of the discs during each compression test is measured with a total of 4 linear potentiometers. The potentiometers are located all around the disc at approximately each quadrant of the disc. An average value of all linear potentiometers is used to calculate the modulus of elasticity. The results for the modulus of elasticity exhibits a lot of variability, showing values over 30000 N/mm^2 and even negative values. This extreme variety is in no way realistic behaviour and it indicates that something went wrong with the measurements of the linear potentiometers.

The results of the individual potentiometers show a lot of variety in the measured strain. Some of the potentiometers even showed an elongation of the gauge length during the compression test. These distortions in the strain measurements can be explained by several factors. A distinction is made between local defects and global deformations.

The wood has local defects and these defects can be the cause of the unexpected behaviour of the individual measurements. Examples of such defects are the presence of a soft shell or knots. The strain is measured over a gauge length of 60 mm and with a stroke of only 2 mm, this is quite small in comparison to the size of the defects. In general, a defect has a bigger negative impact when the gauge length is smaller. The defects become more significant for the behaviour of the wood structure within the range of the measurement.

In addition, the brackets of the linear potentiometers are attached to the disc in the area where the cracks are forming and propagating. These cracks occur due to high compressive stresses and are present for all discs, regardless whether there are defects or not. Nevertheless, the cracks often initiate at the location of a defect because these are weak points in the wood structure. Some examples of horizontal cracks that developed during the compression tests are pictured in Figure 6.6.

Crack pattern disc M5M K1 | *Crack pattern disc V5.1M K2* | *Crack pattern disc V3.18M K*

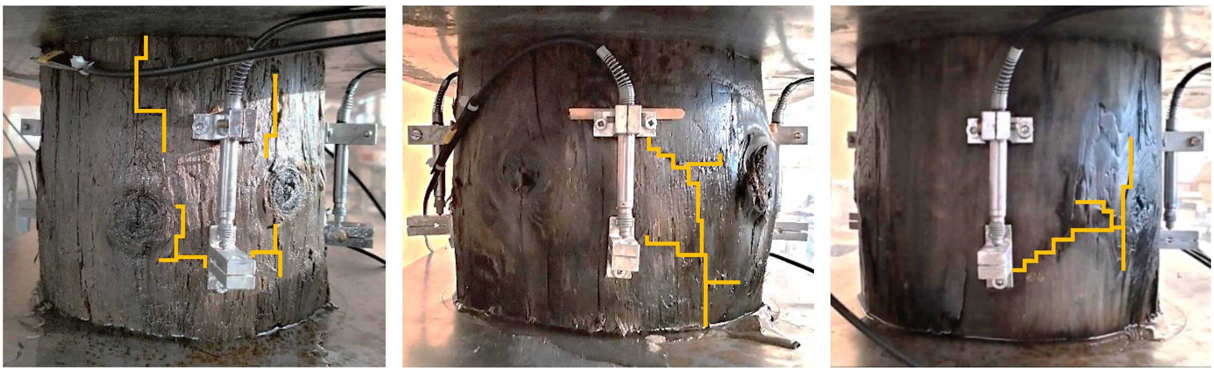

Figure 6.6: Indication of horizontal crack patterns that occur during disc compression tests

The discs deform during the compression test and in the most ideal situation there is a uniform compression with gradual shortening until failure occurs. However, based on the observed behaviour of the discs, there are mainly 2 possible ways a disc can deform during the compression test that seem to have a negative effect on the measurements of the strain. These deformations consist of rotation of the loading-head and barrelling of the disc.

Rotations of the loading-head cause uneven deformations of the disc. The top plate of the loading-head is hinged and able to rotate during the compression tests. This rotation is very limited in most cases, but in some of the cases a severe distortion is evident. The rotation of the loading-head is mainly noticeable in the stress-strain curves of the linear potentiometers.

An example of a disc in compression with the rotation of the loading-head is presented in Figure 6.7. It is visible that the stress-strain curves deviate depending on the linear potentiometer. Note that potentiometers D1 and D3 are positioned opposite from each other, just as D2 and D4 are located in opposite places. It becomes apparent that potentiometers D2 and D3 experience more shortening than potentiometers D1 and D4, meaning that a slight rotation of the loading-head occurs. The average strain can be computed and lies somewhere in the middle which seems to be still useful for the calculation of the modulus of elasticity.

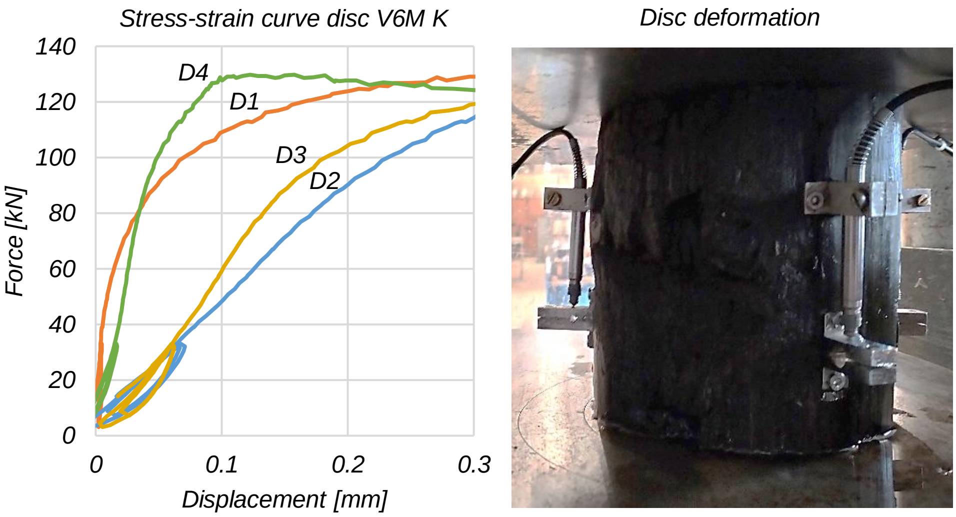

Figure 6.7: Example of a disc in compression with rotation of the loading-head

Barrelling of a disc occurs when the disc deforms under compression and the initially plane sides start bulging. The side of the disc takes on a rounder shape which can cause the brackets of the linear potentiometers to rotate slightly away from each other. The gauge length becomes a bit larger which distorts the measurements of the stain. This phenomenon has been observed to varying extents, with a small or a large effect and with an area ranging from only one side to the entire disc.

An example of extreme barrelling is pictured in Figure 6.8. All measurements from the linear potentiometers indicated a negative displacement at some point, which means an increase in gauge length. This means that the data from the linear potentiometers are not suitable for the calculation of the modulus of elasticity. Also, the sides are rounded and the rotation of the brackets is clearly visible.

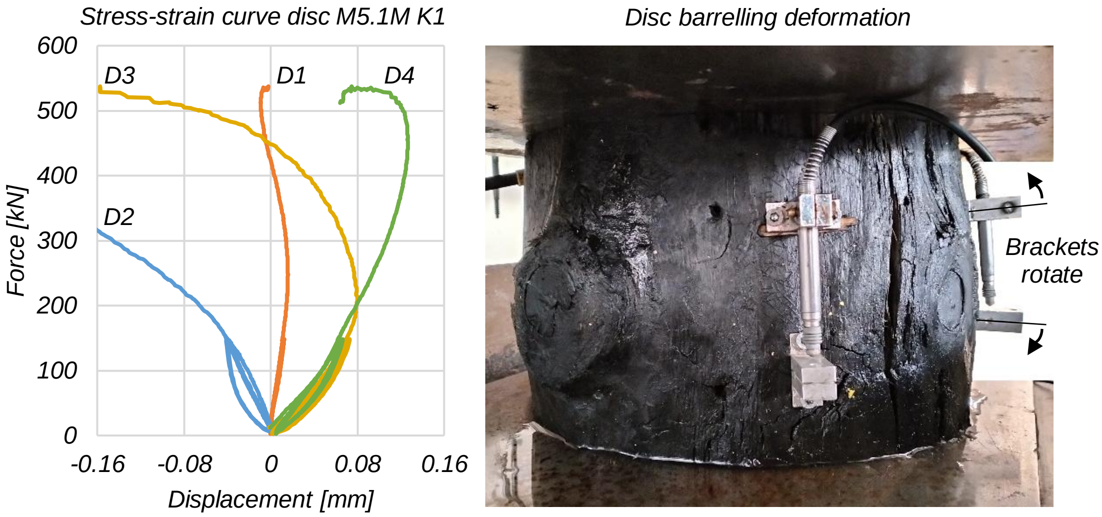

Figure 6.8: Example of barrelling deformation of a compressed disc

All of the aforementioned distortions can happen simultaneously. The stress-strain curves of the linear potentiometers can go in all directions, especially when barrelling of the disc occurs.

The inconsistencies in the signal of the linear potentiometers occurred on all types of discs and it does not matter if they are old or new, with or without knots and/or biological degradation. It seems to be mainly related to the size of the discs that cause the inaccurate measurements. In general, it unfortunately seems to be not feasible to determine the modulus of elasticity of the discs based on the results from the linear potentiometers.

That being the case, the displacement of the jack has also been examined to investigate whether it was a useful measure for the strain of the disc. The moduli of elasticity that were determined in this way seem to result in very low values that do not correspond with the values measured for the pile segments. Some reasons could be that the displacement of the jack includes the preloading and it also measures the deformation of the part where the load is introduced in the specimen. This makes it seem not possible to get a reliable measure for the modulus of elasticity by only performing compression tests on small discs from a pile.

7. Conclusions

Discs were taken from degraded and non-degraded spruce foundation piles. The discs were subjected to testing and the results were then analysed. The conclusions are outlined in this section, followed by a discussion including some limitations and recommendations.

7.1 Main findings

The aim of this study is to find out whether it is possible to determine the mechanical properties of timber foundation piles by performing tests on discs. The mechanical properties that are considered are the short-term wet compressive strength and the static modulus of elasticity. These properties have been computed by performing small-scale compression tests on the discs from timber foundation piles. The main findings of this study can be summarised in five separate conclusions. The first four conclusions cover the results regarding the strength and the last conclusion is about the elasticity. Each conclusion is followed by a brief explanation that sums up the reasoning behind it.

1) **The wet compressive strength from the small-scale tests on discs corresponds well with the wet compressive strength from the large-scale tests on segments.**

   A total of 45 discs were tested in compression and their results were compared with the values from previously performed large-scale tests on segments. The segments are the same ones from which the discs were taken, making it possible to use the values from the segment tests to validate the values retrieved from the tests on discs.

   The wet compressive strength of the discs is very similar to the wet compressive strength of the segments. A total of 25 from the 45 discs had a strength value with less than 10% difference from the strength of the corresponding segments. Another 17 from the 45 discs measured a strength that ranges within the 10% and 20% difference from the segment strength. The remaining 3 discs are considered outliers in this context. Note that it is not possible to test the exact same section twice until failure and wood is inhomogeneous with defects, so some variations between the results from the disc and segment compression tests can be expected. In general it can be said that the results are well aligned and the strength of the discs turn out to have a good correlation with the strength of the segments.

2) **The amount of bacterial degradation in a cross-section is proportional to a decrease in the wet compressive strength.**

   The biological degradation of the examined piles consists of bacterial decay which develops as a soft shell around the perimeter of the pile. For this study, piles with different building years and different amounts of degradation were selected to investigate their conditions. The amount of degradation was examined and quantified with a micro-drill. The effect that the degradation has on the strength of the discs can be well demonstrated by looking at the results from the tests on clear wood discs without knots.

The discs with almost no biological degradation originate from 1922 / 2019 and have an average wet compressive strength of 15.4 ± 0.8 N/mm^2. The discs from 1886 are moderately degraded, have a remaining sound sectional area between 80% and 100% with an average compressive strength of 13.4 ± 1.3 N/mm^2. The severely degraded discs are from 1727, have a sound sectional area between 50% and 80% with an average compressive strength of 9.4 ± 1.6 N/mm^2. All in all, when the degraded discs are compared with the non-degraded discs, it can be seen that the moderately degraded discs have a strength that is 14% lower and the severely degraded discs have a strength that is 39% lower. The amount of degradation is found to be directly related to the loss in strength that it causes, which is an indication that the strength of the soft shell is close to zero and the soft shell contributes very little to the load-carrying capacity of the pile.

3) The sections with the highest knot ratios are the weakest points with the lowest wet compressive strength along the length of a timber pile.

The section with the highest knot ratio from each segment was isolated in a disc and they were tested in compression. It is possible to compare the strength of the clear wood discs directly to the strength of the discs with large knots in order to investigate the differences. Here the strength of the soft shell is neglected which ensures that the remaining strength is no longer dependent on the amount of biological degradation and the focus shifts to the effect of the knots.

Clear wood discs without knots have an average strength of 15.0 ± 1.2 N/mm^2, discs with a knot ratio between the 0.07 and 0.15 have an average strength of 14.0 ± 1.4 N/mm^2 and discs with a high knot ratio ranging between 0.15 and 0.32 have an average strength of 13.0 ± 1.0 N/mm^2. So, when the knotted discs are compared with the clear wood discs, it turns out that discs with a knot ratio between 0.07 and 0.15 have a 7% lower strength and discs with a knot ratio between 0.15 and 0.32 have a strength that is 14% lower. The section with the highest knot ratio ultimately has the lowest strength, regardless of the amount of degradation and the building year. Therefore it can be stated that the sections with the highest knot ratios govern the strength of the pile.

4) The small-scale compression tests on discs can be applied to successfully retrieve the wet compressive strength of a timber pile.

The strength of a timber pile is a measure for the highest load it can endure without the occurrence of failure. It can be stated that the strength of a pile is identical to the strength of the weakest part along the length of the pile because this part governs the failure of the pile. In this study it was observed that the wet compressive strength of a disc is very similar to that of a larger segment of the pile. Thus, it is possible to obtain an accurate value for the wet compressive strength of a pile, simply by isolating the weakest section in a disc and by performing compression tests on that disc. This provides an alternative to the conventional large-scale compression tests which can save a lot of time and resources. In practice this can be used to reduce the extensive experimental efforts needed to obtain the strength of a pile.

It was found that a soft shell has a negligible strength and a knot ratio above 0.10 can cause a strength reduction up to 30%, meaning that the wet compressive strength of an aged timber pile is mostly dominated by the presence of biological degradation and a high knot ratio. Here it should be noted that the bacterial degradation occurs over the entire length of the pile and there is no specific position along the length of the pile that is more susceptible to bacterial attack. However, the pile tip generally contains the most knots and also the largest knots in comparison to the head and middle of the pile. This information, combined with the smaller circumference, ensures that the pile tip principally contains the highest knot ratio and therefore also the section with the lowest strength. If such a section is then captured in a disc and tested in compression, it would lead to a strength value that is representative for the minimum compressive resistance of the pile.

5) **It is not possible to get a reliable measure for the modulus of elasticity from the small-scale disc compression tests.**

   The modulus of elasticity is an measure for the stiffness of the wood. In general, it can be determined by investigating the stress-strain relationship in the elastic region of the material in question. The strain is measured during each compression test with 4 linear potentiometers that are mounted on the exterior of the disc. It turns out that the data from these linear potentiometers show a lot of variations and distortions.

   The main reason for the inconsistencies in the data of the linear potentiometers seem to be related to the short height of the disc. The brackets of the potentiometers are located in the crack propagation zone and any wood defects have a big negative effect on the strain measurements. Furthermore, the discs deform and barrelling occurs which can even cause an elongation of the potentiometers’ stroke during the compression tests. The results from the linear potentiometers are unfortunately not suitable for the derivation of the modulus of elasticity.

These findings provide valuable insights into the performance of aged timber piles and the factors that influence their mechanical properties. The values obtained from the tests on the discs contribute to add more data to the body of knowledge within this field of study. It can also be utilized to improve damage accumulation models and reliability based studies on the remaining strength of aged timber piles.

The outcomes of this study can be used as a reference in further research and as a comparison for practical situations. However, it should be kept in mind that the given information is obtained by testing spruce roundwood with a moisture content around the water saturation point and with signs of bacterial decay only.

Note that the data in this report, and specifically this section, is for informational purposes only and the given values are not intended to be used as input for structural calculations. They are not meant to be used for deriving characteristic values for calculations and practical engineering design directly.

7.2 Answer to the research question

Only the main research question in answered in section. The answers to the various sub research questions can be found in the chapters of this thesis.

The main research question, as stated in the introduction, was formulated as follows:
How can the wet mechanical properties of a degraded spruce timber pile be determined through small-scale mechanical tests on discs sawn from the pile?

The answer to the research question is a combination of the main findings, in particular conclusions 4 and 5. Therefore it can already be stated that it is possible to obtain the strength, but not the elasticity, from small-scale mechanical tests on discs. The way the small-scale compression testing can be applied to compute the strength of the pile is described below.

First it is important to locate the weakest section of the pile. The strength of the pile is mainly influenced by the presence of bacterial degradation and knots. So, in order to find the weakest section, the amount of bacterial degradation and knots need to be quantified and compared with each other.

The distribution and the amount of bacterial degradation can be investigated by performing non-destructive tests at different locations over the length of each pile. A micro-drill can be used to measure the thickness of the soft shell and to classify the amount of biological degradation for each section. It is also possible to use a handheld piercer tool as a low-tech and cheaper option to estimate the soft shell thickness, but these measurements are generally less precise than the values resulting from the micro-drilling tests.

As for the presence of multiple knots in one section of round wood, these can be expressed in a knot ratio that represents the percentage of the cross-sectional area that is occupied by the knots. The knot ratio can be determined from dimensions on the outside of the pile. This means that it is possible to point out the sections with highest knot ratios without the need to damage or saw the pile.

The weakest section of the pile is mainly the section with the highest knot ratio, provided that the thickness of the soft shell has also been taken into consideration. This section can then be isolated by sawing it into a disc. After this, the disc is tested in compression until failure to determine the maximum force that the section can withstand. The maximum force can be divided by the area of the remaining sound inner part of the pile and the result is an accurate value for the short-term wet compressive strength of the pile.

As previously mentioned, the disadvantage of this small-scale compression testing method is that is not possible to determine the modulus of elasticity. Having said this, it is not really considered a problem. The importance of the elasticity predominantly lies in the fact that it is well correlated with the strength and, in practice, it is often desirable to be able to determine the elasticity in-situ as a way to predict the strength. So, even if the elasticity cannot be assessed with small-scale testing, the fact that the strength can be determined with such tests means that the inability to measure the elasticity is considered to be no longer significant for the outcome of this study.

7.3 Limitations
The limitations mainly deal with uncertainties and/or assumptions that occurred during the experimental phase of this project. They are linked to some of the choices that were made during the testing of the specimens. The three main limitations that were recognized are specifically related to the oversimplification of a complex problem, the sample size and the artificial test set-up.

Generally, in this type of experimental research, complex problems are a bit simplified so certain relations can be made clear. An example of this principle, specifically related to this study, could be that a disc with a lot of degradation has been tested and afterwards it is assumed that the observed decrease in strength comes directly from the presence of this degradation. In reality there are many factors that play a role, influence the strength and also influence each other, which means that the researcher should be careful when attributing the reduced strength to the presence of the degradation.

What is also considered important in this context is the sample size and the characteristics of the samples. Here the well-known statement “what you put in is what you get out” explains what is meant by this. For this study, the specimens originated from a total of 6 spruce foundation piles which ultimately resulted in 45 discs. These piles were specifically selected with different building years and different amounts of degradation. By doing this, the research is already set up in such a way that mainly the differences between the degradation can be measured during the testing of the specimens. This could make one inclined to lose sight of the other factors that may influence the results of the tests. The researcher’s biases can also play a role, these may determine that the research is heading in a certain direction and the findings that follow. Increasing the number of samples with different characteristics and seeking advice from other researchers can be helpful when it comes to avoiding these kinds of tunnel visions.

The test-set up in the laboratory consisted of a compression bank that applied an axial load parallel to the fibre direction. If this is compared to the situation where the pile is in the ground then there is a certain ground pressure around the pile that can give support in lateral direction. This means that the discs were freer to expand laterally during the tests, which in itself should not have a big effect on the strength measurements. However, during the segment compression tests it could indeed influence the strength because the segment is free to buckle sideways, which may mean that a segments in a compression test would fail more easily with a buckling type of failure mechanism. The strength of the segments was used in this study to validate the strength of the discs, which means that the noted difference could have an influence on the findings of this study.

It was also the case that during the disc compression tests it was not possible to fix the loading-head in place, which means that the loading-head was able to rotate during the compression tests. Because the loading-head could rotate, bending stresses could potentially develop in the test pieces. Since the height of the discs are very limited, it is likely that any bending stresses, if they occurred at all, would not have affected the strength measurement too much. Moreover, there are a couple of more differences between the artificial test set-up and the real-world scenario that can be mentioned, but these are considered of lesser importance and are therefore left out of this thesis.

7.4 Recommendations

Some recommendations for further research are given. The recommendations are related to the mechanical degradation that affects the strength of aged timber piles, the crack propagation of the different failure mechanisms and the possibility to develop a reliability based method for the strength of aged timber piles.

This study elaborated on the effects of biological degradation and knots on the strength of aged timber piles. However, besides the presence of biological degradation and knots, there is also mechanical degradation that can have a major effect on the strength of aged timber foundation piles. It is known that a higher load and a longer load duration can increase the mechanical degradation and result in a lower strength. Having said that, the precise loading history of the foundation piles is not known and it was not possible to assess the mechanical degradation during this study. So, as a recommendation for further research, it is interesting to investigate the exact effect of the mechanical degradation on the strength of the timber piles from Amsterdam.

When the different specimens are tested in compression, it can be observed that the discs generally experience a crushing failure and the segments mainly fail due to buckling. Despite the different failure mechanisms, it was discovered that the strength of the discs matches the strength of the segments. It may be interesting for further research to map out how these failure mechanisms work and what there similarities/differences are. This could be done by developing a numerical model to investigate how the stresses develop in an aged timber pile. It can also be interesting to create a crack propagation model to examine how the failure develops around the presence of knots in the wood structure of the pile.

The correlation between the strength and the amount of degradation or the knot ratio were found to be strong. In addition, it turned out that the negative effects of the biological degradation and the presence of knots seem to work alongside each other. It is also important to note that both the amount of degradation and the knot ratio can be quantified by performing non-destructive testing. These outcomes give possibility to create a straight-forward method to estimate the remaining strength of an aged timber pile in practice, without having to damage or destroy the pile. In order to develop such a reliability based method, a lot more data is needed and therefore more tests need to be carried out. Also, the data needs to be subjected to a statistical analysis to see how they are distributed and to see if they are statistically significant.

An indication of what such a method would look like is as follows. The degradation and knots can be examined and quantified separately, whereby it may even be manageable to relate these directly to a reduction factor for the strength of the pile. The negative effects of both the degradation and knots can then be combined to obtain an estimate for the strength reduction that they induce on the aged timber pile. When this reduction is then considered in comparison with the strength of a sound pile it can be possible to obtain a good value for the strength of this pile.

References

[1] R. K. W. M. Klaassen and J. G. M. Creemers, “Wooden foundation piles and its underestimated relevance for cultural heritage,” SHR Timber Research, Wageningen, 2012.

[2] Forest Products Laboratory, Wood handbook—Wood as an engineering material. General Technical Report FPL-GTR-190, Madison: U.S. Department of Agriculture, Forest Service, Forest Products Laboratory, 2010.

[3] H. J. Blaß and C. Sandhaas, Timber Engineering - Principles for Design, Karlsruhe: KIT Scientific Publishing, 2017.

[4] R. K. W. M. Klaassen, “Bacterial decay in wooden foundation piles—Patterns and causes: A study of historical pile foundations in the Netherlands,” Int. Biodeterior. Biodegradation 61-1, 2008.

[5] G. Pagella, “Durability of timber structures: damage detection, quantification and inspection techniques,” Delft University of Technology, Delft, 2022.

[6] European Standard EN 1995, “Eurocode 5 - Design of timber structures,” CEN - European Committee for Standardization, 2004.

[7] J. W. G. van de Kuilen, “Bepaling van de karakteristieke druksterkte van houten heipalen - TNO report 94-CON-R0271,” TNO, Delft, 1994.

[8] S. Aicher and G. Stapf, “Compressive strength parallel to the fiber of spruce with high moisture content,” University of Stuttgart, Stuttgart, 2016.

[9] Delft University of Technology, “Strength of wooden pile foundations in Amsterdam,” December 03 2020. [Online]. Available: https://www.tudelft.nl/en/2020/citg/strength-of-wooden-pile-foundations-in-amsterdam. [Accessed 12 December 2024].

[10] G. Pagella, “Mechanical Characterisation of New and Existing Timber Foundation Piles: For the assessment of historical timber foundations and their contemporary applications in structural design,” Delft University of Technology, Delft, 2025.

[11] G. Pagella, M. Mirra, G. J. P. Ravenshorst and J. W. G. van de Kuilen, Influence of knots and density distribution on compressive strength of wooden foundation piles, Delft: Delft University of Technology, 2022.

[12] C. Gambarin, “Influence of knots on the compressive strength of wooden foundation piles,” University of Padova, Padua, 2022.

[13] H. Rietdijk, “Amsterdam on poles,” 9 February 2017. [Online]. Available: https://www.holandiabeztajemnic.pl/?page_id=24061&lang=en. [Accessed 21 April 2023].

[14] R. K. W. M. Klaassen, “Life Expectation of Wooden Foundations - a Non-Destructive Approach,” SHR Timber Research, Wageningen, 2015.

[15] R. K. W. M. Klaassen and e. al., “Preserving cultural heritage by preventing bacterial decay of wood in foundation piles and archaeological sites (EVK4-CT-2001-00043),” European Commission, Wageningen, 2005.

[16] G. van den Berg, Interviewee, *Director of RHS Rondhout at Hierden (NL).* [Interview]. 28 November 2023.

[17] J. Bijnagte and R. P. Boeije, “Funderingsherstel Schiedam,” Deltares (GeoDelft), Delft, 2009.

[18] X. Li, H. X. Wu and S. G. Southerton, “Transcriptome profiling of wood maturation in Pinus radiata identifies differentially expressed genes with implications in juvenile and mature wood variation,” CSIRO Plant Industry, Canberra, 2011.

[19] J. M. Dinwoodie, Timber - Its nature and behaviour, London and New York: Taylor & Francis e-Library, 2000.

[20] S. Anupoju, “Types of Defects in Timber as a Construction Material,” [Online]. Available: https://theconstructor.org/building/types-of-defects-in-timber/21521/. [Accessed 4 May 2023].

[21] J. G. Collin, Timber Pile - Design & Construction Manual, USA: Southern Pressure Treaters' Association, 2016.

[22] C. Meredieu and Y. Caraglio, “External indicators of living branches with missing rings within a tree crown of Corsican pine,” French National Institute for Agriculture, Food and Environment (INRAE), Cestas, 2002.

[23] C. Lantinga, “De resterende (geotechnische) draagkracht van bestaande houten funderingspalen,” Technische Universiteit, Eindhoven, 2015.

[24] G. Pagella, G. J. P. Ravenshorst and J. W. G. van de Kuilen, “Analysis of the mechanical properties in relation to RPD measurements of 60 timber piles retrieved from bridge 30 and 41 in Amsterdam,” Delft University of Technology, Delft, 2023.

[25] M. Bather, “Guide to statistics in the Eurocodes for timber engineers,” University of Liverpool, Liverpool, 2021.

[26] G. Granello and A. Palermo, “Creep in Timber: Research Overview and Comparison between Code,” New Zealand Timber Design Journal, Canterbury, 2019.

[27] W. F. Gard, G. J. P. Ravenshorst and J. W. G. van de Kuilen, “Historical Wood Pile Foundations in Amsterdam: An Integrated Approach for the Estimation of Structural Performance and Residual Service Life,” SAHC 2023 - Vol. 1, pp. 1370-1382, Delft, 2023.

[28] S. Ujang, A. H. H. Wong and E. B. Gareth Jones, “Wood Degrading Fungi,” Mushroom Research Centre, University of Malaya and Ministry of Natural Resourcesa nd Environment Malaysia, 2007.

[29] G. Daniel, “Fungal and Bacterial Biodegradation: White Rots, Brown Rots, Soft Rots, and Bacteria,” Swedish University of Agricultural Sciences, Uppsala, 2014.

[30] A. Roy, G. J. P. Ravenshorst, W. F. Gard and J. W. G. van de Kuilen, “Handleiding Soft Shell Calculator TU Delft versie 0.1,” Delft University of Technology, Delft, 2021.

[31] G. Pagella and G. J. P. Ravenshorst, “Characterization of the mechanical properties of 60 timber piles retrieved from bridge 30 and 41 in Amsterdam,” Delft University of Technology, Delft, 2023.

[32] M. Lee, “Cross Sectional Analysis Of The Mechanical And Physical Properties Of Spruce Foundation Piles,” Delft University of Technology, Delft, 2023.

[33] M. Mirra, G. Pagella, W. F. Gard, G. J. P. Ravenshorst and J. W. G. van de Kuilen, “Influence of moisture content on the assessment of decay levels by micro-drilling measurements in wooden foundation piles,” Delft University of Technology, Delft, 2023.

[34] Rijksdienst voor het Cultureel Erfgoed, “Rijksmonumenten Amsterdam plaat- of balkbrug,” [Online]. Available: https://rijksmonumenten.nl/monumenten/plaat-of-balkbrug/gemeente=amsterdam. [Accessed 22 May 2024].

[35] S. Honardar, “Geotechnical Bearing Capacity of Timber Piles in the City of Amsterdam,” Delft University of Technology, Delft, 2020.